

Space-Time Block Codes for Multi-Input
Single-Output Channels and Simple Maximum
Likelihood Detection

SPACE-TIME BLOCK CODES FOR MULTI-INPUT
SINGLE-OUTPUT CHANNELS AND SIMPLE MAXIMUM
LIKELIHOOD DETECTION

BY
ANZHONG WONG, B.Eng.

A THESIS
SUBMITTED TO THE DEPARTMENT OF ELECTRICAL & COMPUTER ENGINEERING
AND THE SCHOOL OF GRADUATE STUDIES
OF MCMASTER UNIVERSITY
IN PARTIAL FULFILMENT OF THE REQUIREMENTS
FOR THE DEGREE OF
MASTER OF APPLIED SCIENCE

© Copyright by Anzhong Wong, September 2010

All Rights Reserved

Master of Applied Science (2010)
(Electrical & Computer Engineering)

McMaster University
Hamilton, Ontario, Canada

TITLE: Space-Time Block Codes for Multi-Input Single-Output
Channels and Simple Maximum Likelihood Detection

AUTHOR: Anzhong Wong
B.Eng., (Electrical Engineering)
McMaster University, Hamilton, Canada

SUPERVISOR: Dr. Jian-Kang Zhang

NUMBER OF PAGES: xii, 97

I would like to dedicate this work to my father and mother, for their constant love and support throughout all my endeavours. Their principle of “a good life is one inspired by love and guided by knowledge” is a continuous reminder that, while new areas of knowledge are being explored, the fundamentals of love and honour must not be abandoned.

Abstract

Multi-input multi-output (MIMO) technology has been used to improve wireless communications systems over the past several years. The multiple antennas of MIMO systems are used to increase data rates through multiplexing gain and/or increase the reliability of the system through diversity gain. It is known that an optimum trade-off between diversity gain and multiplexing gain can be achieved by having proper space-time block code (STBC) designs. The current STBC designs minimizing the pair-wise error probability (PEP) of the maximum likelihood (ML) detector are based mainly on the rank and the determinant criteria.

In this thesis, we study a special case of the MIMO system. This consists of a coherent communication system equipped with M_t transmitter antennas and a single receiver antenna, i.e., a multi-input single-output (MISO) system. Such systems are often encountered in mobile down-link communications for which a MIMO realization may be expensive or for which the mobile receiver may not be able to support multiple antennas (e.g. a mobile phone). Given a full-rate data transmission, the PEP of the ML detector for such systems can be minimized by using the rotated quasi-orthogonal STBC design, which enables full diversity and optimal coding gains for the system. The efficiency of fast ML decoding for orthogonal STBC is also largely preserved for such quasi-orthogonal STBC. However, for large constellations, the performance of

such “optimum” codes deteriorates due to the increase of the number of the nearest neighbours per symbol.

To correct such a deficiency of the code, in this thesis, we propose to include the number of nearest neighbors in the design criterion. We show that for the current optimal rotated quasi-orthogonal code, the number of nearest neighbours tends to infinity when the size of constellation becomes infinite. However, we show that by having a particular value of rotation, not only full diversity and maximum coding gain will be achieved, but also a small number of nearest neighbours will be maintained even for very large constellations.

Also, at present, STBC designs in a MIMO system are mainly based on the PEP (or its upper bound). This is because the geometrical structure of the decision regions for a general MIMO channel, equipped with the ML detector, is so irregular that it would be impossible to obtain an exact error probability formula for the ML receiver. This means that the error probability formula cannot be utilized as a criterion for the design of the optimal transmitter for the MIMO systems and the current STBC designs may not be truly optimum in terms of the exact error probability.

To rectify this problem, in this thesis, we first find a closed form algorithm for ML detection, for a 4×1 MISO system equipped with a ML detector, transmitting signals from a four signal quadrature amplitude modulation (4-QAM) constellation. This algorithm is derived such that given a received signal and the channel, the transmitted signal can be obtained using a threshold decision. Then, using this ML detection algorithm, a closed form of the exact error probability of this system is derived. This closed form decoding algorithm is then applied to the 4-group decodable STBC, in order to obtain the optimal rotation angle to minimize the ML error probability.

Acknowledgements

I would like to first and foremost express my gratitude to my supervisor, Dr. J.K. Zhang, for his encouragement and guidance during the course of this work. His direction and supervision were invaluable to the success of this work and his dedication to research is most inspiring.

I would also like to thank other professors and colleagues of the communications research group at McMaster University for their helpful discussions and suggestions. In particular, the courses of Drs. T.N. Davidson and K.M. Wong, apart from being directly applicable, are motivating and interesting, and their valuable advice is gratefully acknowledged.

Finally, I would like to thank Drs. D. Zhao and S. Dumitrescu for taking their time to be a part of my Master's thesis defence committee and sharing their valuable comments and critiques on my thesis.

Notation and Abbreviations

e.g. \mathbf{A}	matrices are denoted by uppercase boldface characters
e.g. \mathbf{b}	column vectors are denoted by lowercase boldface characters
\mathbf{I}_K	the $K \times K$ identity matrix
$\mathbf{0}_K$	the $K \times K$ zeros matrix
\mathbf{a}_i	the i th column of a matrix \mathbf{A}
$(\cdot)_i$	the i th element of a vector
$(\cdot)_{ij}$	the ij th element of a matrix
$(\cdot)^*$	the conjugate of a vector or matrix
$(\cdot)^T$	the transpose of a vector or matrix
$(\cdot)^H$	the Hermitian transpose of a vector or matrix
$\ \cdot\ $	the norm of a vector or a matrix
$ \cdot $	the magnitude operator or the determinant operator
$\det(\cdot)$	the determinant operator
$\text{tr}[\cdot]$	the trace operator
$\mathbb{E}[\cdot]$	the statistical expectation operator
$\langle \cdot, \cdot \rangle$	the inner product operator
j	$\sqrt{-1}$

\mathbb{Z}	the field of integers
\mathbb{R}	the field of real numbers
\mathbb{C}	the field of complex numbers
IID	independent identically distributed
ISI	intersymbol interference
LD	linear dispersion
MIMO	multi-input multi-output
MISO	multi-input single-output
ML	maximum likelihood
PEP	pair-wise error probability
PSD	positive semi-definite
QAM	quadrature amplitude modulation
SNR	signal-to-noise ratio
STBC	space-time block code

Contents

Abstract	iv
Acknowledgements	vi
Notation and Abbreviations	vii
1 Introduction	1
1.1 Background Knowledge of MIMO Systems and STBC Design	1
1.2 Contributions	5
2 The MISO Channel, Orthogonal STBC and STBC Criterion	8
2.1 Channel Model and Orthogonal STBC	8
2.2 PEP Code Design Criterion	13
3 The Quasi-Orthogonal STBC	16
3.1 The Rotated Quasi-Orthogonal STBC and Novel Design Criterion . .	17
3.2 Code Properties and Performance Analysis of the Su-Xia Rotation Angle	20
3.3 Code Properties and Performance Analysis of the Novel Quasi-Optimal Angle	25
3.4 Simulations	28

4	The 4×1 MISO Channel and Simple ML Detection	31
4.1	Channel Model and 4-Group Decodable STBC	32
4.2	Closed Form ML Decoding Algorithm for the 4-QAM Constellation .	36
4.3	Decision Regions for the ML Receiver for the 4-QAM Constellation .	41
5	Symbol Error Probability Analysis and Optimal Rotation Angle	45
5.1	Relationships Between Correct Probability Decision Regions for the 4-QAM Constellation	46
5.2	Gaussian Probability Integrals and the Q -function	50
5.3	Analysis of the Average Probability of Correct Decision for the 4-QAM Constellation	54
5.4	Optimal Rotation Angle for the Minimum Probability of Error for the 4-Group Decodable STBC	61
6	Summary and Conclusion	63
6.1	Summary	63
6.2	Future Work	65
6.3	Conclusion	66
A	Proofs of Lemmas in Chapter 3	67
A.1	Proof of Lemma 2	67
A.2	Proof of Lemma 3	71
B	Proofs of Properties in Chapter 5	76
B.1	Proof of Property 3	76
B.2	Proof of Property 4	78

B.3	Proof of Property 5	79
B.4	Proof of Property 6	81
B.5	Proof of Property 7	82
B.6	Proof of Property 8	83
B.7	Proof of Property 9	86
C	Proofs of Lemmas in Chapter 5	88
C.1	Proof of Lemma 4	88
C.2	Proof of Lemma 5	89

List of Figures

3.1	Performance Comparison of the Su-Xia [1] Rotated Quasi-Orthogonal STBC and Our Rotated Quasi-Orthogonal STBC for 16-QAM	28
3.2	Performance Comparison of the Su-Xia [1] Rotated Quasi-Orthogonal STBC and Our Rotated Quasi-Orthogonal STBC for 64-QAM	29
4.1	4×1 MISO system	32
4.2	ML Decision Regions for Hypotheses $H_i, i = 1, \dots, 4$	42
5.1	Integral Domain in Lemma 4	51
5.2	Integral Domain in Lemma 5	53
5.3	The Coding Gain as a Function of the Rotation Angle of a 4-Group Decodable STBC	62

Chapter 1

Introduction

1.1 Background Knowledge of MIMO Systems and STBC Design

Over the last several years, MIMO technology has been used to improve wireless communications systems since it offers many advantages over conventional single-antenna communications. For instance, multiple antennas can be used to increase transmission reliability and/or to increase the data transmission rates of the system. Increase in transmission reliability in a MIMO system is made possible by having an increased number of transmission data copies over the independent fading paths from each transmitter antenna to each receiver antenna [2]. This results in a higher probability of receiving the correct data by combining all the faded copies of data at the receiver. Increase in transmission data rate in a MIMO system, on the other hand, is made possible by utilizing the available multiple antennas to increase the number of different data streams sent over the independent fading paths from each

transmitter antenna to each receiver antenna. This allows for a gain in the amount of data transmitted, i.e., a capacity gain, at no additional power or bandwidth requirements. *Full data rate* is achieved when on average, for each transmitter antenna, a symbol is transmitted in each time slot. The increase in transmission data rate is usually measured by the *multiplexing gain* [2]. However, from the fundamental limit in communication theory, increase in data transmission invariably leads to a decrease in system performance. This results in a fundamental trade-off between data rate and performance in a MIMO design [3]. From the above discussion, we can see that MIMO technology allows for the improvement of data transmission rates as well as system performance (measured in terms of probability of error), where each can be optimized according to the trade-off limit to provide superior wireless communication systems. In addition to the increases in data rate and system performance, ISI and interference from other users in a MIMO system can be reduced using certain antenna techniques such as beamforming and precoder designs [4].

The improvement of transmission data rate and system performance in a MIMO system can be achieved by efficient STBC designs. Due to the fact that an increase in data rate invariably results in a loss of performance, the current optimum STBC designs aim to fix the data rate (usually fix at full rate) and design the code to optimize the performance measured in terms of the probability of error in the receiver. In particular, the PEP of the ML detector at the receiver is often used as the objective of optimal code design. Here, the objective function contains two parts, viz., the rank and determinant [5, 6, 7], which respectively govern the *diversity gain* and the *coding gain* of the MIMO system. More detailed explanations of these two gains will be given in Chapter 2. Roughly, the diversity gain refers to the gradient of the

probability of error curve against SNR ratio, and measures how fast the probability of error decreases with the increase of SNR. The coding gain measures the distance between the descending probability of error curve from the ordinate axis and is an indication of how high the SNR is before the probability of error curve starts to fall. For the MIMO system, we seek to design an optimum STBC to achieve maximum diversity gain or *full diversity*, and maximum coding gain or *optimal coding gain*.

A STBC is usually represented by an $L \times M_t$ matrix in which each column represents the transmission symbols of a particular antenna for all L time slots, and each row represents the transmitted symbols in one time slot for all M_t transmitter antennas. Thus, each entry in the matrix represents the transmitted symbol of one antenna during a particular time slot. Over the past several years, various STBC schemes [8, 9, 10, 11, 12, 13, 14] have been developed to take advantage of the MIMO communication channel. Among these different schemes, orthogonal STBC [15, 16, 17, 18] are attractive, since they can provide maximum diversity using a linear processing ML detector and provide simple linear optimal decoding. For instance, the *Alamouti Code* was designed for two transmission antennas, and is famous for being the only orthogonal STBC to provide full transmission rate [15]. In fact, if the number of the transmitter antennas is greater than two, no orthogonal STBC can achieve full data rate (i.e., achieving full MIMO channel capacity) [18, 19].

To improve on the low transmission rate, Jafarkhani [20], Tirkkonen-Boariu-Hottinen [21], and Papadias-Foschini [22] proposed STBC with quasi-orthogonal designs. While the quasi-orthogonal structures still support simple, fast ML decoding, they no longer provide optimal linear decoding or achieve full diversity. To overcome these shortcomings so that both full diversity and fast ML decoding are

maintained, Su and Xia [1] designed a rotated quasi-orthogonal STBC with the optimal coding gain for commonly used square QAM constellations which inspired other similar designs which focus on maintaining full diversity and non-vanishing determinants [12, 13, 14], enabling the optimal tradeoff of diversity and multiplexing gains [3].

While MIMO systems offer valuable advantages over conventional single antenna systems, the expenses associated with implementing critical MIMO designs in order to maximize the efficiency of each antenna for both diversity and multiplexing can be unrealistically high [3, 5] for some practical applications. One of the main costs for the performance enhancements of MIMO communication channels is the cost of deploying multiple antennas. The space and circuitry required for these extra antennas, and the added complexity required for multi-dimensional signal processing [4], may not be affordable in many communication systems, especially when mobility is a factor. Thus, in view of the antenna cost in a mobile system, in this thesis, instead of a general MIMO system, our attention focuses on the study of a coherent MISO system equipped with multiple transmitter antennas and a single receiver antenna. A MISO wireless communication system is, in fact, a particular case of a MIMO system. It may lose some of the benefits (such as reduction in multiplexing and diversity gains) of a general MIMO system, but it reduces the costs in antenna and space required in a mobile environment. Thus, MISO systems are often encountered in mobile down-link communications for which a MIMO system may be too expensive, or the mobile receiver (e.g. a mobile phone) may not be able to support multiple antennas.

1.2 Contributions

While the optimum designs of STBC codes for a ML detector focus on the maximization of the diversity and coding gains, governed by the rank and determinant factors in the criterion of PEP, one problem that has been unaddressed is performance deterioration of the “optimum” codes when the transmission symbols are selected from a large constellation. This is due to the fact that when the PEP is averaged, the average probability of error not only depends on the distance between the pair-wise neighbours, but also on the average number of neighbours that are separated by the same distance. Furthermore, this average probability of error is dominated by the average number of neighbours separated by the minimum distance, i.e., the *average number of nearest neighbours*. To correct this problem, in this thesis, we propose a new design criterion which uses the average nearest neighbour number as a novel additional factor to the current design criterion of the rotated quasi-orthogonal STBC. We first prove that, despite the fact that the rotated quasi-orthogonal STBC with angle $\pi/4$, proposed by Su and Xia [1], enables full diversity as well as the optimal coding gain for the commonly used square QAM constellation, the code is no longer optimal in terms of our new design criterion. In fact, by making use of the Pell Diophantine equation and Diophantine approximation theory [23], we prove that the average number of nearest neighbors tends to infinity for the Su-Xia code when the size of the constellation is infinite. Also, we propose a new rotated quasi-orthogonal STBC design with a new rotation angle that, in addition to both maximizing the rank and the coding gain, attempts to make the average number of the nearest neighbors small. Based on verifications using the Pell Diophantine equation, we obtain the new rotation angle to be $\pi/6$ and prove that the resulting rotated quasi-orthogonal STBC

not only provides full diversity and the optimal coding gain, but also has an average nearest neighbor number per symbol which tends to 8 when the constellation size tends to infinity.

In this thesis, we also address a MIMO system problem which is generally overlooked: At present, STBC designs in a MIMO system are mainly based on the PEP (or its upper bound). This is because the geometrical structure of the decision regions, for a general MIMO channel equipped with the ML detector, is so irregular that it would be impossible to obtain an explicit exact error probability formula for the ML receiver [5]. This means that the error probability formula cannot be utilized as a criterion for the design of the optimal transmitter for MIMO systems, and the current STBC designs may not be truly optimum in terms of the exact error probability. Therefore, the current STBC designs use the union bound instead, which sums up all the prior-probability-weighted PEP of the ML detector, to establish the rank and determinant criterion of optimizing the error performance dominant term. Alternatively, the sphere bound can be employed, instead of the union bound, as a design criterion to successfully construct the non-vanishing determinant STBC [14]. This enables the optimal tradeoff of diversity and multiplexing gains based on the logarithm criterion, which governs the decay order of error performance in terms of SNR, but cannot control the coding gain. As a consequence, two distinct STBC, both of which enable the optimal tradeoff of diversity and multiplexing gains, may have significantly different error performance.

To rectify this problem, in this thesis, a closed form of the exact error probability for a 4×1 MISO system, equipped with a ML detector transmitting signals from a

4-QAM constellation, is derived based on novel analyses of different Gaussian probability integrals. For such a system, we first obtain a closed-form algorithm for ML detection such that given a received signal and the channel, the transmitted signal can be obtained by a simple threshold decision. Then, its decision regions for all the transmitted signal points are completely and explicitly determined. The decision regions obtained have a geometrical structure with symmetric properties, allowing for a much simplified calculation of the closed form error probability. This closed form error probability specifically analyzes the asymptotic behavior of its average error performance taken over all random channel coefficients, when SNR is high. Finally, this problem is specifically employed on the 4-group decodable STBC [24, 25, 26, 27, 28, 29] and the optimal rotation angle is obtained to minimize the probability of error, based on the asymptotic closed form probability of error formula.

To the best knowledge of the author, this thesis is the first attempt to utilize the average number of nearest neighbours as an optimization design criterion for STBC using a ML receiver. As well, this thesis is the first to derive a closed form algorithm for ML detection in a MISO system with the 4-group decodable STBC.

Chapter 2

The MISO Channel, Orthogonal STBC and STBC Criterion

MIMO technology and the orthogonal STBC structure have been used to improve the performance of wireless communications systems over the last several years [15, 16, 17, 18]. In this chapter, the MIMO channel model, and in particular the MISO channel which is used throughout this thesis, will be introduced. Additionally, other relevant topics such as orthogonal STBC, the ML receiver, and the current STBC design criteria for the ML receiver will be discussed in detail.

2.1 Channel Model and Orthogonal STBC

Existing MIMO communication systems rely on the use of M_t transmitter antennas and M_r receiver antennas which enables the communication system to exploit both the high performance provided by the space diversity available, and the high data rate provided by the capacity obtainable in the MIMO channels [6, 7]. A MISO

system is a particular case of a MIMO system in which there is only one ($M_r = 1$) receiver antenna. A MISO system alleviates the burden of having multiple antennas at the receiver which demands extra cost and space often unavailable in a mobile environment. A coherent flat fading MISO wireless communication system having M_t transmitter antennas and a single receiver antenna operates as follows: For each time slot (usually called a “channel use”), each of the M_t transmitter antennas is fed a coded symbol for transmission. Each of these transmitter antennas is linked to the receiver antenna through a channel h_m , $m = 1, \dots, M_t$. At the receiver of such a system, for time slots $\ell = 1, \dots, L$, an L -dimensional signal vector $\mathbf{y} = [y_1 \ y_2 \ \dots \ y_L]^T$ is received, which according to the input-output model of the system, can then be written as

$$\mathbf{y} = \sqrt{\frac{\rho}{M_t}} \mathbf{X}(\mathbf{s})\mathbf{h} + \boldsymbol{\xi} \quad (2.1)$$

where $\mathbf{X}(\mathbf{s})$ is an $L \times M_t$ coding matrix with a normalized average energy $M_t L$, each row of which consists of coded versions of the symbols s_k , $k = 1, 2, \dots, K$ fed to the M_t transmitter antennas during a particular time slot, \mathbf{h} is an $M_t \times 1$ channel vector, ρ is the average SNR per symbol, and $\boldsymbol{\xi}$ is an $L \times 1$ complex noise vector. Since there is only a single receiver antenna in a MISO system, if within one time slot the receiver antenna receives all the transmitted K symbols, i.e., $L = K$, this is called *full-rate* (or rate 1) transmission for the system. The coding of the symbols in $\mathbf{X}(\mathbf{s})$ can take on different forms. A popular code is the *linear dispersion* (LD) code which can be written as:

$$\mathbf{X}(\mathbf{s}) = \sum_{k=1}^K \mathbf{A}_k s_k + \sum_{k=1}^K \mathbf{B}_k s_k^* \quad (2.2)$$

where \mathbf{s} denotes a $K \times 1$ transmission symbol vector such that $\mathbf{s} = [s_1 \ s_2 \ \cdots \ s_K]^T$ containing the K information symbols selected from an alphabet, \mathcal{S} , of complex numbers to be transmitted within the L time slots, where $s_k = (s_k)_{\text{re}} + j(s_k)_{\text{im}}$ and \mathbf{A}_k and \mathbf{B}_k each denotes an $L \times M_t$ real matrix.

Definition 1. Let $\{\mathbf{A}_i, \mathbf{B}_i\}_{i=1}^K$ be a sequence of $L \times M_t$ matrices with $L \geq M_t$. The LD code formed using these matrices is said to be a complex orthogonal STBC if the following conditions are satisfied:

$$\mathbf{A}_m^H \mathbf{A}_n + \mathbf{B}_n^H \mathbf{B}_m = \delta_{mn} \mathbf{I}_{M_t} \quad (2.3)$$

$$\mathbf{A}_m^H \mathbf{B}_n + \mathbf{A}_n^H \mathbf{B}_m = \mathbf{0}_{M_t} \quad (2.4)$$

for any $1 \leq m, n \leq K$, where $\delta_{mn} = \begin{cases} 1 & \text{if } m = n \\ 0 & \text{if } m \neq n \end{cases}$.

Example 1. The following Alamouti orthogonal STBC [15], for a wireless communication system, has two transmitter antennas and a single receiver antenna. For this code, we can observe that $L = K = 2$ (full rate). It is a very important code in the sense that it is the only complex orthogonal code that supports full symbol rate transmission in a MISO system:

$$\mathbf{X}(\mathbf{s}) = \begin{bmatrix} s_1 & s_2 \\ -s_2^* & s_1^* \end{bmatrix} \quad (2.5)$$

where by simple inspection of Eq.(2.5), the coefficient matrices of the code are given

by

$$\mathbf{A}_1 = \begin{bmatrix} 1 & 0 \\ 0 & 0 \end{bmatrix} \quad \mathbf{A}_2 = \begin{bmatrix} 0 & 1 \\ 0 & 0 \end{bmatrix} \quad \mathbf{B}_1 = \begin{bmatrix} 0 & 0 \\ 0 & 1 \end{bmatrix} \quad \mathbf{B}_2 = \begin{bmatrix} 0 & 0 \\ -1 & 0 \end{bmatrix}$$

Example 2. Another typical example [17] is a 4×4 orthogonal code with a symbol rate $3/4$,

$$\mathbf{X}(\mathbf{s}) = \begin{bmatrix} s_1 & s_2 & s_3 & 0 \\ -s_2^* & s_1^* & 0 & -s_3 \\ -s_3^* & 0 & s_1^* & s_2 \\ 0 & s_3^* & -s_2^* & s_1 \end{bmatrix} \quad (2.6)$$

Here, the code is for $M_t = 4$ antennas, and within $L = 4$ time-slots, there are only $K = 3$ symbols s_1, s_2, s_3 transmitted making the transmission rate equal to $\frac{K}{L} = \frac{3}{4}$. The coefficient matrices \mathbf{A}_i and $\mathbf{B}_i, i = 1, 2, 3$ can be similarly constructed by inspection of Eq.(2.6).

More examples of orthogonal space-time block codes can be found in [16, 18, 30]. Notice that Eq.(2.1) can be rewritten as

$$\mathbf{y} = \mathbf{H}_a \mathbf{s} + \mathbf{H}_b \mathbf{s}^* + \boldsymbol{\xi} \quad (2.7)$$

where \mathbf{H}_a and \mathbf{H}_b are $L \times K$ matrices given by

$$\mathbf{H}_a = \begin{bmatrix} \mathbf{A}_1 \mathbf{h} & \mathbf{A}_2 \mathbf{h} & \cdots & \mathbf{A}_K \mathbf{h} \end{bmatrix} \quad (2.8a)$$

$$\mathbf{H}_b = \begin{bmatrix} \mathbf{B}_1 \mathbf{h} & \mathbf{B}_2 \mathbf{h} & \cdots & \mathbf{B}_K \mathbf{h} \end{bmatrix} \quad (2.8b)$$

Taking the conjugate on both sides of Eq.(2.7) leads to

$$\mathbf{y}^* = \mathbf{H}_b^* \mathbf{s} + \mathbf{H}_a^* \mathbf{s}^* + \boldsymbol{\xi}^* \quad (2.9)$$

Let

$$\mathcal{H} = \begin{bmatrix} \mathbf{H}_a & \mathbf{H}_b \\ \mathbf{H}_b^* & \mathbf{H}_a^* \end{bmatrix} \quad (2.10)$$

\mathcal{H} is the $2L \times 2K$ matrix called the *virtual MISO channel*. Then Eqs.(2.7) and (2.9) can be expressed in a compact matrix form as

$$\begin{pmatrix} \mathbf{y} \\ \mathbf{y}^* \end{pmatrix} = \begin{bmatrix} \mathbf{H}_a & \mathbf{H}_b \\ \mathbf{H}_b^* & \mathbf{H}_a^* \end{bmatrix} \begin{pmatrix} \mathbf{s} \\ \mathbf{s}^* \end{pmatrix} + \begin{pmatrix} \boldsymbol{\xi} \\ \boldsymbol{\xi}^* \end{pmatrix}$$

or,

$$\tilde{\mathbf{y}} = \mathcal{H} \tilde{\mathbf{s}} + \tilde{\boldsymbol{\xi}} \quad (2.11)$$

Thus, the following property can be deduced:

Property 1. *The following three statements are equivalent:*

1. $\{\mathbf{A}_i, \mathbf{B}_i\}_{i=1}^K$ constitutes a complex orthogonal STBC
2. $\mathbf{X}^H(\mathbf{s})\mathbf{X}(\mathbf{s}) = \|\mathbf{s}\|^2 \mathbf{I}_{M_t}$ for any $K \times 1$ complex vector \mathbf{s}
3. $\mathcal{H}^H \mathcal{H} = \|\mathbf{h}\|^2 \mathbf{I}_{2K}$ for any $M_t \times 1$ complex channel vector \mathbf{h}

The proof of the above statement follows directly from Definition 1 and the expressions of $\mathbf{X}(\mathbf{s})$ and \mathcal{H} in Eqs. (2.2) and (2.10), respectively. From Property 1, one can see that orthogonal STBC allow for symbol-by-symbol detection at the receiver end,

which is desirable because of the simplicity in implementation. In the next section, the general optimal STBC design currently employed in practice will be discussed.

2.2 PEP Code Design Criterion

Before the current STBC design criteria can be introduced, throughout this thesis, the following statements are assumed:

Assumption 1. *The complex channel vector $\mathbf{h} = \mathbf{h}_{\text{re}} + j\mathbf{h}_{\text{im}}$, where \mathbf{h}_{re} and \mathbf{h}_{im} are the real and imaginary parts of the channel vector, respectively, and \mathbf{h}_{re} and \mathbf{h}_{im} are both independent identically distributed (IID) real Gaussian distributed random vectors, with zero-mean and covariance matrix $\frac{1}{2}\mathbf{I}_{M_t}$.*

Assumption 2. *The complex noise vector $\boldsymbol{\xi} = \boldsymbol{\xi}_{\text{re}} + j\boldsymbol{\xi}_{\text{im}}$, where $\boldsymbol{\xi}_{\text{re}}$ and $\boldsymbol{\xi}_{\text{im}}$ are the real and imaginary parts of the noise vector, respectively, and $\boldsymbol{\xi}_{\text{re}}$ and $\boldsymbol{\xi}_{\text{im}}$ are both IID real Gaussian noise vectors with zero mean and covariance matrix $\frac{1}{2}\mathbf{I}_L$.*

Assumption 3. *Complete channel state information is available at the receiver and ML detection is employed.*

Assumption 4. *The transmitted signal vector, \mathbf{s} , contains signals, $s_k, k = 1, 2, \dots, K$, independently and equally likely chosen from a square 2^{2q} -QAM constellation, where q is a positive integer.*

Under Assumptions 1-4, given a channel realization \mathbf{h} and a transmitted signal vector \mathbf{s} , the probability of transmitting \mathbf{s} and deciding in favor of $\mathbf{s}' \neq \mathbf{s}$ at the ML detector can be evaluated as

$$P(\mathbf{s} \rightarrow \mathbf{s}' | \mathbf{h}) = Q\left(\frac{d(\mathbf{s} \rightarrow \mathbf{s}')}{\sqrt{2}}\right) \quad \mathbf{s}' \neq \mathbf{s} \quad (2.12)$$

where $Q(z) = (1/\sqrt{2\pi}) \int_z^\infty e^{-x^2/2} dx$ and $d(\mathbf{s} \rightarrow \mathbf{s}')$ is the Euclidean distance between the received code words $\mathcal{H}\mathbf{s}$ and $\mathcal{H}\mathbf{s}'$; i.e.,

$$d^2(\mathbf{s} \rightarrow \mathbf{s}') = \frac{\rho}{M_t} \text{tr} [\mathbf{X}^H(\mathbf{s} - \mathbf{s}') \mathbf{h}^H \mathbf{h} \mathbf{X}(\mathbf{s} - \mathbf{s}')] \quad (2.13)$$

where $\mathbf{X}(\cdot)$ denotes the coding formula given by Eq.(2.2). To evaluate this probability, it is convenient to use the following expression for the Q -function [31],

$$Q(z) = \frac{1}{\pi} \int_0^{\pi/2} \exp\left(-\frac{z^2}{2 \sin^2 \phi}\right) d\phi \quad (2.14)$$

Also, utilizing the property of trace [32], we can rewrite Eq.(2.13) as

$$d^2(\mathbf{s} \rightarrow \mathbf{s}') = \frac{\rho}{M_t} \mathbf{h}^H [\mathbf{X}^T(\mathbf{e}) \mathbf{X}^*(\mathbf{e})] \mathbf{h} \quad (2.15)$$

where $\mathbf{e} = \mathbf{s} - \mathbf{s}'$. By substituting Eqs.(2.14) and (2.15) into Eq.(2.12) and then taking the average over the random vector \mathbf{h} , whose statistics are given in Assumption 1 above, the average PEP at the ML detector can be written as [33]

$$P(\mathbf{s} \rightarrow \mathbf{s}') = \frac{1}{\pi} \int_0^{\pi/2} \frac{d\phi}{\det\left(\mathbf{I}_{M_t} + \frac{\rho}{4M_t \sin^2 \phi} \mathbf{X}^H(\mathbf{e}) \mathbf{X}(\mathbf{e})\right)} \quad (2.16)$$

Eq.(2.16) expresses the exact PEP, and since $|\sin \phi| \leq 1$, we can replace $\sin \phi$ with unity in the above integral and obtain the upper bound of the PEP, such that

$$P(\mathbf{s} \rightarrow \mathbf{s}') \leq \frac{1}{2} \det\left(\mathbf{I}_{M_t} + \frac{\rho}{4M_t} \mathbf{X}^H(\mathbf{e}) \mathbf{X}(\mathbf{e})\right)^{-1} \quad (2.17)$$

Eq.(2.17) is called the Chernoff bound of the PEP. Thus, the average PEP over

possible channels, $P(\mathbf{s} \rightarrow \mathbf{s}')$, of transmitting \mathbf{s} and deciding in favor of $\mathbf{s}' \neq \mathbf{s}$ at the decoder can be bounded by

$$P(\mathbf{s} \rightarrow \mathbf{s}') \leq \frac{1}{2} \left(\frac{\rho}{4M_t} \right)^{-r(\mathbf{e})} \left(\prod_{i=1}^{r(\mathbf{e})} \lambda_i \right)^{-1} \quad (2.18)$$

where $r(\mathbf{e})$ denotes the rank of the matrix $\mathbf{X}^H(\mathbf{e})\mathbf{X}(\mathbf{e})$, and λ_i for $i = 1, 2, \dots, r(\mathbf{e})$ are the non-zero eigenvalues of the matrix $\mathbf{X}^H(\mathbf{e})\mathbf{X}(\mathbf{e})$. Eq.(2.18) is often used as a criterion for designing STBC to keep the Chernoff Bound low. This necessitates the examination of the following two terms of Eq.(2.18) [5]:

1. **The Rank:** At high SNR, $\left(\frac{\rho}{4M_t} \right)^{-r(\mathbf{e})}$ in Eq.(2.18) dominates and therefore to keep the Chernoff bound as low as possible, we should make the exponent, $r(\mathbf{e})$, i.e., the rank of the matrix $\mathbf{X}^H(\mathbf{e})\mathbf{X}(\mathbf{e})$, as large as possible. The minimum rank of $\mathbf{X}(\mathbf{e}) = \mathbf{X}(\mathbf{s}) - \mathbf{X}(\mathbf{s}')$ taken over all distinct pairs $\{\mathbf{s}, \mathbf{s}'\}$ is the *diversity gain*, r , and should be maximized, i.e., the matrix $\mathbf{X}^H(\mathbf{e})\mathbf{X}(\mathbf{e})$ should be of full rank. Thus, maximum diversity or *full diversity* occurs when $r = M_t$ if the number of channels used, $L \geq M_t$.
2. **The Determinant:** The second term consists of the product of the non-zero eigenvalues of the matrix $\mathbf{X}^H(\mathbf{e})\mathbf{X}(\mathbf{e})$. The r th root of the minimum value of the second term, taken over all distinct symbol vector pairs $\{\mathbf{s}, \mathbf{s}'\}$, is called the *coding gain* and must be maximized, i.e., $\min_{\mathbf{e}} \left(\prod_{i=1}^r \lambda_i \right)^{1/r}$ must be maximized.

One can verify that orthogonal STBC are optimal in terms of the above two criteria.

Chapter 3

The Quasi-Orthogonal STBC

Even though true orthogonal codes satisfy the optimum conditions of maximum rank and maximum determinant in the PEP design criterion, they cannot achieve full data rate when there are more than two transmitter antennas. To improve on the low rate, quasi-orthogonal STBC [20, 21, 22] have been proposed. However, these are not optimal in terms of diversity and coding gains. Su and Xia proposed the rotated quasi-orthogonal STBC structure [1] which achieved optimality maximizing the rank and determinant of PEP design criterion. Here in this chapter, attention is focused on the application of the rotated quasi-orthogonal STBC to MISO transmission. In particular, the employment of the Su-Xia optimal rotated quasi-orthogonal STBC structure [1] will be studied.

Furthermore, the PEP criterion in Eq.(2.18) only considers a pair of signals in the constellation and does not give the average error probability over all pairs. Therefore, in this chapter, we re-examine the design criterion by averaging over all possible symbols. This results in a new STBC design criterion which, in addition to the current

STBC design factors, includes a new feature of the *average number of nearest neighbours*. We show that the Su-Xia “optimal” rotated quasi-orthogonal STBC structure is no longer optimal by this more general criterion. An optimal rotation angle is then obtained to satisfy this new criterion, which is verified to have superior performance over the Su-Xia STBC, especially when the transmission signal constellation is large.

3.1 The Rotated Quasi-Orthogonal STBC and Novel Design Criterion

Quasi-orthogonal codes of full rate have been proposed to overcome the shortcoming of orthogonal codes, which cannot achieve full transmission rate. As an example, for a four transmitter antennas system transmitting signals from a square 2^{2q} -QAM constellation, where q is a positive integer, the special quasi-orthogonal STBC structure proposed by Tirkkonen-Boariu-Hottinen [21] has a coding matrix of the form:

$$\mathbf{X}(\mathbf{s}) = \begin{bmatrix} s_1 & s_2 & s_3 & s_4 \\ -s_2^* & s_1^* & -s_4^* & s_3^* \\ s_3 & s_4 & s_1 & s_2 \\ -s_4^* & s_3^* & -s_2^* & s_1^* \end{bmatrix}$$

The symbol transmission rate of this code is one per channel use, and thus is full-rate. We note that the code is not entirely orthogonal (e.g., $\langle \mathbf{x}_1, \mathbf{x}_2 \rangle = \langle \mathbf{x}_1, \mathbf{x}_4 \rangle = 0$, but $\langle \mathbf{x}_1, \mathbf{x}_3 \rangle \neq 0$ with \mathbf{x}_i being the i th column of $\mathbf{X}(\mathbf{s})$), thus, giving rise to the name “quasi-orthogonal”. Since signal constellations in the quasi-orthogonal STBC schemes are chosen arbitrarily, their codes may not necessarily provide full diversity.

For a MISO system with M_t transmitter antennas, transmitting $K = 2p$ symbols selected from a square 2^{2q} -QAM constellation in L time-slots, Su and Xia [1] proposed the rotated quasi-orthogonal STBC designs from the generalized orthogonal STBC with the following codeword structure:

$$\mathbf{X}(\mathbf{s}) = \sqrt{\frac{3L}{4p(2^{2q} - 1)}} \begin{bmatrix} \mathcal{O}(\mathbf{s}_1) & \mathcal{O}(e^{j\theta}\mathbf{s}_2) \\ \mathcal{O}(e^{j\theta}\mathbf{s}_2) & \mathcal{O}(\mathbf{s}_1) \end{bmatrix} \quad (3.1)$$

where $\mathbf{s}_1 = (s_1 \ s_2 \ \cdots \ s_p)^T$, $\mathbf{s}_2 = (s_{p+1} \ s_{p+2} \ \cdots \ s_{2p})^T$, $\mathbf{s} = (\mathbf{s}_1^T \ \mathbf{s}_2^T)^T = (s_1 \ s_2 \ \cdots \ s_{2p})^T$, and $\mathcal{O}(\mathbf{s}_i)$ for $i = 1, 2$ are any two $L/2 \times M_t/2$ generalized orthogonal codes with $L \geq M_t$. For orthogonal codes, the rules governing the restrictions on the length, p , of the transmitted signal vectors, \mathbf{s}_1 and \mathbf{s}_2 , given a specific number of time slots, L , can be found in detail in [18]. For example, complex square orthogonal designs for $M_t = 4, 8, 16$ transmitter antennas, yields a maximum transmitted symbol rate of $\frac{p}{L} = \frac{3}{4}, \frac{1}{2}, \frac{5}{16}$, respectively. In this thesis, Eq.(3.1) is presented in a slightly different way from the original Su-Xia code, such that each $\mathcal{O}(\mathbf{s}_i)$ is no longer required to be a square matrix as in the original Su-Xia code, but is allowed to be a “tall” rectangular matrix. Su and Xia [1] also found that the optimal rotation angle for the code to enable both full diversity and the maximum coding gain, with reference to the criterion in Eq.(2.18), for the square QAM constellation, is $\theta = \pi/4$.

While the Su-Xia code satisfies the optimality of Eq.(2.18), the criterion only considers the probability of error between individual pairs of signal vectors \mathbf{s} and \mathbf{s}' for the ML detector. Therefore, the average error for the transmission for all the possible signal vectors is not taken into account. To overcome this shortcoming, we can average both sides of Eq.(2.18) by multiplying with the probability, $P(\mathbf{s})$, of each

s and then sum up the product resulting in the following “snug” bound on the average block error probability, P_{ble} [34]:

$$P_{ble} \leq \sum_{\mathbf{s} \neq \mathbf{s}'} P(\mathbf{s}) P(\mathbf{s} \rightarrow \mathbf{s}') \leq \frac{1}{2} \left(\frac{\rho}{4M_t} \right)^{-r} \sum_{\mathbf{s} \neq \mathbf{s}'} P(\mathbf{s}) \left(\prod_{i=1}^r \lambda_i \right)^{-1} \quad (3.2)$$

where r denotes the minimum rank among all the possible matrices $\mathbf{X}^H(\mathbf{e})\mathbf{X}(\mathbf{e})$, $\mathbf{e} = \mathbf{s} - \mathbf{s}'$. With each choice of \mathbf{s} and \mathbf{s}' ($\mathbf{s}' \neq \mathbf{s}$), we obtain a value of $\prod_{i=1}^r \lambda_i$. Running through all the possible choices of \mathbf{s} and \mathbf{s}' in the signal constellation, we obtain a number of different products, $\prod_{i=1}^r \lambda_i$, some of which may be equal in value. Let us denote each of the different values of the products $\prod_{i=1}^r \lambda_i$ by d_n , for $n = 1, 2, \dots, N$, and align them in increasing order so that $d_1 < d_2 < \dots < d_N$. Thus, let the average number of cases in which d_n occurs be denoted by K_n . Then, Eq.(3.2) can be written as

$$P_{ble} \leq \frac{1}{2} \left(\frac{\rho}{4M_t} \right)^{-r} \left[\sum_{n=1}^N \frac{K_n}{d_n} \right] \quad (3.3)$$

where $K_n = \sum_{\mathbf{s}} P(\mathbf{s}) \sum_{\mathbf{s}' \neq \mathbf{s}, \prod_{i=1}^r \lambda_i = d_n} 1$. In particular, since d_1 denotes the lowest value of the product $\prod_{i=1}^r \lambda_i$, K_1 is called the *average number of nearest neighbours* or more descriptively, the *average kissing number* [35].

From the average union bound in Eq.(3.3) one can observe that the rank, r , controls how fast the error performance decays with respect to the average SNR per symbol, ρ , and thus, must first be maximized [5]. Then, we note that among all the terms of d_n , the one that dominates the sum in the brackets is d_1 , which is the coding gain, and is the second most significant factor to affect the error performance. Hence, it should be maximized. These are the two current factors in the criterion

used for optimal STBC design as discussed in Chapter 2. Since d_1 is the dominating factor among all d_n for the error bound, the average number of nearest neighbours, K_1 in Eq.(3.3), must also be another significant performance index. Therefore, in the following, the average number of nearest neighbours is proposed as a novel third factor associated with the criterion to design rotated quasi-orthogonal STBC. We have the following statement:

Assertion 1. *For the optimal design of transmission codes for a MISO system equipped with a ML receiver, the following three factors have to be optimized:*

1. *The minimum possible value of **the rank** of the matrix $\mathbf{X}^H(\mathbf{e})\mathbf{X}(\mathbf{e})$, r , has to be maximized;*
2. *The minimum possible value of **the determinant** of the matrix $\mathbf{X}^H(\mathbf{e})\mathbf{X}(\mathbf{e})$, d_1 , has to be maximized;*
3. ***The average number of nearest neighbours** in the design code, K_1 , must be minimized.*

In the following section we will prove that the Su-Xia code, which uses a rotation angle of $\theta = \pi/4$, is not optimal in terms of the above assertion.

3.2 Code Properties and Performance Analysis of the Su-Xia Rotation Angle

We now examine the Su-Xia code and discuss the optimality, in terms of Assertion 1, of setting $\theta = \pi/4$ in the rotated quasi-orthogonal STBC. The Su-Xia code has

been shown to be optimal in the sense of design factors 1 and 2. In other words, the code enables full diversity and the maximum coding gain [1]. However, we will show here that it is not optimal according to factor 3. In fact, we will show that its average number of nearest neighbors per symbol tends to infinity if the size of the QAM constellation is large. To achieve this, we need the following lemma on a specific Pell Diophantine equation [23].

Lemma 1. *The solutions to the Pell equation $\alpha^2 - \gamma\beta^2 = 1$, specifically for $\gamma = 2$, are given by*

$$\alpha_k = \pm \frac{(3 + 2\sqrt{2})^k + (3 - 2\sqrt{2})^k}{2} \quad (3.4a)$$

$$\beta_k = \pm \frac{(3 + 2\sqrt{2})^k - (3 - 2\sqrt{2})^k}{2\sqrt{2}} \quad (3.4b)$$

where $k \in \mathbb{Z}$.

Theorem 1. *For the rotated quasi-orthogonal STBC in Eq.(3.1) with $\theta = \pi/4$, the number of nearest neighbors per symbol for a 2^{2q} -QAM constellation, with q being a positive integer, tends to infinity if q tends to infinity.*

Proof. First, we notice that the codeword matrix, $\mathbf{X}(\mathbf{s})$, from a rotated quasi-orthogonal STBC in Eq.(3.1) can be decomposed into a block-diagonal, orthogonal, “multi-group decodable” STBC [26, 36] in the following way:

$$\frac{1}{2} \begin{bmatrix} \mathbf{I}_{\frac{L}{2}} & \mathbf{I}_{\frac{L}{2}} \\ \mathbf{I}_{\frac{L}{2}} & -\mathbf{I}_{\frac{L}{2}} \end{bmatrix}^H \mathbf{X}(\mathbf{s}) \begin{bmatrix} \mathbf{I}_{\frac{M_t}{2}} & \mathbf{I}_{\frac{M_t}{2}} \\ \mathbf{I}_{\frac{M_t}{2}} & -\mathbf{I}_{\frac{M_t}{2}} \end{bmatrix} = \sqrt{\frac{3L}{4p(2^{2q} - 1)}} \begin{bmatrix} \mathcal{O}(\mathbf{s}_1 + e^{j\theta}\mathbf{s}_2) & \mathbf{0} \\ \mathbf{0} & \mathcal{O}(\mathbf{s}_1 - e^{j\theta}\mathbf{s}_2) \end{bmatrix} \quad (3.5)$$

Substituting \mathbf{e} for \mathbf{s} in \mathbf{X} , we can note that

$$\begin{aligned} & \left| \frac{1}{4} \left(\begin{bmatrix} \mathbf{I}_{\frac{L}{2}} & \mathbf{I}_{\frac{L}{2}} \\ \mathbf{I}_{\frac{L}{2}} & -\mathbf{I}_{\frac{L}{2}} \end{bmatrix}^H \mathbf{X}(\mathbf{e}) \begin{bmatrix} \mathbf{I}_{\frac{M_t}{2}} & \mathbf{I}_{\frac{M_t}{2}} \\ \mathbf{I}_{\frac{M_t}{2}} & -\mathbf{I}_{\frac{M_t}{2}} \end{bmatrix} \right)^H \left(\begin{bmatrix} \mathbf{I}_{\frac{L}{2}} & \mathbf{I}_{\frac{L}{2}} \\ \mathbf{I}_{\frac{L}{2}} & -\mathbf{I}_{\frac{L}{2}} \end{bmatrix}^H \mathbf{X}(\mathbf{e}) \begin{bmatrix} \mathbf{I}_{\frac{M_t}{2}} & \mathbf{I}_{\frac{M_t}{2}} \\ \mathbf{I}_{\frac{M_t}{2}} & -\mathbf{I}_{\frac{M_t}{2}} \end{bmatrix} \right) \right| \\ &= \frac{\det(\mathbf{X}^H(\mathbf{e})\mathbf{X}(\mathbf{e}))}{2^{M_t}} \left| \begin{bmatrix} \mathbf{I}_{\frac{M_t}{2}} & \mathbf{I}_{\frac{M_t}{2}} \\ \mathbf{I}_{\frac{M_t}{2}} & -\mathbf{I}_{\frac{M_t}{2}} \end{bmatrix}^H \right| \left| \begin{bmatrix} \mathbf{I}_{\frac{M_t}{2}} & \mathbf{I}_{\frac{M_t}{2}} \\ \mathbf{I}_{\frac{M_t}{2}} & -\mathbf{I}_{\frac{M_t}{2}} \end{bmatrix} \right| = \det(\mathbf{X}^H(\mathbf{e})\mathbf{X}(\mathbf{e})) \end{aligned} \quad (3.6)$$

where \mathbf{e} denotes the error vector between the transmitted signal vector \mathbf{s} and the erroneous signal vector \mathbf{s}' , i.e., $\mathbf{e} = \mathbf{s} - \mathbf{s}'$, $\mathbf{s} \neq \mathbf{s}'$, and

$$\left| \begin{bmatrix} \mathbf{I}_{\frac{M_t}{2}} & \mathbf{I}_{\frac{M_t}{2}} \\ \mathbf{I}_{\frac{M_t}{2}} & -\mathbf{I}_{\frac{M_t}{2}} \end{bmatrix}^H \right| = \left| \begin{bmatrix} \mathbf{I}_{\frac{M_t}{2}} & \mathbf{I}_{\frac{M_t}{2}} \\ \mathbf{I}_{\frac{M_t}{2}} & -\mathbf{I}_{\frac{M_t}{2}} \end{bmatrix} \right| = \det(2\mathbf{I}_{\frac{M_t}{2}}) = 2^{M_t/2}$$

From Property 1, we have $\mathcal{O}^H(\mathbf{e})\mathcal{O}(\mathbf{e}) = \|\mathbf{e}\|^2 \mathbf{I}_{\frac{M_t}{2}} \Rightarrow \det(\mathcal{O}^H(\mathbf{e})\mathcal{O}(\mathbf{e})) = (\|\mathbf{e}\|^2)^{M_t/2}$, and using this together with Eq.(3.5) in Eq.(3.6), we have

$$\begin{aligned} \det(\mathbf{X}^H(\mathbf{e})\mathbf{X}(\mathbf{e})) &= \left(\frac{3L}{4p(2^{2q}-1)} \right)^{M_t} \times \\ & \left(\sum_{m=1}^p |e_m + e^{j\theta} e_{m+p}|^2 \right)^{M_t/2} \left(\sum_{n=1}^p |e_n - e^{j\theta} e_{n+p}|^2 \right)^{M_t/2} \end{aligned} \quad (3.7)$$

Since $\mathbf{s} \neq \mathbf{s}'$, there must be at least one non-zero entry in the vector \mathbf{e} . Let e_k and e_{k+p} be such a pair of entries, at least one being non-zero, in \mathbf{e} with $1 \leq k \leq p$. Then,

we have

$$\det(\mathbf{X}^H(\mathbf{e})\mathbf{X}(\mathbf{e})) \geq \left(\frac{3L}{4p(2^{2q}-1)}\right)^{M_t} \times |(e_k + e^{j\theta}e_{k+p})(e_k - e^{j\theta}e_{k+p})|^{M_t} \quad (3.8)$$

where equality holds if and only if minimum error occurs, i.e., if and only if $e_m = e_{m+p} = 0$ for $m = 1, 2, \dots, p$ and $m \neq k$. In addition, we note that

$$|(e_k + e^{j\theta}e_{k+p})(e_k - e^{j\theta}e_{k+p})| = |(e_k + e^{j\theta}e_{k+p})(e_k^* - e^{-j\theta}e_{k+p}^*)| \quad (3.9)$$

We also notice, from Eq.(3.9), that

$$(e_k + e^{j\theta}e_{k+p})(e_k^* - e^{-j\theta}e_{k+p}^*) = E_{\text{re}} + E_{\text{im}} \quad (3.10)$$

where $E_{\text{re}} = |e_k|^2 - |e_{k+p}|^2$ and $E_{\text{im}} = e_k^*e_{k+p}e^{j\theta} - e_k e_{k+p}^*e^{-j\theta}$. Since each e_k and e_{k+p} , $1 \leq k \leq p$, is the difference between two square QAM constellation points, we can observe that E_{re} is a real integer and E_{im} is a purely imaginary number. Also, it can be observed that the difference between two square QAM constellation points is always an even complex integer. Thus, for discussion convenience, we let $e_k = 2\bar{e}_k$ and $e_{k+p} = 2\bar{e}_{k+p}$, with \bar{e}_k and \bar{e}_{k+p} being two complex integers. Hence, $E_{\text{re}} = 4(|\bar{e}_k|^2 - |\bar{e}_{k+p}|^2)$ and $E_{\text{im}} = 4(\bar{e}_k^*\bar{e}_{k+p}e^{j\theta} - \bar{e}_k\bar{e}_{k+p}^*e^{-j\theta})$.

Combining Eqs.(3.8) and (3.10), and substituting in the value of $\theta = \pi/4$ for the Su-Xia code, $E_{\text{im}} = 2\sqrt{2}(\bar{e}_k^*\bar{e}_{k+p}(1+j) - \bar{e}_k\bar{e}_{k+p}^*(1-j))$. Since $1+j$, $1-j$, \bar{e}_k and \bar{e}_{k+p} are all complex integers, let $\bar{e}_k^*\bar{e}_{k+p} = u + jv$, $u, v \in \mathbb{Z}$. Then, $E_{\text{im}} = 4\sqrt{2}j(u+v)$. Therefore, the minimum non-zero value for $|E_{\text{re}}| = 4$ and the minimum non-zero value for $|E_{\text{im}}| = 4\sqrt{2}$, when $u = 0$ or $v = 0$. Then, the minimum possible value for

$\det(\mathbf{X}^H(\mathbf{e})\mathbf{X}(\mathbf{e}))$ occurs when $|E_{\text{re}}| = 4$ and $|E_{\text{im}}| = 0$, and thus, the optimal coding gain is achieved if and only if the error symbols satisfy the following two Diophantine equations:

$$|\bar{e}_k|^2 - |\bar{e}_{k+p}|^2 = \pm 1 \quad (3.11a)$$

$$\bar{e}_k^* \bar{e}_{k+p} (1+j) - \bar{e}_k \bar{e}_{k+p}^* (1-j) = 0 \quad (3.11b)$$

It is clear that if one of \bar{e}_k and \bar{e}_{k+p} is zero, then, the other must be ± 1 or $\pm j$. Thus, we only need to consider the case when both \bar{e}_k and \bar{e}_{k+p} are not zero. In this case, from Eq.(3.11b), we obtain

$$\bar{e}_k \bar{e}_{k+p}^* = j \bar{e}_k^* \bar{e}_{k+p} \quad (3.12)$$

Since Eq.(3.11a) has to be satisfied as well, then the only solutions will be either $\bar{e}_k = j\eta \bar{e}_k^*$ and $\bar{e}_{k+p} = \eta \bar{e}_{k+p}^*$, or $\bar{e}_k = \eta \bar{e}_k^*$ and $\bar{e}_{k+p} = j\eta \bar{e}_{k+p}^*$, where η is the unit, i.e., $\eta = \pm 1, \pm j$.

For the first solution, let $\bar{e}_k = (\bar{e}_k)_{\text{re}} + j(\bar{e}_k)_{\text{im}}$ and let $\bar{e}_{k+p} = (\bar{e}_{k+p})_{\text{re}} + j(\bar{e}_{k+p})_{\text{im}}$, then

$$\bar{e}_k \bar{e}_k^* = (\bar{e}_k)_{\text{re}}^2 (1 + |\eta|^2) = 2(\bar{e}_k)_{\text{re}}^2 \quad (3.13a)$$

$$\bar{e}_{k+p} \bar{e}_{k+p}^* = \begin{cases} |\eta|^2 (\bar{e}_{k+p})_{\text{re}}^2 = (\bar{e}_{k+p})_{\text{re}}^2 \\ \text{or} \\ |\eta|^2 (\bar{e}_{k+p})_{\text{im}}^2 = (\bar{e}_{k+p})_{\text{im}}^2 \end{cases} \quad (3.13b)$$

Substituting these two conditions into Eq.(3.11a) leads us to the consideration of the Pell Diophantine equation $\alpha^2 - 2\beta^2 = \pm 1$. The second solution also leads to the same consideration of the Pell Diophantine equation. Now, Lemma 1 tells us that there

is an infinite number of solutions to the equation in the integer ring. This implies that the average number of nearest neighbours per symbol tends to infinity when the QAM constellation size is infinite. This completes the proof of Theorem 1. \square

3.3 Code Properties and Performance Analysis of the Novel Quasi-Optimal Angle

Since the Su-Xia code does not fully satisfy the optimality factors in Assertion 1, it is desirable to seek for angles other than $\theta = \pi/4$ for the rotated quasi-orthogonal code to be fully optimal. In this section, we show that by using a novel rotation angle of $\theta = \pi/6$ for the rotated quasi-orthogonal STBC of Eq.(3.1), the code not only provides full diversity gain and optimal coding gain, but also has a fixed small number of nearest neighbours per symbol. This result is given in the following theorem:

Theorem 2. *For $\theta = \pi/6$ in Eq.(3.1), the resulting rotated quasi-orthogonal STBC for a 2^{2q} -QAM constellation, with q being a positive integer, have the following properties:*

1. *The code provides full diversity for the ML receiver.*
2. *The maximum coding gain $G_{opt} = \frac{3L}{p(2^{2q}-1)}$ is achieved.*
3. *The average number of nearest neighbours per symbol tends to 8 when q tends to infinity.*

In order to prove this theorem, we need to first establish the following two lemmas:

Lemma 2. For $a, b \in \mathbb{Z}$, let

$$\Delta(a, b) = 2\sqrt{3}ab + (a^2 - b^2) \quad (3.14)$$

Then, $|\Delta(a, b)| > 1$ for any non-zero integers a and b .

Lemma 3. For $a, b \in \mathbb{Z}$, let

$$\mathcal{E}(a, b) = 2ab + \sqrt{3}(a^2 - b^2) \quad (3.15)$$

Then, $|\mathcal{E}(a, b)| > 1$ for any non-zero integers a and b .

The proofs of Lemmas 2 and 3 are provided in Appendix A. We are now in a position to prove Theorem 2.

Proof. The proof of Theorem 2 follows a similar argument from Eq.(3.5) to Eq.(3.10) of the proof of Theorem 1. Thus, consider Eq.(3.10) with $\theta = \pi/6$, we have

$$(e_k + e^{j\pi/6} e_{k+p})(e_k^* - e^{-j\pi/6} e_{k+p}^*) = E_{\text{re}} + E_{\text{im}} \quad (3.16)$$

where $E_{\text{re}} = |e_k|^2 - |e_{k+p}|^2$ and $E_{\text{im}} = e_k^* e_{k+p} e^{j\pi/6} - e_k e_{k+p}^* e^{-j\pi/6}$. Now the proofs for statements 1, 2 and 3 are as follows:

For Statement 1: If $E_{\text{im}} = 0$, then, we have $\bar{e}_k \bar{e}_{k+p}^* = \bar{e}_k^* \bar{e}_{k+p} e^{j2\pi/6}$. Since $e^{j2\pi/6} = \frac{1}{2} + \frac{\sqrt{3}}{2}j$ is an irrational number, we conclude that either $e_k = 0$ or $e_{k+p} = 0$. Since one of e_k and e_{k+p} is not zero, $E_{\text{re}} \neq 0$. Now, combining this with Eqs.(3.8), (3.9) and (3.16) results in $\det(\mathbf{X}^H(\mathbf{e})\mathbf{X}(\mathbf{e})) > 0$. It is clear that the result $\det(\mathbf{X}^H(\mathbf{e})\mathbf{X}(\mathbf{e})) > 0$ is also true when $E_{\text{im}} \neq 0$. Hence, our code with $\theta = \pi/6$ yields

full rank for the matrix $\mathbf{X}^H(\mathbf{e})\mathbf{X}(\mathbf{e})$, i.e., it enables full diversity for the ML receiver. This completes the proof of statement 1.

For Statements 2 and 3 we consider the following two cases:

Case 1. $E_{\text{re}} \neq 0$:

Combining this condition with Eqs.(3.8) and (3.16), we arrive at the fact that the optimal coding gain is achieved if and only if the error symbols satisfy the following two Diophantine equations:

$$|\bar{e}_k|^2 - |\bar{e}_{k+p}|^2 = \pm 1 \quad (3.17a)$$

$$\bar{e}_k^* \bar{e}_{k+p} e^{j\pi/6} - \bar{e}_k \bar{e}_{k+p}^* e^{-j\pi/6} = 0 \quad (3.17b)$$

From Eq.(3.17b), we have $\bar{e}_k \bar{e}_{k+p}^* = \bar{e}_k^* \bar{e}_{k+p} e^{j2\pi/6}$. Since $e^{j2\pi/6}$ is an irrational number then either \bar{e}_k or \bar{e}_{k+p} must be zero. Since \bar{e}_k and \bar{e}_{k+p} cannot be both zero, then to satisfy Eq.(3.17a), we must have either $\bar{e}_k = 0$ and $\bar{e}_{k+p} = \pm 1, \pm j$, or $\bar{e}_{k+p} = 0$ and $\bar{e}_k = \pm 1, \pm j$.

Case 2. $E_{\text{re}} = 0$:

This means $|\bar{e}_k|^2 - |\bar{e}_{k+p}|^2 = 0 \Rightarrow \bar{e}_k \bar{e}_k^* = \bar{e}_{k+p} \bar{e}_{k+p}^*$. Thus, both \bar{e}_k and \bar{e}_{k+p} are not zero because of the fact that one of them is not zero. Let the greatest common divisor of \bar{e}_k and \bar{e}_{k+p} be g . Then, $\bar{e}_k = gg_k$, $\bar{e}_{k+p} = gg_{k+p}$, and thus, $g_k g_k^* = g_{k+p}^* g_{k+p}$, where g, g_k and g_{k+p} are complex integers, and g_k and g_{k+p} are co-prime. Since the Gaussian integer ring is the unique factorization ring, i.e., g_k and g_{k+p} have no other common factor other than the unit, we have $g_k = \eta g_{k+p}^*$, where η is the unit, i.e., $\eta = \pm 1, \pm j$. If $\eta = \pm j$, then, $E_{\text{im}} = 4|g|^2 (g_k^* g_{k+p} e^{j\pi/6} - g_k g_{k+p}^* e^{-j\pi/6}) = 4\eta |g|^2 ((g_k^*)^2 e^{j\pi/6} + g_k^2 e^{-j\pi/6})$. If we let $g_k = a + jb$, with a and b being real integers, then $E_{\text{im}} = 8\eta |g|^2 ((a^2 - b^2) \cos(\pi/6) + 2ab \sin(\pi/6)) = 4\eta |g|^2 \mathcal{E}(a, b)$. By Lemma 3, we

obtain $|E_{\text{im}}| > 4$, since one of a and b is not zero.

Similarly, if $\eta = \pm 1$, then, $E_{\text{im}} = 4\eta|g|^2((g_k^*)^2 e^{j\pi/6} - g_k^2 e^{-j\pi/6}) = 4j\eta|g|^2(-4ab \cos(\pi/6) + 2(a^2 - b^2) \sin(\pi/6)) = 4j\eta|g|^2 \Delta(a, -b)$. Now, using Lemma 2, we know that $|E_{\text{im}}| > 4j|g|^2 \geq 4$ for $a \neq 0$ and $b \neq 0$. It is clear that if either $a = 0, b \neq 0$ or $b = 0, a \neq 0$, then, $|E_{\text{im}}| \geq 4\eta|g|^2 \geq 4$, where equalities hold if and only if either $|g| = 1$ and $a = \pm 1, b = 0$ or $|g| = 1$ and $a = 0, b = \pm 1$.

Therefore, in this case, substituting either $\bar{e}_k = \pm 1$ and $\bar{e}_{k+p} = \pm 1$, or $\bar{e}_k = \pm j$ and $\bar{e}_{k+p} = \pm j$, into Eq.(3.7), the optimal coding gain, $G_{\text{opt}} = \frac{3L}{p(2^{2q}-1)}$, is achieved. Therefore, when constellation size is large, we have 8 nearest neighbor points per symbol to achieve the optimal coding. This completes the proof of Statements 2 and 3, and thus, Theorem 2. \square

3.4 Simulations

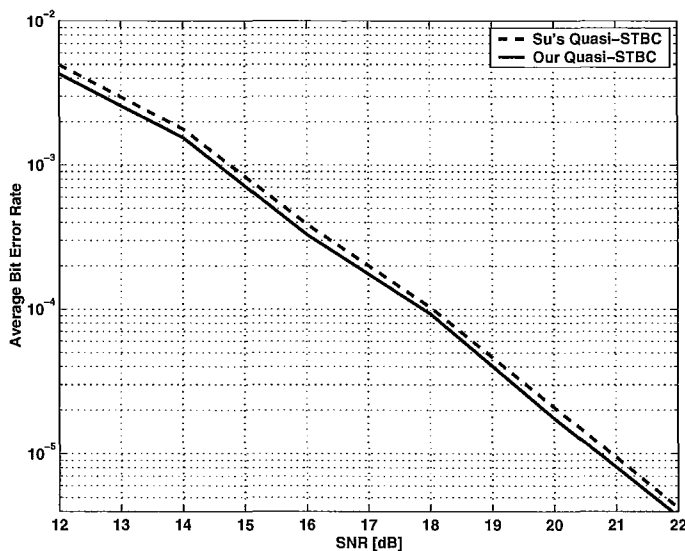


Figure 3.1: Performance Comparison of the Su-Xia [1] Rotated Quasi-Orthogonal STBC and Our Rotated Quasi-Orthogonal STBC for 16-QAM

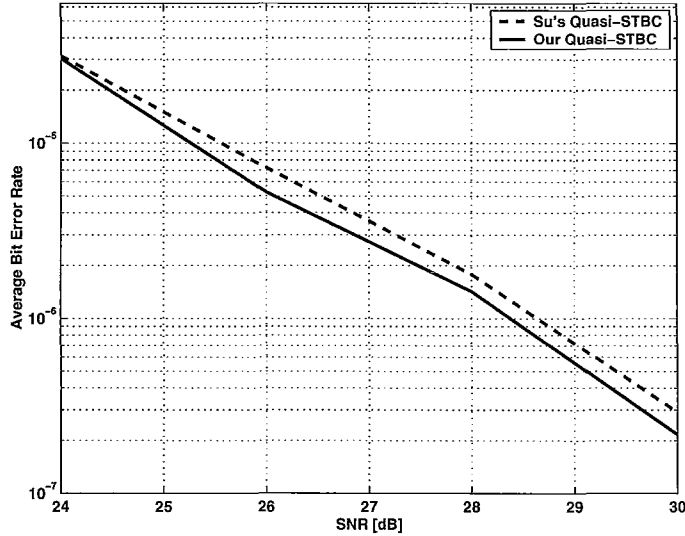


Figure 3.2: Performance Comparison of the Su-Xia [1] Rotated Quasi-Orthogonal STBC and Our Rotated Quasi-Orthogonal STBC for 64-QAM

In this section, we consider a MISO system with 4 transmitter antennas and a single receiver antenna. We examine the performance of the following rotated quasi-orthogonal STBC,

$$\mathbf{X}(\mathbf{s}) = \sqrt{\frac{3}{2(2^{2q} - 1)}} \begin{bmatrix} s_1 & s_2 & e^{j\theta} s_3 & e^{j\theta} s_4 \\ -s_2^* & s_1^* & -e^{-j\theta} s_4^* & e^{-j\theta} s_3^* \\ e^{j\theta} s_3 & e^{j\theta} s_4 & s_1 & s_2 \\ -e^{-j\theta} s_4^* & e^{-j\theta} s_3^* & -s_2^* & s_1^* \end{bmatrix} \quad (3.18)$$

where the symbols $\{s_i\}$, $i = 1, \dots, 4$, to be transmitted are selected from the square 2^{2q} -QAM constellation, where q is a positive integer. Comparing Eqs.(3.18) and (3.1), we see that $p = 2$, and the two symbol vectors to be transmitted are $\mathbf{s}_1 = [s_1 \ s_2]$ and

$\mathbf{s}_2 = [s_3 \ s_4]$. We also note that

$$\mathcal{O}(\mathbf{s}_1) = \begin{bmatrix} s_1 & s_2 \\ -s_2^* & s_1^* \end{bmatrix} \quad \text{and} \quad \mathcal{O}(e^{j\theta} \mathbf{s}_2) = \begin{bmatrix} e^{j\theta} s_3 & e^{j\theta} s_4 \\ -e^{-j\theta} s_4^* & e^{-j\theta} s_3^* \end{bmatrix}$$

The code is quasi-orthogonal because the columns of the code matrix in Eq.(3.18) are not all orthogonal. For $\theta = \pi/4$, the code matrix yields the Su-Xia code [1]. We compare the performance of the Su-Xia code to the performance of the code with $\theta = \pi/6$, proposed in this chapter. White Gaussian noise is added during transmission. In both cases, the ML detector is used to decode the received signal, and thus, in both cases, we have the same complexity of decoding. Four symbols form the 2^{2q} -QAM constellation selected for transmission and are detected at the receiver each time. This is repeated 10,000,000 times for each SNR, and the error-rate is computed.

Figs. 3.1 and 3.2 show computer simulation results for both codes when the transmitted symbols are respectively selected from the 16-QAM and the 64-QAM constellations. It can be seen from Fig. 3.1 that the quasi-orthogonal STBC in Eq.(3.18) with $\theta = \pi/6$ obtains the gain of 0.15 dB over the Su-Xia code at the bit error rate of 10^{-5} , when the 16-QAM signaling points are transmitted. When the QAM constellation size is increased to 64, we observe from Fig. 3.2 that the gain is increased to about 0.3 dB, at the bit error rate of 10^{-6} . Such observations confirm that, as the size of the square QAM constellation increases, the performance using the quasi-orthogonal STBC with $\theta = \pi/6$ becomes increasingly superior to that of the Su-Xia code, and thus the theoretic analysis in this chapter is clearly verified.

Chapter 4

The 4×1 MISO Channel and Simple ML Detection

In Chapters 2 and 3 the conventional STBC design criterion and a new design factor were introduced for optimization. These optimizations are based on minimizing the worst case average of the PEP of the ML detector. This is because the geometrical structure of the decision regions, for a general MIMO channel equipped with the ML detector, is so irregular that it would be impossible to obtain an explicit exact error probability formula for the ML receiver [5]. This means that the error probability formula cannot be utilized as a criterion for the design of the optimal transmitter for the MIMO systems, and the current STBC designs may not be truly optimum in terms of the exact error probability. In this chapter, for the 4×1 MISO system transmitting signals from a 4-QAM constellation, a simplified closed form algorithm will be derived for ML detection such that given a received signal and the channel, the transmitted signal can be obtained by a threshold decision. Then, its decision regions for all the transmitted signal points will be completely and explicitly determined. This

detection algorithm will be specifically employed on the 4-group decodable STBC [24, 25, 26, 27, 28, 29].

4.1 Channel Model and 4-Group Decodable STBC

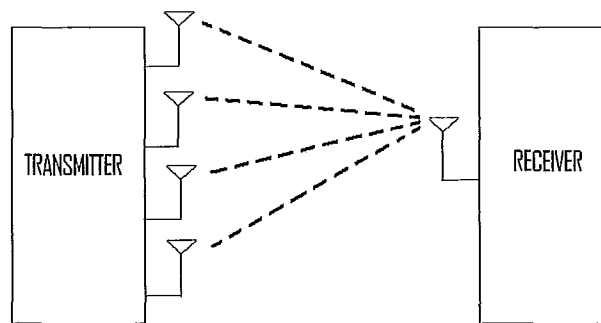


Figure 4.1: 4×1 MISO system

A general model of a MISO system has been given in Chapter 2. This will be used specifically for the case where $M_t = 4$ as shown in Fig. 4.1 such that

$$\mathbf{y} = \frac{\sqrt{\rho}}{2} \mathbf{X} \mathbf{h} + \boldsymbol{\xi} \quad (4.1)$$

where \mathbf{y} is a 4×1 complex received signal vector, \mathbf{h} is a 4×1 vector, $\boldsymbol{\xi}$ is a 4×1 vector, and \mathbf{X} is a 4×4 , complex rotated transmitted signal matrix. Specifically, \mathbf{X}

is a 4-group decodable matrix [26], where,

$$\mathbf{X} = \begin{bmatrix} x_1 & x_3 & 0 & 0 \\ -x_3^* & x_1^* & 0 & 0 \\ 0 & 0 & x_2 & x_4 \\ 0 & 0 & -x_4^* & x_2^* \end{bmatrix} \quad (4.2)$$

Here, each symbol $x_i, i = 1, \dots, 4$ represents a rotated version of a symbol selected from the 4-QAM constellation. This particular STBC structure was chosen since simple ML decoding is possible due to its orthogonal structure, and the fact that each group of 4 transmitted signals can be decoded separately. Comparing \mathbf{X} in Eq.(4.2) to the right side of Eq.(3.5), we can see that this codeword \mathbf{X} is a result of decomposing a rotated quasi-orthogonal STBC using Eq.(3.5),

$$\begin{aligned} \begin{bmatrix} x_1 & x_3 \\ x_2 & x_4 \end{bmatrix}_{\text{re}} &= \mathbf{R} \begin{bmatrix} s_1 & s_3 \\ s_2 & s_4 \end{bmatrix}_{\text{re}} \\ \begin{bmatrix} x_1 & x_3 \\ x_2 & x_4 \end{bmatrix}_{\text{im}} &= \mathbf{R} \begin{bmatrix} s_1 & s_3 \\ s_2 & s_4 \end{bmatrix}_{\text{im}} \end{aligned} \quad (4.3)$$

where \mathbf{R} is a real rotation matrix, such that

$$\mathbf{R} = \begin{bmatrix} \cos \theta & \sin \theta \\ -\sin \theta & \cos \theta \end{bmatrix}$$

and $\mathbf{s} = (s_1 \ s_2 \ s_3 \ s_4)^T$ is the signal vector from the 4-QAM constellation prior to

rotation. Eq.(4.1) can now be re-written in terms of a channel matrix, \mathcal{H} , such that

$$\tilde{\mathbf{y}} = \frac{\sqrt{\rho}}{2} \mathcal{H} \tilde{\mathbf{x}} + \boldsymbol{\xi} \quad (4.4)$$

where $\tilde{\mathbf{y}} = (y_1 \ y_2^* \ y_3 \ y_4^*)^T$, $\tilde{\mathbf{x}} = (x_1 \ x_3 \ x_2 \ x_4)^T$ and

$$\mathcal{H} = \begin{bmatrix} h_1 & h_2 & 0 & 0 \\ h_2^* & -h_1^* & 0 & 0 \\ 0 & 0 & h_3 & h_4 \\ 0 & 0 & h_4^* & -h_3^* \end{bmatrix}$$

Multiplying both sides of Eq.(4.4) by $\frac{2}{\sqrt{\rho}} \mathcal{H}^H$,

$$\mathbf{r} = \frac{2}{\sqrt{\rho}} \mathcal{H}^H \tilde{\mathbf{y}} = \begin{bmatrix} (|h_1|^2 + |h_2|^2) \mathbf{I}_2 & \mathbf{0}_2 \\ \mathbf{0}_2 & (|h_3|^2 + |h_4|^2) \mathbf{I}_2 \end{bmatrix} \tilde{\mathbf{x}} + \tilde{\boldsymbol{\xi}} \quad (4.5)$$

where $\tilde{\boldsymbol{\xi}} = \frac{2}{\sqrt{\rho}} \mathcal{H}^H \boldsymbol{\xi}$. Using the properties of the structure of the STBC in Eq.(4.2), we can separately decode the individual blocks of symbols. Thus, taking the real part of the first and third rows of Eq.(4.5) and using Eq.(4.3),

$$\begin{aligned} \mathbf{e}_1 &= \begin{pmatrix} r_1 \\ r_3 \end{pmatrix}_{\text{re}} = \begin{bmatrix} (|h_1|^2 + |h_2|^2) & 0 \\ 0 & (|h_3|^2 + |h_4|^2) \end{bmatrix} \begin{pmatrix} x_1 \\ x_2 \end{pmatrix}_{\text{re}} + \boldsymbol{\zeta}_1 \\ &= \mathbf{A} \mathbf{R} \tilde{\mathbf{s}}_1 + \boldsymbol{\zeta}_1 \end{aligned} \quad (4.6)$$

where $\tilde{\mathbf{s}}_1 = (s_1 \ s_2)_{\text{re}}^T$,

$$\mathbf{\Lambda} = \begin{bmatrix} (|h_1|^2 + |h_2|^2) & 0 \\ 0 & (|h_3|^2 + |h_4|^2) \end{bmatrix}$$

and $\zeta_1 = (\tilde{\xi}_1 \ \tilde{\xi}_3)_{\text{re}}^T$, with the variance of ζ_1 being

$$E[\zeta_1 \zeta_1^T] = \frac{4}{\rho} \begin{bmatrix} (|h_1|^2 + |h_2|^2) & 0 \\ 0 & (|h_3|^2 + |h_4|^2) \end{bmatrix}$$

We can express $\boldsymbol{\varrho}_2 = (r_1 \ r_3)_{\text{im}}^T$, $\boldsymbol{\varrho}_3 = (r_2 \ r_4)_{\text{re}}^T$ and $\boldsymbol{\varrho}_4 = (r_2 \ r_4)_{\text{im}}^T$ similarly, such that

$$\boldsymbol{\varrho}_2 = \mathbf{\Lambda} \mathbf{R} \tilde{\mathbf{s}}_2 + \zeta_2 \quad (4.7a)$$

$$\boldsymbol{\varrho}_3 = \mathbf{\Lambda} \mathbf{R} \tilde{\mathbf{s}}_3 + \zeta_3 \quad (4.7b)$$

$$\boldsymbol{\varrho}_4 = \mathbf{\Lambda} \mathbf{R} \tilde{\mathbf{s}}_4 + \zeta_4 \quad (4.7c)$$

where $\tilde{\mathbf{s}}_2 = (s_1 \ s_2)_{\text{im}}^T$, $\tilde{\mathbf{s}}_3 = (s_3 \ s_4)_{\text{re}}^T$ and $\tilde{\mathbf{s}}_4 = (s_3 \ s_4)_{\text{im}}^T$, and $\zeta_2 = (\tilde{\xi}_1 \ \tilde{\xi}_3)_{\text{im}}^T$, $\zeta_3 = (\tilde{\xi}_2 \ \tilde{\xi}_4)_{\text{re}}^T$ and $\zeta_4 = (\tilde{\xi}_2 \ \tilde{\xi}_4)_{\text{im}}^T$. Here, $\zeta_i, i = 1, 2, 3, 4$ are all zero mean Gaussian noise having the same variance. Each of the four simplified MISO systems in Eqs.(4.6) and (4.7) consists of similar vectors of real symbols, so we can simply consider all of them using the same representation. Thus, whitening the noise in Eq.(4.6) or Eq.(4.7),

the MISO system becomes

$$\begin{aligned}
\tilde{\mathbf{r}}_i &= \begin{bmatrix} \frac{1}{\sqrt{|h_1|^2 + |h_2|^2}} & 0 \\ 0 & \frac{1}{\sqrt{|h_3|^2 + |h_4|^2}} \end{bmatrix} \mathbf{e}_i \\
&= \begin{bmatrix} \sqrt{|h_1|^2 + |h_2|^2} & 0 \\ 0 & \sqrt{|h_3|^2 + |h_4|^2} \end{bmatrix} \mathbf{R}\tilde{\mathbf{s}}_i + \begin{bmatrix} \frac{1}{\sqrt{|h_1|^2 + |h_2|^2}} & 0 \\ 0 & \frac{1}{\sqrt{|h_3|^2 + |h_4|^2}} \end{bmatrix} \zeta_i \\
&= \tilde{\mathbf{H}}\tilde{\mathbf{s}}_i + \tilde{\zeta}_i \quad i = 1, 2, 3, 4 \tag{4.8}
\end{aligned}$$

where $\tilde{\mathbf{H}} = \mathbf{\Lambda}^{\frac{1}{2}}\mathbf{R}$ and

$$\tilde{\zeta}_i = \begin{bmatrix} \frac{1}{\sqrt{|h_1|^2 + |h_2|^2}} & 0 \\ 0 & \frac{1}{\sqrt{|h_3|^2 + |h_4|^2}} \end{bmatrix} \zeta_i$$

with the variance of $\tilde{\zeta}_i$ being $E[\tilde{\zeta}_i\tilde{\zeta}_i^T] = \frac{4}{\rho}\mathbf{I}_2$.

4.2 Closed Form ML Decoding Algorithm for the 4-QAM Constellation

In the previous section, we have seen that for 4×1 MISO system transmitting signals selected from 4-QAM constellation, the received signal can be separated into four independent groups, each having a general expression given by Eq.(4.8). In this section, we are going to develop a closed form ML detection algorithm for these received signal groups. Due to the similarity between these received signal groups, the algorithm developed will be equally applicable to each and therefore, in the following,

we simplify by omitting the subscript denoting these signal groups and write

$$\tilde{\mathbf{r}} = \tilde{\mathbf{H}}\tilde{\mathbf{s}} + \tilde{\boldsymbol{\zeta}} \quad (4.9)$$

Given that the transmitted symbols are selected from a 4-QAM constellation, we note that $\tilde{\mathbf{s}}$ is *real* and its elements \tilde{s}_1 and \tilde{s}_2 are of the binary set $\{-1, 1\}$. The ML detector at the receiver detects the signal by selecting a signal $\tilde{\mathbf{s}}$ which minimizes the distance between the received signal $\tilde{\mathbf{r}}$ and the ideal received signal $\tilde{\mathbf{H}}\tilde{\mathbf{s}}$. Thus, the detection algorithm is:

$$\begin{aligned} \min_{\tilde{\mathbf{s}}} \|\tilde{\mathbf{r}} - \tilde{\mathbf{H}}\tilde{\mathbf{s}}\|^2 &= \min_{\tilde{\mathbf{s}}} (\tilde{\mathbf{r}} - \tilde{\mathbf{H}}\tilde{\mathbf{s}})^T (\tilde{\mathbf{r}} - \tilde{\mathbf{H}}\tilde{\mathbf{s}}) \\ &= \min_{\tilde{\mathbf{s}}} (\|\tilde{\mathbf{r}}\|^2 + 2\mathbf{z}^T\tilde{\mathbf{s}} + \tilde{\mathbf{s}}^T\mathbf{A}\tilde{\mathbf{s}}) \end{aligned} \quad (4.10)$$

where

$$\mathbf{z} = (z_1 \ z_2)^T = -\tilde{\mathbf{H}}^T\tilde{\mathbf{r}} \quad (4.11)$$

and

$$\mathbf{A} = \tilde{\mathbf{H}}^T\tilde{\mathbf{H}} = \mathbf{R}^T\boldsymbol{\Lambda}\mathbf{R} \quad (4.12)$$

Note that \mathbf{A} is a positive semi-definite (PSD) matrix, and substituting the parameters of \mathbf{R} and $\boldsymbol{\Lambda}$, we have

$$\mathbf{A} = \begin{bmatrix} a_{11} & a_{12} \\ a_{12} & a_{22} \end{bmatrix} = \begin{bmatrix} \frac{\lambda_1 + \lambda_2}{2} + \frac{\lambda_1 - \lambda_2}{2} \cos 2\theta & \frac{\lambda_1 - \lambda_2}{2} \sin 2\theta \\ \frac{\lambda_1 - \lambda_2}{2} \sin 2\theta & \frac{\lambda_1 + \lambda_2}{2} - \frac{\lambda_1 - \lambda_2}{2} \cos 2\theta \end{bmatrix} \quad (4.13)$$

where $\lambda_1 = |h_1|^2 + |h_2|^2$ and $\lambda_2 = |h_3|^2 + |h_4|^2$. Since $h_i = (h_i)_{\text{re}} + j(h_i)_{\text{im}}, i = 1, \dots, 4$, where $(h_i)_{\text{re}}$ and $(h_i)_{\text{im}}$ are IID Gaussian random variables with properties given in

Assumption 1, then each $\lambda_i, i = 1, 2$, is a chi-squared random variable with 4 degrees of freedom, i.e., χ_4^2 . Now, since $\|\tilde{\mathbf{r}}\|^2$ is the received signal energy and is constant, Eq.(4.10) is equivalent to

$$\min_{\tilde{\mathbf{s}}} (\tilde{\mathbf{s}}^T \mathbf{A} \tilde{\mathbf{s}} + 2\mathbf{z}^T \tilde{\mathbf{s}}) \quad (4.14)$$

Also, since this problem is binary, from Eq.(4.14), $a_{11}\tilde{s}_1^2$ and $a_{22}\tilde{s}_2^2$ are constant, and Eq.(4.14) is further reduced to:

$$\min_{\tilde{s}_1, \tilde{s}_2} (a_{12}\tilde{s}_1\tilde{s}_2 + z_1\tilde{s}_1 + z_2\tilde{s}_2) \quad (4.15)$$

Now, the ML objective function has been reduced to Eq.(4.15), consisting of three terms. To minimize this likelihood function we choose the estimated signals $\hat{\tilde{s}}_1$ and $\hat{\tilde{s}}_2$ so that the most dominant two terms are minimized (made negative), with the constraint that $\|\hat{\tilde{s}}_1\| = \|\hat{\tilde{s}}_2\| = 1$.

Theorem 3. *The optimal estimates of \tilde{s} , $\hat{\tilde{s}}$, for the 4-group decodable STBC with signals taken from a 4-QAM constellation and the ML detector, can be determined as follows:*

(a) For $a_{12} \geq 0$:

(1) $|z_1| \geq |z_2| \geq a_{12}$: Here, $|z_1|$ and $|z_2|$ are the most significant terms. Therefore we minimize the Eq.(4.15) by choosing the ML detected output to be

$$\begin{aligned} \hat{\tilde{s}}_1 &= -\text{sgn}(z_1) \\ \hat{\tilde{s}}_2 &= -\text{sgn}(z_2) \end{aligned} \quad (4.16)$$

(2) $|z_2| \geq |z_1| \geq a_{12}$: Following the same argument, minimizing Eq.(4.15), the

ML receiver output is

$$\begin{aligned}\hat{s}_1 &= -\text{sgn}(z_1) \\ \hat{s}_2 &= -\text{sgn}(z_2)\end{aligned}\tag{4.17}$$

(3) $|z_1| \geq a_{12} \geq |z_2|$: *Minimizing Eq.(4.15), the ML receiver output is*

$$\begin{aligned}\hat{s}_1 &= -\text{sgn}(z_1) \\ \hat{s}_2 &= \text{sgn}(z_1)\end{aligned}\tag{4.18}$$

(4) $|z_2| \geq a_{12} \geq |z_1|$: *Minimizing Eq.(4.15), the ML receiver output is*

$$\begin{aligned}\hat{s}_1 &= \text{sgn}(z_2) \\ \hat{s}_2 &= -\text{sgn}(z_2)\end{aligned}\tag{4.19}$$

(5) $a_{12} \geq |z_1| \geq |z_2|$: *Minimizing Eq.(4.15), the ML receiver output is*

$$\begin{aligned}\hat{s}_1 &= -\text{sgn}(z_1) \\ \hat{s}_2 &= \text{sgn}(z_1)\end{aligned}\tag{4.20}$$

(6) $a_{12} \geq |z_2| \geq |z_1|$: *Minimizing Eq.(4.15), the ML receiver output is*

$$\begin{aligned}\hat{s}_1 &= \text{sgn}(z_2) \\ \hat{s}_2 &= -\text{sgn}(z_2)\end{aligned}\tag{4.21}$$

(b) For $a_{12} < 0$:

(1) $|z_1| \geq |z_2| \geq -a_{12}$: Minimizing Eq.(4.15), the ML receiver output is

$$\begin{aligned}\hat{s}_1 &= -\text{sgn}(z_1) \\ \hat{s}_2 &= -\text{sgn}(z_2)\end{aligned}\tag{4.22}$$

(2) $|z_2| \geq |z_1| \geq -a_{12}$: Minimizing Eq.(4.15), the ML receiver output is

$$\begin{aligned}\hat{s}_1 &= -\text{sgn}(z_1) \\ \hat{s}_2 &= -\text{sgn}(z_2)\end{aligned}\tag{4.23}$$

(3) $|z_1| \geq -a_{12} \geq |z_2|$: Minimizing Eq.(4.15), the ML receiver output is

$$\begin{aligned}\hat{s}_1 &= -\text{sgn}(z_1) \\ \hat{s}_2 &= -\text{sgn}(z_1)\end{aligned}\tag{4.24}$$

(4) $|z_2| \geq -a_{12} \geq |z_1|$: Minimizing Eq.(4.15), the ML receiver output is

$$\begin{aligned}\hat{s}_1 &= -\text{sgn}(z_2) \\ \hat{s}_2 &= -\text{sgn}(z_2)\end{aligned}\tag{4.25}$$

(5) $-a_{12} \geq |z_1| \geq |z_2|$: Minimizing Eq.(4.15), the ML receiver output is

$$\begin{aligned}\hat{s}_1 &= -\text{sgn}(z_1) \\ \hat{s}_2 &= -\text{sgn}(z_1)\end{aligned}\tag{4.26}$$

(6) $-a_{12} \geq |z_2| \geq |z_1|$: *Minimizing Eq.(4.15), the ML receiver output is*

$$\begin{aligned}\hat{s}_1 &= -\text{sgn}(z_2) \\ \hat{s}_2 &= -\text{sgn}(z_2)\end{aligned}\tag{4.27}$$

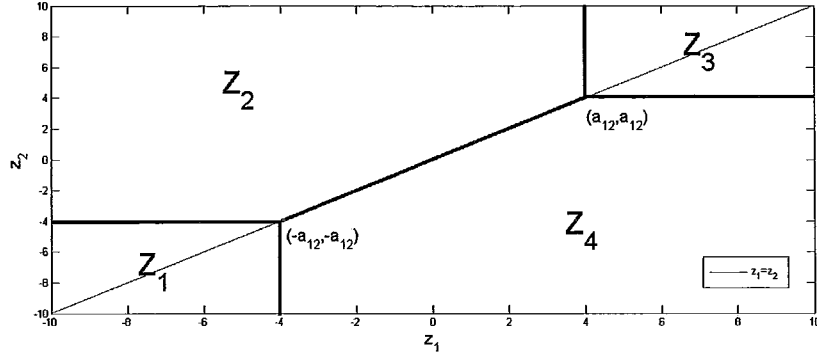
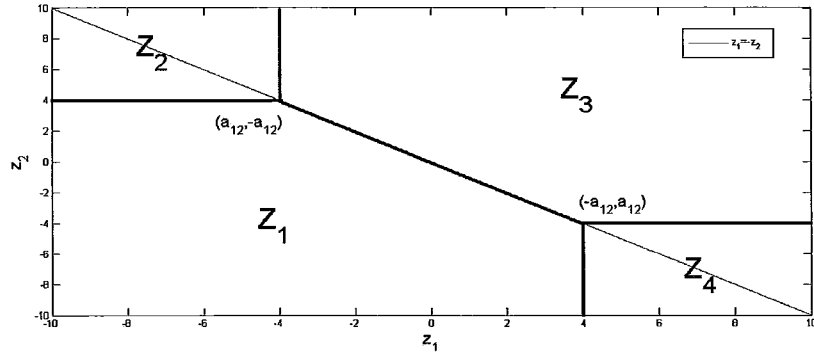
If we assume that \tilde{s}_1 and \tilde{s}_2 are of the same sign, then the decisions in cases (a)-(3) to (a)-(6), from Theorem 3, represent definitely erroneous decisions contradictory to our assumption. On the other hand, if we assume that \tilde{s}_1 and \tilde{s}_2 are of different signs, none of the decisions in case (a) are contradictory to our assumption. If we assume that \tilde{s}_1 and \tilde{s}_2 are of different signs, then the decisions in cases (b)-(3) to (b)-(6), from Theorem 3, represent definitely erroneous decisions contradictory to our assumption. On the other hand, if we assume that \tilde{s}_1 and \tilde{s}_2 are of the same sign, none of the decisions in case (b) are contradictory to our assumption.

4.3 Decision Regions for the ML Receiver for the 4-QAM Constellation

In the previous section, we have established the decision rules of the ML detector for the 4×1 MISO system transmitting symbols from a 4-QAM constellation in Theorem 3. In this section, we will establish the decision regions for the ML detection of the transmitted symbols based on the observed vector $\mathbf{z} = (z_1 \ z_2)^T = -\tilde{\mathbf{H}}\tilde{\mathbf{r}}$.

Since there are four cases of signals $\boldsymbol{\varsigma}_1 = (1 \ 1)^T$, $\boldsymbol{\varsigma}_2 = (1 \ -1)^T$, $\boldsymbol{\varsigma}_3 = (-1 \ -1)^T$, and $\boldsymbol{\varsigma}_4 = (-1 \ 1)^T$ to decide upon, we need to establish the following four hypotheses:

- (1) H_1 : $\tilde{\mathbf{s}} = \boldsymbol{\varsigma}_1$; (2) H_2 : $\tilde{\mathbf{s}} = \boldsymbol{\varsigma}_2$; (3) H_3 : $\tilde{\mathbf{s}} = \boldsymbol{\varsigma}_3$; (4) H_4 : $\tilde{\mathbf{s}} = \boldsymbol{\varsigma}_4$.

(a) Decision Regions for $a_{12} \geq 0$ (b) Decision Regions for $a_{12} < 0$ Figure 4.2: ML Decision Regions for Hypotheses $H_i, i = 1, \dots, 4$

The decision also depends on the observed value of a_{12} . Therefore, we establish the decision regions in the $z_1 z_2$ -plane as follows:

Theorem 4. *The ML decision regions, for each transmitted signal point of the closed form ML detector determined in Theorem 3, can be characterized as follows:*

(a) For $a_{12} \geq 0$: Let us denote the region in which we decide on $\tilde{\mathbf{s}} = \boldsymbol{\varsigma}_i, i = 1, \dots, 4$ by $\mathcal{Z}_i|_{a_{12} \geq 0}$. These regions are shown in Fig. 4.2(a). From Eqs.(4.16) to (4.21) in the previous section, we have

(1) For the decision region for $\tilde{\mathbf{s}} = \boldsymbol{\varsigma}_1$, applying the conditions of Eq.(4.16) such

that $\hat{s}_1 = -\text{sgn}(z_1)$, $\hat{s}_2 = -\text{sgn}(z_2)$, and since both symbols of ς_1 are +1, then

$$\mathcal{Z}_1|_{a_{12} \geq 0} = \{(z_1, z_2) : z_1 \leq -a_{12}, z_2 \leq -a_{12}\} \quad (4.28)$$

(2) Similar to (1),

$$\begin{aligned} \mathcal{Z}_2|_{a_{12} \geq 0} &= \{(z_1, z_2) : z_1 \leq -a_{12}, z_2 \geq -a_{12}\} \\ &\cup \{(z_1, z_2) : |z_1| \leq a_{12}, z_2 \geq z_1\} \end{aligned} \quad (4.29)$$

(3) Similar to (1),

$$\mathcal{Z}_3|_{a_{12} \geq 0} = \{(z_1, z_2) : z_1 \geq a_{12}, z_2 \geq a_{12}\} \quad (4.30)$$

(4) Similar to (1),

$$\begin{aligned} \mathcal{Z}_4|_{a_{12} \geq 0} &= \{(z_1, z_2) : z_1 \geq a_{12}, z_2 \leq a_{12}\} \\ &\cup \{(z_1, z_2) : |z_1| \leq a_{12}, z_2 \leq z_1\} \end{aligned} \quad (4.31)$$

(b) For $a_{12} < 0$: Let us denote the region in which we decide on $\tilde{s} = \varsigma_i, i = 1, \dots, 4$ by $\mathcal{Z}_i|_{a_{12} < 0}$. These regions are shown in Fig. 4.2(b). From Eqs.(4.22) to (4.27) in the previous section, we have

(1) Similar to (a)-(1),

$$\begin{aligned} \mathcal{Z}_1|_{a_{12} < 0} &= \{(z_1, z_2) : z_1 \leq a_{12}, z_2 \leq -a_{12}\} \\ &\cup \{(z_1, z_2) : |z_1| \leq -a_{12}, z_2 \leq -z_1\} \end{aligned} \quad (4.32)$$

(2) *Similar to (a)-(1),*

$$\mathcal{Z}_2|_{a_{12}<0} = \{(z_1, z_2) : z_1 \leq a_{12}, z_2 \geq -a_{12}\} \quad (4.33)$$

(3) *Similar to (a)-(1),*

$$\begin{aligned} \mathcal{Z}_3|_{a_{12}<0} &= \{(z_1, z_2) : z_1 \geq -a_{12}, z_2 \geq a_{12}\} \\ &\cup \{(z_1, z_2) : z_2 \geq -z_1, |z_1| \leq -a_{12}\} \end{aligned} \quad (4.34)$$

(4) *Similar to (a)-(1),*

$$\mathcal{Z}_4|_{a_{12}<0} = \{(z_1, z_2) : z_1 \geq -a_{12}, z_2 \leq a_{12}\} \quad (4.35)$$

The establishment of the decision regions in Theorem 4 facilitates the analysis of the performance of the ML detector, developed in Theorem 3. The analysis will be presented in the following chapter.

Chapter 5

Symbol Error Probability Analysis and Optimal Rotation Angle

In Chapter 4, we focused our attention on the special case of a 4×1 MISO system transmitting symbols selected from a rotated 4-QAM constellation. We transformed the signal transmission model so that the received signals can be detected pair-wise in their real and imaginary parts. This reduces the ML detection to a series of threshold detections resulting in different decision regions in the plane of the observables. In this chapter, we utilize the decision regions established in Chapter 4 to calculate the closed form symbol error probability for the ML detector. This will be achieved by evaluating the probabilities of all correct decisions made by our threshold ML detector and deriving an asymptotic formula for the average error probability. Using this closed form symbol error probability we then find the optimal (yielding the minimum probability of detection error) rotation angle for the 4-group decodable STBC in Eq.(4.2), of which the transmission symbols are selected from the 4-QAM constellation.

5.1 Relationships Between Correct Probability Decision Regions for the 4-QAM Constellation

From Eqs.(4.11) and (4.12), the observable vector is $\mathbf{z} = -\tilde{\mathbf{H}}^T \tilde{\mathbf{r}}$ and $\mathbf{A} = \tilde{\mathbf{H}}^T \tilde{\mathbf{H}}$.

Substituting the expression of $\tilde{\mathbf{r}}$ in Eq.(4.9), we have

$$\mathbf{z} = -\tilde{\mathbf{H}}^T \tilde{\mathbf{H}} \tilde{\mathbf{s}} - \tilde{\mathbf{H}}^T \tilde{\boldsymbol{\zeta}} = \mathbf{z}_0 + \boldsymbol{\nu} \quad (5.1)$$

where $\mathbf{z}_0 = -\mathbf{A} \tilde{\mathbf{s}}$ and $\boldsymbol{\nu} = -\tilde{\mathbf{H}}^T \tilde{\boldsymbol{\zeta}}$, with the variance of $\boldsymbol{\nu}$ being

$$\boldsymbol{\Sigma}_{\boldsymbol{\nu}\boldsymbol{\nu}} = E[\boldsymbol{\nu}\boldsymbol{\nu}^T] = \frac{4}{\rho} \mathbf{A} \quad (5.2)$$

From Eq.(4.12), the eigen-decomposition of \mathbf{A} is $\mathbf{A} = \mathbf{R}^T \boldsymbol{\Lambda} \mathbf{R}$, where $\boldsymbol{\Lambda} = \text{diag}(\lambda_1, \lambda_2)$, and let $\boldsymbol{\lambda} = (\lambda_1 \ \lambda_2)^T$. Since $\boldsymbol{\nu}$ results from a linear transformation of Gaussian random variables, then the conditional probability density function of \mathbf{z} given H_i , $\boldsymbol{\lambda}$ and θ , denoted by $p(\mathbf{z}|H_i, \boldsymbol{\lambda}, \theta)$, is expressed by

$$p(\mathbf{z}|H_i, \boldsymbol{\lambda}, \theta) = \frac{1}{2\pi \sqrt{\det(\boldsymbol{\Sigma}_{\boldsymbol{\nu}\boldsymbol{\nu}})}} \exp\left(-\frac{1}{2}(\mathbf{z} - \mathbf{z}_0)^T \boldsymbol{\Sigma}_{\boldsymbol{\nu}\boldsymbol{\nu}}^{-1}(\mathbf{z} - \mathbf{z}_0)\right) \quad i = 1, \dots, 4 \quad (5.3)$$

where \mathbf{z}_0 is a function of $\tilde{\mathbf{s}}$, and $\tilde{\mathbf{s}}$ can assume any one of the four forms $\boldsymbol{\varsigma}_i, i = 1, \dots, 4$ corresponding to the four hypotheses $H_i, i = 1, \dots, 4$, as mentioned in Section 4.3.

Therefore, if we let $\hat{\tilde{\mathbf{s}}}$ be the detected symbol vector, then, the conditional probabilities

of correct decisions can be calculated by evaluating the following integrals:

$$P_c(\hat{\mathbf{s}}|H_i, \theta, \boldsymbol{\lambda}, a_{12} \geq 0) = \iint_{z_i|_{a_{12} \geq 0}} p(\mathbf{z}|H_i, \boldsymbol{\lambda}, \theta) d\mathbf{z} \quad i = 1, \dots, 4 \quad (5.4a)$$

$$P_c(\hat{\mathbf{s}}|H_i, \theta, \boldsymbol{\lambda}, a_{12} < 0) = \iint_{z_i|_{a_{12} < 0}} p(\mathbf{z}|H_i, \boldsymbol{\lambda}, \theta) d\mathbf{z} \quad i = 1, \dots, 4 \quad (5.4b)$$

We note from Eq.(4.13) that $a_{12} = \frac{\lambda_1 - \lambda_2}{2} \sin 2\theta$, and, thus, $a_{12} \geq 0 \Rightarrow \lambda_1 \geq \lambda_2$ and $a_{12} \leq 0 \Rightarrow \lambda_1 \leq \lambda_2$ for the rotating angle $0 \leq \theta \leq \pi/2$. The range of $0 \leq \theta \leq \pi/2$ is the only range of θ that needs to be considered, since the 4-QAM signal constellation is symmetrical between all four quadrants in the complex plane. Also, from Assumption 4, each entry of $\tilde{\mathbf{s}}$ is independently and equally likely chosen from the 4-QAM constellation. Thus, all hypotheses $H_i, i = 1, \dots, 4$, are equally likely, and the average conditional probability of correct decision is simply the arithmetic average of the probabilities of correct decisions, such that

$$\begin{aligned} P_c(\hat{\mathbf{s}}|\theta, \boldsymbol{\lambda}, \lambda_1 \geq \lambda_2) &= \sum_{i=1}^4 P(H_i) P_c(\hat{\mathbf{s}}|H_i, \theta, \boldsymbol{\lambda}, \lambda_1 \geq \lambda_2) \\ &= \frac{1}{4} \sum_{i=1}^4 P_c(\hat{\mathbf{s}}|H_i, \theta, \boldsymbol{\lambda}, \lambda_1 \geq \lambda_2) \end{aligned} \quad (5.5a)$$

$$\begin{aligned} P_c(\hat{\mathbf{s}}|\theta, \boldsymbol{\lambda}, \lambda_1 < \lambda_2) &= \sum_{i=1}^4 P(H_i) P_c(\hat{\mathbf{s}}|H_i, \theta, \boldsymbol{\lambda}, \lambda_1 < \lambda_2) \\ &= \frac{1}{4} \sum_{i=1}^4 P_c(\hat{\mathbf{s}}|H_i, \theta, \boldsymbol{\lambda}, \lambda_1 < \lambda_2) \end{aligned} \quad (5.5b)$$

Therefore, the average conditional probability of correct decisions taken over the random vector $\boldsymbol{\lambda}$ and given the rotation angle θ , denoted by $P_c(\hat{\mathbf{s}}|\theta)$, is determined by

$$P_c(\hat{\mathbf{s}}|\theta) = E_{\lambda_1 \geq \lambda_2} \left[P_c(\hat{\mathbf{s}}|\theta, \boldsymbol{\lambda}, \lambda_1 \geq \lambda_2) \right] + E_{\lambda_1 < \lambda_2} \left[P_c(\hat{\mathbf{s}}|\theta, \boldsymbol{\lambda}, \lambda_1 < \lambda_2) \right] \quad (5.6)$$

One of our main goals in this chapter is to obtain the asymptotic formula of $P_c(\hat{\mathbf{s}}|\theta)$ when the SNR is large. To do that, let us explore the relationships among the probabilities of correct decisions. From Eqs.(4.28) - (4.35), the ML decision regions shown in Figs. 4.2(a) and 4.2(b) possess some symmetric properties directly resulting in the following property:

Property 2. Let $P_c(\hat{\mathbf{s}}|H_i, \theta, \boldsymbol{\lambda}, \lambda_1 \geq \lambda_2)$ and $P_c(\hat{\mathbf{s}}|H_i, \theta, \boldsymbol{\lambda}, \lambda_1 < \lambda_2)$ be defined by Eq.(5.4). Then, we have

$$P_c(\hat{\mathbf{s}}|H_1, \theta, \boldsymbol{\lambda}, \lambda_1 \geq \lambda_2) = P_c(\hat{\mathbf{s}}|H_3, \theta, \boldsymbol{\lambda}, \lambda_1 \geq \lambda_2)$$

$$P_c(\hat{\mathbf{s}}|H_2, \theta, \boldsymbol{\lambda}, \lambda_1 \geq \lambda_2) = P_c(\hat{\mathbf{s}}|H_4, \theta, \boldsymbol{\lambda}, \lambda_1 \geq \lambda_2)$$

$$P_c(\hat{\mathbf{s}}|H_2, \theta, \boldsymbol{\lambda}, \lambda_1 < \lambda_2) = P_c(\hat{\mathbf{s}}|H_4, \theta, \boldsymbol{\lambda}, \lambda_1 < \lambda_2)$$

$$P_c(\hat{\mathbf{s}}|H_1, \theta, \boldsymbol{\lambda}, \lambda_1 < \lambda_2) = P_c(\hat{\mathbf{s}}|H_3, \theta, \boldsymbol{\lambda}, \lambda_1 < \lambda_2)$$

Due to this property, we need only consider the probabilities $P_c(\hat{\mathbf{s}}|H_1, \theta, \boldsymbol{\lambda}, \lambda_1 \geq \lambda_2)$ and $P_c(\hat{\mathbf{s}}|H_3, \theta, \boldsymbol{\lambda}, \lambda_1 \geq \lambda_2)$ when $a_{12} \geq 0$, and the probabilities $P_c(\hat{\mathbf{s}}|H_2, \theta, \boldsymbol{\lambda}, \lambda_1 < \lambda_2)$ and $P_c(\hat{\mathbf{s}}|H_4, \theta, \boldsymbol{\lambda}, \lambda_1 < \lambda_2)$ when $a_{12} < 0$. To further simplify the integrals, Eq.(5.4), we need to develop an important property on the conditional probability density function $p(\mathbf{z}|H_i, \boldsymbol{\lambda}, \theta)$, $i = 1, 2, 3$.

Property 3. *The probability density function $p(\mathbf{z}|H_i, \boldsymbol{\lambda}, \theta)$, defined by Eq.(5.3), has the following property:*

$$p(\mathbf{z}|H_1, (\lambda_1 \ \lambda_2)^T, \theta) = p(\bar{\mathbf{z}}|H_2, (\lambda_2 \ \lambda_1)^T, \theta) \quad (5.7a)$$

$$p(\mathbf{z}|H_2, (\lambda_1 \ \lambda_2)^T, \theta) = p(\bar{\mathbf{z}}|H_3, (\lambda_2 \ \lambda_1)^T, \theta) \quad (5.7b)$$

where $\bar{\mathbf{z}} = (z_2 \ -z_1)^T$.

The proof of Property 3 is given in Appendix B.1. Using this property, we can find a relationship between probabilities $P_c(\hat{\mathbf{s}}|H_i, \theta, \boldsymbol{\lambda}, \lambda_1 \geq \lambda_2)$ and $P_c(\hat{\mathbf{s}}|H_i, \theta, \boldsymbol{\lambda}, \lambda_1 < \lambda_2)$, $i = 1, 2, 3$.

Property 4. *If we let*

$$P_c(\hat{\mathbf{s}}|H_i, \theta, \lambda_1 \geq \lambda_2) = E_{\lambda_1 \geq \lambda_2} [P_c(\hat{\mathbf{s}}|H_i, \theta, \boldsymbol{\lambda}, \lambda_1 \geq \lambda_2)] \quad i = 1, 2, 3$$

$$P_c(\hat{\mathbf{s}}|H_i, \theta, \lambda_1 < \lambda_2) = E_{\lambda_1 < \lambda_2} [P_c(\hat{\mathbf{s}}|H_i, \theta, \boldsymbol{\lambda}, \lambda_1 < \lambda_2)] \quad i = 1, 2, 3$$

then, we have

$$P_c(\hat{\mathbf{s}}|H_3, \theta, \lambda_1 < \lambda_2) = P_c(\hat{\mathbf{s}}|H_2, \theta, \lambda_1 \geq \lambda_2) \quad (5.8a)$$

$$P_c(\hat{\mathbf{s}}|H_2, \theta, \lambda_1 < \lambda_2) = P_c(\hat{\mathbf{s}}|H_1, \theta, \lambda_1 \geq \lambda_2) \quad (5.8b)$$

Property 2 and Property 4, the proof of which is given in Appendix B.2, together tell us that only the probabilities of the correct decisions, $P_c(\hat{\mathbf{s}}|H_2, \theta, \lambda_1 \geq \lambda_2)$ and $P_c(\hat{\mathbf{s}}|H_1, \theta, \lambda_1 \geq \lambda_2)$, need to be considered to obtain the overall probability of correct decisions. In other words, the calculation of $P_c(\hat{\mathbf{s}}|\theta)$, based on Eqs.(5.6) and (5.5), is

significantly simplified to the following equation:

$$\begin{aligned} P_c(\hat{\mathbf{s}}|\theta) &= \mathbb{E}_{\lambda_1 \geq \lambda_2} [P_c(\hat{\mathbf{s}}|H_1, \theta, \boldsymbol{\lambda}, \lambda_1 \geq \lambda_2)] + \mathbb{E}_{\lambda_1 \geq \lambda_2} [P_c(\hat{\mathbf{s}}|H_2, \theta, \boldsymbol{\lambda}, \lambda_1 \geq \lambda_2)] \\ &= P_c(\hat{\mathbf{s}}|H_1, \theta, \lambda_1 \geq \lambda_2) + P_c(\hat{\mathbf{s}}|H_2, \theta, \lambda_1 \geq \lambda_2) \end{aligned} \quad (5.9)$$

Therefore, the focus of the remaining sections of this chapter will be calculating $\mathbb{E}_{\lambda_1 \geq \lambda_2} [P_c(\hat{\mathbf{s}}|H_1, \theta, \boldsymbol{\lambda}, \lambda_1 \geq \lambda_2)]$ and $\mathbb{E}_{\lambda_1 \geq \lambda_2} [P_c(\hat{\mathbf{s}}|H_2, \theta, \boldsymbol{\lambda}, \lambda_1 \geq \lambda_2)]$.

5.2 Gaussian Probability Integrals and the Q -function

Since the evaluation of the probability of correct decisions in Eq.(5.9) involves the integrals of Gaussian densities, the results will be intimately related to the Q -function [31, 37]. In this section, we establish two fundamental lemmas which will be helpful to simplify the probability integrals involving Gaussian distributions. The Q -function is defined as

$$Q(x) = \frac{1}{\sqrt{2\pi}} \int_x^\infty \exp\left(-\frac{u^2}{2}\right) du \quad (5.10)$$

Alternatively, the following two equivalent formulae [31, 37] of the Q -function play an important role in the diversity analysis of error performance for wireless communication systems:

$$Q(x) = \frac{1}{\pi} \int_0^{\frac{\pi}{2}} \exp\left(-\frac{x^2}{2 \sin^2 \phi}\right) d\phi \quad \text{for } x \geq 0 \quad (5.11a)$$

$$Q^2(x) = \frac{1}{\pi} \int_0^{\frac{\pi}{4}} \exp\left(-\frac{x^2}{2 \sin^2 \phi}\right) d\phi \quad \text{for } x \geq 0 \quad (5.11b)$$

In the following, we will derive two expressions for a two-dimensional vector, $\mathbf{x} = (x_1 \ x_2)^T$, that will be used to simplify the correct probability integrals established in the previous section. For notation and discussion convenience, we let $f(\mathbf{x})$ denote the function $f(\mathbf{x}) = \exp(-\mathbf{x}^T \mathbf{P} \mathbf{x})$, where \mathbf{P} is a 2×2 PSD matrix, i.e., $\mathbf{P} \succeq 0$.

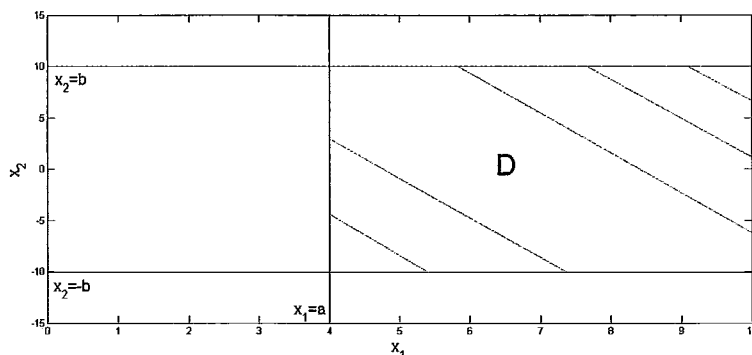


Figure 5.1: Integral Domain in Lemma 4

Lemma 4. Let $I_1 = \iint_{\mathcal{D}} f(\mathbf{x}) dx_2 dx_1$, where $\mathcal{D} = \{(x_1, x_2) : x_1 \geq a, -b \leq x_2 \leq b; a, b \geq 0\}$ as shown in Fig. 5.1. Then, we have

$$I_1 = \int_{-\tan^{-1} b/a}^{\tan^{-1} b/a} \frac{\exp\left(-\frac{a^2 \mathbf{x}^T(\phi) \mathbf{P} \mathbf{x}(\phi)}{\cos^2 \phi}\right) - \exp\left(-\frac{b^2 \mathbf{x}^T(\phi) \mathbf{P} \mathbf{x}(\phi)}{\sin^2 \phi}\right)}{2 \mathbf{x}^T(\phi) \mathbf{P} \mathbf{x}(\phi)} d\phi \quad (5.12)$$

The proof of Lemma 4 can be found in Appendix C.1. In particular, consider the case when $\mathbf{P} = \frac{1}{2} \mathbf{I}$, $a = 0$ and $b = x$ in Lemma 4. Then, using the definition of \mathcal{D} , we have

$$\begin{aligned} I_1 &= \int_0^\infty \exp\left(-\frac{x_1^2}{2}\right) dx_1 \int_{-x}^x \exp\left(-\frac{x_2^2}{2}\right) dx_2 \\ &= \pi \times \left(1 - 2Q(x)\right) \end{aligned}$$

and using the result in Eq.(5.12), we have

$$\begin{aligned}
I_1 &= \int_{-\frac{\pi}{2}}^{\frac{\pi}{2}} \left(1 - \exp\left(-\frac{x^2}{2\sin^2\phi}\right) \right) d\phi \\
&= 2 \int_0^{\frac{\pi}{2}} d\phi - 2 \int_0^{\frac{\pi}{2}} \exp\left(-\frac{x^2}{2\sin^2\phi}\right) d\phi \\
&= \pi - 2 \int_0^{\frac{\pi}{2}} \exp\left(-\frac{x^2}{2\sin^2\phi}\right) d\phi
\end{aligned}$$

Therefore, we have $Q(x) = \frac{1}{\pi} \int_0^{\frac{\pi}{2}} \exp\left(-\frac{x^2}{2\sin^2\phi}\right) d\phi$, which is exactly the same as Eq.(5.11a). In addition, when $\mathbf{P} = \frac{1}{2}\mathbf{I}$ and $a = b = x$ in Lemma 4, using the definition of \mathcal{D} , we have

$$\begin{aligned}
I_1 &= \int_x^\infty \exp\left(-\frac{x_1^2}{2}\right) dx_1 \int_{-x}^x \exp\left(-\frac{x_2^2}{2}\right) dx_2 \\
&= 2\pi \times Q(x) \times (1 - 2Q(x))
\end{aligned}$$

On the other hand, using the result in Eq.(5.12), we obtain

$$\begin{aligned}
I_1 &= \int_{-\frac{\pi}{4}}^{\frac{\pi}{4}} \left(\exp\left(-\frac{x^2}{2\cos^2\phi}\right) - \exp\left(-\frac{x^2}{2\sin^2\phi}\right) \right) d\phi \\
&= 2 \int_0^{\frac{\pi}{2}} \exp\left(-\frac{x^2}{\cos^2\phi}\right) d\phi - 2 \int_{\frac{\pi}{4}}^{\frac{\pi}{2}} \exp\left(-\frac{x^2}{\cos^2\phi}\right) d\phi \\
&\quad - 2 \int_0^{\frac{\pi}{4}} \exp\left(-\frac{x^2}{\sin^2\phi}\right) d\phi \\
&= 2 \int_0^{\frac{\pi}{2}} \exp\left(-\frac{x^2}{\sin^2\phi}\right) d\phi - 4 \int_0^{\frac{\pi}{4}} \exp\left(-\frac{x^2}{\sin^2\phi}\right) d\phi \\
&= 2\pi \times Q(x) - 4 \int_0^{\frac{\pi}{4}} \exp\left(-\frac{x^2}{\sin^2\phi}\right) d\phi
\end{aligned}$$

Hence, we have $Q^2(x) = \frac{1}{\pi} \int_0^{\frac{\pi}{4}} \exp\left(-\frac{x^2}{\sin^2\phi}\right) d\phi$, which is the Eq.(5.11b). This shows

that our Lemma 4 is a generalization of Eq.(5.11).

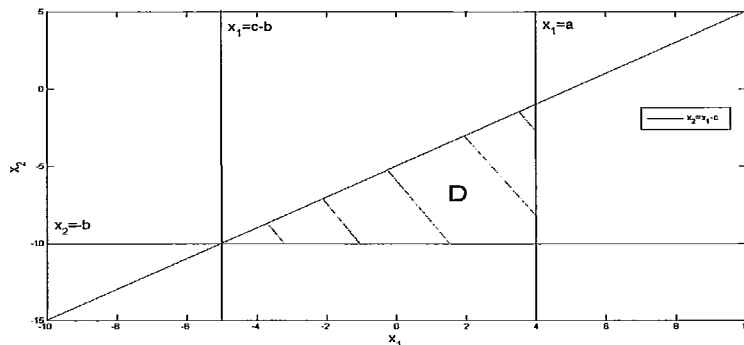


Figure 5.2: Integral Domain in Lemma 5

Lemma 5. Let $I_2 = \iint_{\mathcal{D}} f(\mathbf{x}) dx_2 dx_1$, where $\mathcal{D} = \{(x_1, x_2) : c - b \leq x_1 \leq a, -b \leq x_2 \leq x_1 - c; a, b, c \geq 0\}$ as shown in Fig. 5.2. Then,

$$\begin{aligned}
 I_2 = & \int_{-\tan^{-1} \frac{b}{a}}^{\tan^{-1} \frac{a-c}{a}} \frac{\exp\left(-\frac{c^2 \mathbf{x}^T(\theta) \mathbf{P} \mathbf{x}(\theta)}{(\cos \theta - \sin \theta)^2}\right) - \exp\left(-\frac{a^2 \mathbf{x}^T(\theta) \mathbf{P} \mathbf{x}(\theta)}{\cos^2 \theta}\right)}{2 \mathbf{x}^T(\theta) \mathbf{P} \mathbf{x}(\theta)} d\theta \\
 & + \int_{-\frac{\pi}{2} - \tan^{-1} \frac{b-c}{b}}^{-\tan^{-1} \frac{b}{a}} \frac{\exp\left(-\frac{c^2 \mathbf{x}^T(\theta) \mathbf{P} \mathbf{x}(\theta)}{(\cos \theta - \sin \theta)^2}\right) - \exp\left(-\frac{b^2 \mathbf{x}^T(\theta) \mathbf{P} \mathbf{x}(\theta)}{\sin^2 \theta}\right)}{2 \mathbf{x}^T(\theta) \mathbf{P} \mathbf{x}(\theta)} d\theta
 \end{aligned}$$

The proof of Lemma 5 is given in Appendix C.2.

5.3 Analysis of the Average Probability of Correct Decision for the 4-QAM Constellation

Case 1. $\tilde{\mathbf{s}} = \mathbf{c}_1 = (1 \ 1)^T$:

Let us now examine the probability of the correct decision for $\tilde{\mathbf{s}} = \mathbf{c}_1 = (1 \ 1)^T$ under the condition that $a_{12} \geq 0$. From Eqs.(4.28) and (5.4a), we see that

$$\begin{aligned} P_c(\hat{\mathbf{s}}|H_1, \theta, \boldsymbol{\lambda}, \lambda_1 \geq \lambda_2) &= \iint_{\mathbf{z}_1|_{a_{12} \geq 0}} p(\mathbf{z}|H_1, \boldsymbol{\lambda}, \theta) dz_2 dz_1 \\ &= \int_{-\infty}^{-a_{12}} \int_{-\infty}^{-a_{12}} p(\mathbf{z}|H_1, \boldsymbol{\lambda}, \theta) dz_2 dz_1 \end{aligned}$$

where $p(\mathbf{z}|H_1, \boldsymbol{\lambda}, \theta)$ is defined in Eq.(5.3). Now, let $\tilde{\mathbf{z}} = (\tilde{z}_1 \ \tilde{z}_2)^T = \mathbf{z} - \mathbf{z}_0$, where $\mathbf{z}_0 = -\mathbf{A}\tilde{\mathbf{s}} = -\mathbf{A}(1 \ 1)^T$, then

$$\begin{aligned} P_c(\hat{\mathbf{s}}|H_1, \theta, \boldsymbol{\lambda}, \lambda_1 \geq \lambda_2) &= \int_{-\infty}^{a_{11}} \int_{-\infty}^{a_{22}} p(\tilde{\mathbf{z}}|\boldsymbol{\lambda}, \theta) d\tilde{z}_2 d\tilde{z}_1 \\ &= \int_{-\infty}^{\infty} \int_{-\infty}^{\infty} p(\tilde{\mathbf{z}}|\boldsymbol{\lambda}, \theta) d\tilde{z}_2 d\tilde{z}_1 - \int_{-\infty}^{\infty} \int_{a_{22}}^{\infty} p(\tilde{\mathbf{z}}|\boldsymbol{\lambda}, \theta) d\tilde{z}_2 d\tilde{z}_1 \\ &\quad - \int_{a_{11}}^{\infty} \int_{-\infty}^{\infty} p(\tilde{\mathbf{z}}|\boldsymbol{\lambda}, \theta) d\tilde{z}_2 d\tilde{z}_1 + \int_{a_{11}}^{\infty} \int_{a_{22}}^{\infty} p(\tilde{\mathbf{z}}|\boldsymbol{\lambda}, \theta) d\tilde{z}_2 d\tilde{z}_1 \\ &= 1 - J_1(\boldsymbol{\lambda}, \theta) - J_2(\boldsymbol{\lambda}, \theta) + \Delta_1(\boldsymbol{\lambda}, \theta) \end{aligned} \quad (5.13)$$

where $p(\tilde{\mathbf{z}}|\boldsymbol{\lambda}, \theta)$ is defined as

$$p(\tilde{\mathbf{z}}|\boldsymbol{\lambda}, \theta) = \frac{1}{2\pi \sqrt{\det(\boldsymbol{\Sigma}_{\nu\nu})}} \exp\left(-\frac{1}{2}\tilde{\mathbf{z}}^T \boldsymbol{\Sigma}_{\nu\nu}^{-1} \tilde{\mathbf{z}}\right) \quad (5.14)$$

and $J_1(\boldsymbol{\lambda}, \theta)$, $J_2(\boldsymbol{\lambda}, \theta)$ and $\Delta_1(\boldsymbol{\lambda}, \theta)$ are defined as

$$J_1(\boldsymbol{\lambda}, \theta) = \int_{-\infty}^{\infty} \int_{a_{22}}^{\infty} p(\tilde{\mathbf{z}}|\boldsymbol{\lambda}, \theta) d\tilde{z}_2 d\tilde{z}_1 \quad (5.15a)$$

$$J_2(\boldsymbol{\lambda}, \theta) = \int_{a_{11}}^{\infty} \int_{-\infty}^{\infty} p(\tilde{\mathbf{z}}|\boldsymbol{\lambda}, \theta) d\tilde{z}_2 d\tilde{z}_1 \quad (5.15b)$$

$$\Delta_1(\boldsymbol{\lambda}, \theta) = \int_{a_{11}}^{\infty} \int_{a_{22}}^{\infty} p(\tilde{\mathbf{z}}|\boldsymbol{\lambda}, \theta) d\tilde{z}_2 d\tilde{z}_1 \quad (5.15c)$$

Case 2. $\tilde{\mathbf{s}} = \boldsymbol{\varsigma}_2 = (1 \quad -1)^T$:

For this case, from Eqs.(4.29) and (5.4b), and referring to Fig. 4.2(a), the probability of correct decision for $\tilde{\mathbf{s}} = \boldsymbol{\varsigma}_2 = (1 \quad -1)^T$ when $a_{12} \geq 0$ is given by

$$\begin{aligned} P_c(\hat{\mathbf{s}}|H_2, \theta, \boldsymbol{\lambda}, \lambda_1 \geq \lambda_2) &= \iint_{\mathbf{z}_2|_{a_{12} \geq 0}} p(\mathbf{z}|H_2, \boldsymbol{\lambda}, \theta) dz_2 dz_1 \\ &= \int_{-\infty}^{-a_{12}} \int_{-a_{12}}^{\infty} p(\mathbf{z}|H_2, \boldsymbol{\lambda}, \theta) dz_2 dz_1 \\ &\quad + \int_{-a_{12}}^{a_{12}} \int_{z_1}^{\infty} p(\mathbf{z}|H_2, \boldsymbol{\lambda}, \theta) dz_2 dz_1 \end{aligned}$$

Again, let $\tilde{\mathbf{z}} = (\tilde{z}_1 \quad \tilde{z}_2)^T = \mathbf{z} - \mathbf{z}_0$, where $\mathbf{z}_0 = -\mathbf{A}\tilde{\mathbf{s}} = -\mathbf{A}(1 \quad -1)^T$, then

$$\begin{aligned} P_c(\hat{\mathbf{s}}|H_2, \theta, \boldsymbol{\lambda}, \lambda_1 \geq \lambda_2) &= \int_{-\infty}^{a_{11}-2a_{12}} \int_{-a_{22}}^{\infty} p(\tilde{\mathbf{z}}|\boldsymbol{\lambda}, \theta) d\tilde{z}_2 d\tilde{z}_1 \\ &\quad + \int_{a_{11}-2a_{12}}^{a_{11}} \int_{\tilde{z}_1+2a_{12}-a_{11}-a_{22}}^{\infty} p(\tilde{\mathbf{z}}|\boldsymbol{\lambda}, \theta) d\tilde{z}_2 d\tilde{z}_1 \\ &= \Delta_2(\boldsymbol{\lambda}, \theta) + \Delta_3(\boldsymbol{\lambda}, \theta) \end{aligned} \quad (5.16)$$

where $\Delta_2(\boldsymbol{\lambda}, \theta)$ and $\Delta_3(\boldsymbol{\lambda}, \theta)$ are defined as

$$\Delta_2(\boldsymbol{\lambda}, \theta) = \int_{-\infty}^{a_{11}-2a_{12}} \int_{-a_{22}}^{\infty} p(\tilde{\mathbf{z}}|\boldsymbol{\lambda}, \theta) d\tilde{z}_2 d\tilde{z}_1 \quad (5.17a)$$

$$\Delta_3(\boldsymbol{\lambda}, \theta) = \int_{a_{11}-2a_{12}}^{a_{11}} \int_{\tilde{z}_1+2a_{12}-a_{11}-a_{22}}^{\infty} p(\tilde{\mathbf{z}}|\boldsymbol{\lambda}, \theta) d\tilde{z}_2 d\tilde{z}_1 \quad (5.17b)$$

It is important to note that

$$\begin{aligned} \Delta_1(\boldsymbol{\lambda}, \theta) + \Delta_2(\boldsymbol{\lambda}, \theta) + \Delta_3(\boldsymbol{\lambda}, \theta) &= \int_{-\infty}^{\infty} \int_{-a_{22}}^{\infty} p(\tilde{\mathbf{z}}|\boldsymbol{\lambda}, \theta) d\tilde{z}_2 d\tilde{z}_1 \\ &\quad - \int_{a_{11}}^{\infty} \int_{-a_{22}}^{a_{22}} p(\tilde{\mathbf{z}}|\boldsymbol{\lambda}, \theta) d\tilde{z}_2 d\tilde{z}_1 \\ &\quad - \int_{a_{11}-2a_{12}}^{a_{11}} \int_{-a_{22}}^{\tilde{z}_1-(a_{11}+a_{22}-2a_{12})} p(\tilde{\mathbf{z}}|\boldsymbol{\lambda}, \theta) d\tilde{z}_2 d\tilde{z}_1 \\ &= J_3(\boldsymbol{\lambda}, \theta) - J_4(\boldsymbol{\lambda}, \theta) - J_5(\boldsymbol{\lambda}, \theta) \end{aligned} \quad (5.18)$$

where $J_3(\boldsymbol{\lambda}, \theta)$, $J_4(\boldsymbol{\lambda}, \theta)$ and $J_5(\boldsymbol{\lambda}, \theta)$ are defined by

$$J_3(\boldsymbol{\lambda}, \theta) = \int_{-\infty}^{\infty} \int_{-a_{22}}^{\infty} p(\tilde{\mathbf{z}}|\boldsymbol{\lambda}, \theta) d\tilde{z}_2 d\tilde{z}_1 \quad (5.19a)$$

$$J_4(\boldsymbol{\lambda}, \theta) = \int_{a_{11}}^{\infty} \int_{-a_{22}}^{a_{22}} p(\tilde{\mathbf{z}}|\boldsymbol{\lambda}, \theta) d\tilde{z}_2 d\tilde{z}_1 \quad (5.19b)$$

$$J_5(\boldsymbol{\lambda}, \theta) = \int_{a_{11}-2a_{12}}^{a_{11}} \int_{-a_{22}}^{\tilde{z}_1-(a_{11}+a_{22}-2a_{12})} p(\tilde{\mathbf{z}}|\boldsymbol{\lambda}, \theta) d\tilde{z}_2 d\tilde{z}_1 \quad (5.19c)$$

In the following, we will evaluate the expected value of each $J_i(\boldsymbol{\lambda}, \theta)$ for $i = 1, \dots, 5$ over $\boldsymbol{\lambda}$. First, we have

Property 5. Let $J_1(\boldsymbol{\lambda}, \theta)$, $J_2(\boldsymbol{\lambda}, \theta)$ and $J_3(\boldsymbol{\lambda}, \theta)$ be defined in Eqs.(5.15a), (5.15b)

and (5.19a) respectively. Then,

$$J_1(\boldsymbol{\lambda}, \theta) = Q\left(\frac{\sqrt{\rho a_{22}}}{2}\right) \quad (5.20a)$$

$$J_2(\boldsymbol{\lambda}, \theta) = Q\left(\frac{\sqrt{\rho a_{11}}}{2}\right) \quad (5.20b)$$

$$J_3(\boldsymbol{\lambda}, \theta) = 1 - Q\left(\frac{\sqrt{\rho a_{22}}}{2}\right) \quad (5.20c)$$

where the Q -function is defined in Eq.(5.10).

The proof of Property 5 is provided in Appendix B.3. In order to obtain the expected value of each $J_i(\boldsymbol{\lambda}, \theta)$ for $i = 1, 2, 3$, we need the following property:

Property 6. Let λ_1 and λ_2 be two independently random variables with each being chi-squared distribution χ_4^2 and $\alpha(\lambda_1, \lambda_2)$ be a homogenous linear function of λ_1 and λ_2 such that $\alpha(\lambda_1, \lambda_2) = \lambda_2 \alpha\left(\frac{\lambda_1}{\lambda_2}, 1\right)$. Considering the range $\lambda_1 \geq \lambda_2$, we can let $\lambda_1 = u\lambda_2$, where $u \geq 1$. Then, we have

$$E_{\lambda_1 \geq \lambda_2} \left[Q\left(\frac{\sqrt{\rho \alpha(\lambda_1, \lambda_2)}}{2}\right) \right] = 3360\rho^{-4} \int_1^\infty \frac{u}{\alpha^4(u, 1)} du + O(\rho^{-5}) \quad (5.21)$$

The proof of Property 6 is provided in Appendix B.4. Note that a_{11} , a_{12} and a_{22} are all of the same form of homogenous linear function as $\alpha(\lambda_1, \lambda_2)$ in Lemma 6. Now, taking advantage of Properties 5 and 6, we can obtain the following Property 7:

Property 7. Let $J_1(\boldsymbol{\lambda}, \theta)$, $J_2(\boldsymbol{\lambda}, \theta)$ and $J_3(\boldsymbol{\lambda}, \theta)$ be defined in Eq.(5.20). If we let λ_1 and λ_2 be two independently random variables, each being of chi-squared distribution

χ_4^2 , then, we have

$$\mathbb{E}_{\lambda_1 \geq \lambda_2} [1] = \frac{1}{2} \quad (5.22a)$$

$$\mathbb{E}_{\lambda_1 \geq \lambda_2} [J_1(\boldsymbol{\lambda}, \theta)] = \frac{560(3 - 2 \cos^2 \theta)}{\sin^4 \theta} \rho^{-4} + O(\rho^{-5}) \quad (5.22b)$$

$$\mathbb{E}_{\lambda_1 \geq \lambda_2} [J_2(\boldsymbol{\lambda}, \theta)] = \frac{560(3 - 2 \sin^2 \theta)}{\cos^4 \theta} \rho^{-4} + O(\rho^{-5}) \quad (5.22c)$$

$$\mathbb{E}_{\lambda_1 \geq \lambda_2} [J_3(\boldsymbol{\lambda}, \theta)] = \frac{1}{2} - \frac{560(3 - 2 \cos^2 \theta)}{\sin^4 \theta} \rho^{-4} + O(\rho^{-5}) \quad (5.22d)$$

The proof of Property 7 is given in Appendix B.5.

Now, let us turn our attention to the evaluations of the expected values of $J_4(\boldsymbol{\lambda}, \theta)$ and $J_5(\boldsymbol{\lambda}, \theta)$, which are more complicated than those of $J_1(\boldsymbol{\lambda}, \theta)$, $J_2(\boldsymbol{\lambda}, \theta)$ and $J_3(\boldsymbol{\lambda}, \theta)$. To evaluate $J_4(\boldsymbol{\lambda}, \theta)$, we employ Lemma 4, and in particular, we set $a = a_{11}$ and $b = a_{22}$ and then take the expected value. This gives

Property 8. *Let $J_4(\boldsymbol{\lambda}, \theta)$ be defined in Eq.(5.19b). Letting $\lambda_1 = u\lambda_2$ and expressing $\lambda_2 a_{11}(u, 1) = a_{11}(\lambda_1, \lambda_2)$, $\lambda_2 a_{12}(u, 1) = a_{12}(\lambda_1, \lambda_2)$, and $\lambda_2 a_{22}(u, 1) = a_{22}(\lambda_1, \lambda_2)$, then the expected value of $J_4(\boldsymbol{\lambda}, \theta)$ is given by*

$$\begin{aligned} \mathbb{E}_{\lambda_1 \geq \lambda_2} [J_4(\boldsymbol{\lambda}, \theta)] &= \frac{2048}{\pi \rho^4} \int_1^\infty \frac{u}{a_{11}^4(u, 1)} du \int_{-\frac{a_{22}(u,1)+a_{12}(u,1)}{\sqrt{u}}}^{\frac{a_{22}(u,1)-a_{12}(u,1)}{\sqrt{u}}} \frac{dt}{(t^2 + 1)^5} \\ &\quad - \frac{2048}{\pi \rho^4} \int_1^\infty \frac{u}{a_{22}^4(u, 1)} du \int_{\frac{a_{11}(u,1)-a_{12}(u,1)}{\sqrt{u}}}^\infty \frac{dt}{(t^2 + 1)^5} \\ &\quad - \frac{2048}{\pi \rho^4} \int_1^\infty \frac{u}{a_{22}^4(u, 1)} du \int_{\frac{a_{11}(u,1)+a_{12}(u,1)}{\sqrt{u}}}^\infty \frac{dt}{(t^2 + 1)^5} + O(\rho^{-5}) \end{aligned}$$

The proof of Property 8 is given in Appendix B.6.

We now employ Lemma 5 for the evaluation of $J_5(\boldsymbol{\lambda}, \theta)$. Applying Lemma 5 to $J_5(\boldsymbol{\lambda}, \theta)$, specifically with $a = a_{11}$, $b = a_{22}$ and $c = a_{11} + a_{22} - 2a_{12}$, we can then

take the expected value of $J_5(\boldsymbol{\lambda}, \theta)$. This leads to Property 9, the proof of which is provided in Appendix B.7.

Property 9. *Let $J_5(\boldsymbol{\lambda}, \theta)$ be defined in Eq.(5.19c). Letting $\lambda_1 = u\lambda_2$, and again expressing $\lambda_2 a_{11}(u, 1) = a_{11}(\lambda_1, \lambda_2)$, $\lambda_2 a_{12}(u, 1) = a_{12}(\lambda_1, \lambda_2)$, and $\lambda_2 a_{22}(u, 1) = a_{22}(\lambda_1, \lambda_2)$, then the expected value of $J_5(\boldsymbol{\lambda}, \theta)$ is given by*

$$\begin{aligned}
& E_{\lambda_1 \geq \lambda_2} [J_5(\boldsymbol{\lambda}, \theta)] \\
&= \frac{2048}{\pi \rho^4} \int_1^\infty \frac{u^5 du}{a_{11}^4(u, 1) c^8(u, 1)} \int_{\frac{a_{22}(u, 1) - a_{12}(u, 1)}{\sqrt{u}}}^{\frac{a_{22}(u, 1) + a_{12}(u, 1)}{\sqrt{u}}} \frac{\left(t + \frac{a_{11}(u, 1) - a_{12}(u, 1)}{\sqrt{u}}\right)^8}{(t^2 + 1)^5} dt \\
&+ \frac{2048}{\pi \rho^4} \int_1^\infty \frac{u^5 du}{a_{22}^4(u, 1) c^8(u, 1)} \int_{\frac{a_{11}(u, 1) - a_{12}(u, 1)}{\sqrt{u}}}^{\frac{a_{11}(u, 1) + a_{12}(u, 1)}{\sqrt{u}}} \frac{\left(t + \frac{a_{22}(u, 1) - a_{12}(u, 1)}{\sqrt{u}}\right)^8}{(t^2 + 1)^5} dt \\
&- \frac{2048}{\pi \rho^4} \int_1^\infty \frac{u}{a_{11}^4(u, 1)} du \int_{\frac{a_{22}(u, 1) - a_{12}(u, 1)}{\sqrt{u}}}^{\frac{a_{22}(u, 1) + a_{12}(u, 1)}{\sqrt{u}}} \frac{dt}{(t^2 + 1)^5} \\
&- \frac{2048}{\pi \rho^4} \int_1^\infty \frac{u}{a_{22}^4(u, 1)} du \int_{\frac{a_{11}(u, 1) - a_{12}(u, 1)}{\sqrt{u}}}^{\frac{a_{11}(u, 1) + a_{12}(u, 1)}{\sqrt{u}}} \frac{dt}{(t^2 + 1)^5} + O(\rho^{-5})
\end{aligned}$$

where $c(u, 1) = a_{11}(u, 1) + a_{22}(u, 1) - 2a_{12}(u, 1)$.

Now, combining Eqs.(5.13), (5.16), (5.18) and (5.6) with Property 7, we can arrive at the following:

$$\begin{aligned}
P_c(\hat{\mathbf{s}}|\theta) &= E_{\lambda_1 \geq \lambda_2} [1] - E_{\lambda_1 \geq \lambda_2} [J_1(\boldsymbol{\lambda}, \theta)] - E_{\lambda_1 \geq \lambda_2} [J_2(\boldsymbol{\lambda}, \theta)] + E_{\lambda_1 \geq \lambda_2} [J_3(\boldsymbol{\lambda}, \theta)] \\
&\quad - E_{\lambda_1 \geq \lambda_2} [J_4(\boldsymbol{\lambda}, \theta)] - E_{\lambda_1 \geq \lambda_2} [J_5(\boldsymbol{\lambda}, \theta)] \\
&= 1 - \frac{35(3 - 2 \cos^2 \theta)}{128 \sin^4 \theta} \rho^{-4} - \frac{35(3 - 2 \sin^2 \theta)}{256 \cos^4 \theta} \rho^{-4} - E_{\lambda_1 \geq \lambda_2} [J_4(\boldsymbol{\lambda}, \theta)] \\
&\quad - E_{\lambda_1 \geq \lambda_2} [J_5(\boldsymbol{\lambda}, \theta)] + O(\rho^{-5}) \tag{5.23}
\end{aligned}$$

Using Properties 8 and 9 and grouping together similar terms in the combined equation, we obtain

$$\begin{aligned}
& \mathbb{E}_{\lambda_1 \geq \lambda_2} [J_4(\boldsymbol{\lambda}, \theta)] + \mathbb{E}_{\lambda_1 \geq \lambda_2} [J_5(\boldsymbol{\lambda}, \theta)] \\
&= \frac{4096}{\pi \rho^4} \int_1^\infty \frac{u}{a_{11}^4(u, 1)} du \int_0^{\frac{a_{22}(u, 1) - a_{12}(u, 1)}{\sqrt{u}}} \frac{dt}{(t^2 + 1)^5} \\
&\quad - \frac{280(3 - 2 \cos^2 \theta)}{3 \sin^4 \theta} \rho^{-4} + \frac{4096}{\pi \rho^4} \int_1^\infty \frac{u}{a_{22}^4(u, 1)} du \int_0^{\frac{a_{11}(u, 1) - a_{12}(u, 1)}{\sqrt{u}}} \frac{dt}{(t^2 + 1)^5} \\
&\quad + \frac{2048}{\pi \rho^4} \int_1^\infty \frac{u^5}{a_{11}^4(u, 1) c^8(u, 1)} du \int_{\frac{a_{22}(u, 1) - a_{12}(u, 1)}{\sqrt{u}}}^{\frac{a_{22}(u, 1) + a_{12}(u, 1)}{\sqrt{u}}} \frac{\left(t + \frac{a_{11}(u, 1) - a_{12}(u, 1)}{\sqrt{u}}\right)^8}{(t^2 + 1)^5} dt \\
&\quad + \frac{2048}{\pi \rho^4} \int_1^\infty \frac{u^5}{a_{22}^4(u, 1) c^8(u, 1)} du \int_{\frac{a_{11}(u, 1) - a_{12}(u, 1)}{\sqrt{u}}}^{\frac{a_{11}(u, 1) + a_{12}(u, 1)}{\sqrt{u}}} \frac{\left(t + \frac{a_{22}(u, 1) - a_{12}(u, 1)}{\sqrt{u}}\right)^8}{(t^2 + 1)^5} dt \\
&\quad + O(\rho^{-5}) \tag{5.24}
\end{aligned}$$

where $c(u, 1) = a_{11}(u, 1) + a_{22}(u, 1) - 2a_{12}(u, 1)$. All the above discussions can be summarized as the following theorem:

Theorem 5. *Let $P_e(\hat{\mathbf{s}}|\theta)$ denote the average probability of erroneous decisions, i.e., $P_e(\hat{\mathbf{s}}|\theta) = 1 - P_c(\hat{\mathbf{s}}|\theta)$. Then, for large values of the SNR per symbol, ρ , we have the following asymptotic expression:*

$$P_e(\hat{\mathbf{s}}|\theta) = G(\theta) \rho^{-4} + O(\rho^{-5}) \tag{5.25}$$

where $G(\theta)$ is called the coding gain and is given by

$$G(\theta) = \frac{3080(3 - 2 \cos^2 \theta)}{3 \sin^4 \theta} + \frac{560(3 - 2 \sin^2 \theta)}{\cos^4 \theta} + G_1(\theta) + G_2(\theta) \tag{5.26}$$

with $G_1(\theta)$ and $G_2(\theta)$ defined by

$$\begin{aligned}
G_1(\theta) &= \frac{4096}{\pi} \int_1^\infty \frac{u}{a_{11}^4(u, 1)} du \int_0^{\frac{a_{22}(u,1)-a_{12}(u,1)}{\sqrt{u}}} \frac{dt}{(t^2 + 1)^5} \\
&\quad + \frac{4096}{\pi} \int_1^\infty \frac{u}{a_{22}^4(u, 1)} du \int_0^{\frac{a_{11}(u,1)-a_{12}(u,1)}{\sqrt{u}}} \frac{dt}{(t^2 + 1)^5} \\
G_2(\theta) &= \frac{2048}{\pi} \int_1^\infty \frac{u^5}{a_{11}^4(u, 1)c^8(u, 1)} du \int_{\frac{a_{22}(u,1)-a_{12}(u,1)}{\sqrt{u}}}^{\frac{a_{22}(u,1)+a_{12}(u,1)}{\sqrt{u}}} \frac{\left(t + \frac{a_{11}(u,1)-a_{12}(u,1)}{\sqrt{u}}\right)^8}{(t^2 + 1)^5} dt \\
&\quad + \frac{2048}{\pi} \int_1^\infty \frac{u^5}{a_{22}^4(u, 1)c^8(u, 1)} du \int_{\frac{a_{11}(u,1)-a_{12}(u,1)}{\sqrt{u}}}^{\frac{a_{11}(u,1)+a_{12}(u,1)}{\sqrt{u}}} \frac{\left(t + \frac{a_{22}(u,1)-a_{12}(u,1)}{\sqrt{u}}\right)^8}{(t^2 + 1)^5} dt
\end{aligned}$$

and $c(u, 1) = a_{11}(u, 1) + a_{22}(u, 1) - 2a_{12}(u, 1)$.

Theorem 5 provides us with a closed form expression of the probability of error in terms of the rotation angle θ for the simplified ML detector that can be applied in the 4×1 MISO system. The optimal rotation angle can then be found in order to minimize the probability of error, P_e , when a STBC of the form of Eq.(4.2) is employed.

5.4 Optimal Rotation Angle for the Minimum Probability of Error for the 4-Group Decodable STBC

Theorem 5 provides us with an expression for the coding gain, $G(\theta)$, in terms of the 4-group decodable STBC rotation angle, θ . Here, $G(\theta)$ consists of a sum of two closed-form functions of θ and two Gaussian integrals, $G_1(\theta)$ and $G_2(\theta)$. These Gaussian integrals can be evaluated numerically at different values of θ . These together with the two closed-form functions of θ provides us with the numerical values of $G(\theta)$ enabling

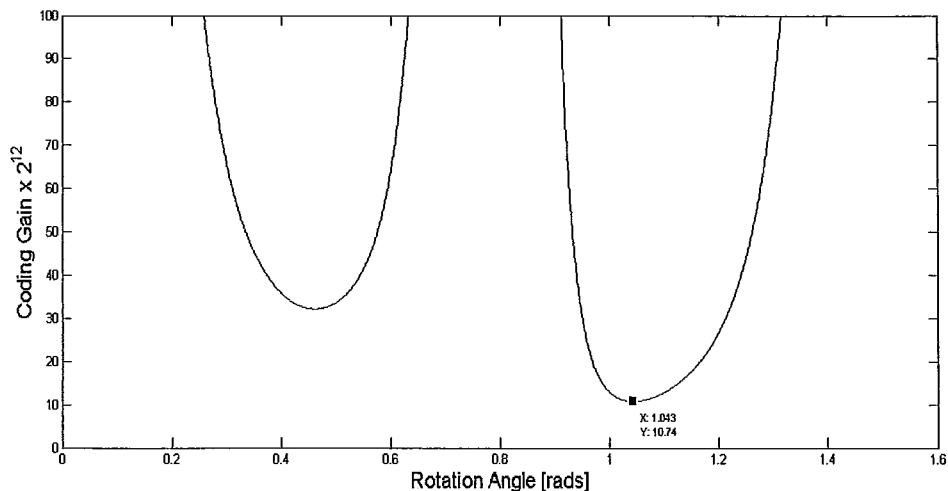


Figure 5.3: The Coding Gain as a Function of the Rotation Angle of a 4-Group Decodable STBC

us to locate the optimal θ yielding the minimum average probability of error. The numerical evaluation of $G(\theta)$ is shown in Fig. 5.3, where the optimal θ was found to be $\theta_{\text{opt}} = 1.043$ rad, yielding a minimum $G(\theta)$, $G_{\min}(\theta) = 10.737 \times 2^{12}$. Thus, θ_{opt} is the optimum angle of rotation for the 4-QAM constellation so that the probability of error is reduced to a minimum when detected by the simplified ML detector. Note that $G(\theta) \rightarrow \infty$ at points $\theta = 0, \pi/4, \pi/2$, which should be impossible since $P_e \leq 1$. This is due to the assumptions made in the proofs of Properties 6, 8 and 9, that the functions J_1, \dots, J_5 all exist as functions of λ_1, λ_2 and ρ^{-4} , for any value of θ . In other words, we assume full diversity for the system when calculating $P_e(\hat{\mathbf{s}}|\theta)$ in Theorem 5. From Appendix B.4, B.6 and B.7, one can see that this assumption does not hold for $\theta = 0, \pi/4, \pi/2$, and the integrals with respect to u tend to ∞ at those values of θ .

Chapter 6

Summary and Conclusion

6.1 Summary

In this thesis, two problems concerning MISO systems have been considered.

The first problem involved the design of STBC codes for the MISO system. We examined the performance of the Su-Xia rotated quasi-orthogonal STBC for large QAM constellation and concluded that the deterioration of performance was due to the increase of the *average number of nearest neighbours*. By examining the average block error probability instead of the PEP, the average number of nearest neighbours was included as a new factor to the conventional rotated quasi-orthogonal STBC design criterion. It was shown that the currently accepted optimal rotation angle of $\pi/4$ in the Su-Xia code is not optimal for square QAM constellations in terms of this new factor. In fact, by making use of the Pell Diophantine equation and Diophantine approximation theory, we proved that the average number of nearest neighbours per symbol tends to infinity for the Su-Xia code, when the size of the constellation is infinite. This result is shown in Theorem 1. Furthermore, we found a novel rotation

angle, $\pi/6$, and proved that the resulting rotated quasi-orthogonal STBC not only provides full diversity and the optimal coding gain, but also has a average number of nearest neighbours per symbol that tends to 8, when the constellation size tends to infinity. This is shown in Theorem 2. The simulation results obtained verify these theoretical analysis.

The second problem that was examined was the irregular geometrical structure of the decision regions, for a general MIMO channel equipped with the ML detector. These decision regions are so irregular that it would be impossible to obtain an explicit exact error probability formula for the ML receiver. Thus, current STBC designs in a MIMO system are mainly based on the PEP (or its upper bound). This means that the exact error probability formula cannot be used as a criterion for the design of the optimal transmitter for the MIMO systems, and the current STBC designs may not be truly optimum in terms of the exact error probability. To rectify this problem, in this thesis, a closed form of the exact error probability for a 4×1 MISO system, equipped with a ML detector transmitting signals from a 4-QAM constellation, was derived based on novel analyses of different Gaussian probability integrals. These analyses are listed as properties and lemmas in Appendix B and C. For such a system, we first obtained a closed-form algorithm for ML detection such that given a received signal and the channel, the transmitted signal was obtained by a simple threshold decision. This result is shown in Theorem 3. Then, the ML decision regions for all the transmitted signal were completely and explicitly determined and are shown in Theorem 4, with the decision regions presented in Figs. 4.2(a) and 4.2(b). These decision regions obtained have a geometrical structure with symmetric properties, allowing for a much simplified calculation of the closed form error probability, and,

thus, a closed form error probability was analyzed utilizing these decision regions. Specifically, we analyzed the asymptotic behavior of the average error performance taken over all random channel coefficients, when SNR is high. This resulted in an asymptotic expression of the probability of error found in Theorem 5. Finally, the closed-form expression of the error probability was applied to the 4-group decodable STBC, and the optimal rotation angle was obtained to minimize the probability of error, based on the asymptotic closed form probability of error formula. This result is shown in Fig. 5.3 with the optimal rotation angle being 1.043 rad.

6.2 Future Work

Looking forward, there are a number of different problems, yet unresolved by this thesis, that can be undertaken. These are listed as follows:

1. Finding the optimal rotation angle with respect to the average number of nearest neighbours criterion: In this thesis, the current optimal rotation angle for rotated quasi-orthogonal STBC, $\pi/4$, was found to be undesirable with respect to the average number of nearest neighbours criterion. Thus, a new rotation angle of $\pi/6$ was introduced, which is optimal in terms of the current STBC design criterion, and, in addition, performs much better than the STBC with an angle of $\pi/4$, when the QAM constellation size tends to infinity. However, it has not been proven if $\pi/6$ is the optimal rotation angle in terms of this new factor.
2. Creating a closed form ML detection algorithm and closed form error probabil-

ity analysis for any general square QAM constellation: A closed form ML detection algorithm and closed form ML probability of error were obtained for a 4×1 MISO system given transmitted signals from a 4-QAM constellation. Further research can be done to extend this algorithm to any general square QAM transmitted signal constellation.

3. Extending the closed form ML detection algorithm to the rotated quasi-orthogonal STBC structures: The closed form ML detection algorithm was solved for a 4-group decodable STBC structure. Further research can be done to extend this algorithm to different STBC structures, such as the rotated quasi-orthogonal STBC.

6.3 Conclusion

In this thesis, a new STBC design criterion for the ML receiver and a closed form ML detection algorithm for a 4-group decodable STBC were created for a 4×1 MISO system. The results obtained are very encouraging and shows that these ideas deserve further exploration. In the previous section, a few elaborations to this research were suggested - these are by no means exhaustive. Until these areas are fully explored, the research on this subject will be far from complete, by which time, other theories will be put forth, and research on MIMO communications will continue onward, allowing for greater knowledge and improvement of wireless communications.

Appendix A

Proofs of Lemmas in Chapter 3

A.1 Proof of Lemma 2

Proof. First, we consider the case where $|b| = 1$. If $b = 1$, then, $\Delta(a, 1) = 2\sqrt{3}a + a^2 - 1$. The two roots of quadratic equation $a^2 + 2\sqrt{3}a - 1 = 0$ are $a_1 = -(1 + \sqrt{3})$ and $a_2 = 2 - \sqrt{3}$ and thus, there are only three integers in the interval $[a_1, a_2]$, i.e., $-2, -1, 0$. In this case, it can be verified by calculation that $|\Delta(-2, 1)| = |3 - 4\sqrt{3}| > 1$ and $|\Delta(-1, 1)| = |-2\sqrt{3}| > 1$.

On the other hand, we know that function $\Delta(a, 1)$ is monotonically decreasing and greater than 0 for $a < a_1$ and that $\Delta(a, 1)$ is monotonically increasing and greater than 0 for $a > a_2$. The integer closest to a_1 is $a_L = -3$ and the integer closest to a_2 is $a_R = 1$. Since $|\Delta(a_L, 1)| > 1$ and $|\Delta(a_R, 1)| > 1$, we arrive at $|\Delta(a, 1)| > 1$ for either $a \leq a_L$ or $a \geq a_R$. Therefore, $|\Delta(a, 1)| > 1$ for any nonzero integer a . Similarly, we can also prove that $|\Delta(a, -1)| > 1$ for any nonzero integer a .

Hence, in the following, we only need to consider the case where $|b| \geq 2$. We

notice that $\Delta(a, b)$ can be decomposed into a product of the following three factors:

$$\Delta(a, b) = b^2 \left(\frac{a}{b} - (2 - \sqrt{3}) \right) \left(\frac{a}{b} + (2 + \sqrt{3}) \right) \quad (\text{A.1})$$

We consider the following two cases:

Case 1: $\frac{a}{b} > -\sqrt{3}$. In this case, let $\delta_1 = \frac{1}{8}$ and examine three possibilities:

1. $-\sqrt{3} < \frac{a}{b} < 2 - \sqrt{3} - \delta_1$. In this situation, we have

$$\begin{aligned} |\Delta(a, b)| &= b^2 \left| \frac{a}{b} - (2 - \sqrt{3}) \right| \left| \frac{a}{b} + (2 + \sqrt{3}) \right| \\ &> 4 \times \delta_1 \times \left| (2 + \sqrt{3}) - \sqrt{3} \right| \\ &= 8\delta_1 = 1 \end{aligned} \quad (\text{A.2})$$

2. $\frac{a}{b} > 2 - \sqrt{3} + \delta_1$. Similar to Situation 1, we can obtain

$$\begin{aligned} |\Delta(a, b)| &= b^2 \left| \frac{a}{b} - (2 - \sqrt{3}) \right| \left| \frac{a}{b} + (2 + \sqrt{3}) \right| \\ &> 4 \times \delta_1 \times \left| (2 - \sqrt{3}) + \delta_1 + (2 + \sqrt{3}) \right| \\ &= 4\delta_1(4 + \delta_1) > 1 \end{aligned} \quad (\text{A.3})$$

3. $2 - \sqrt{3} - \delta_1 < \frac{a}{b} < 2 - \sqrt{3} + \delta_1$. In this situation, for discussion convenience, we let $u_1 = 2 - \sqrt{3}$ and $f_1(u) = u^2 - 4u + 1$. Then, $f_1(u_1) = 0$ and

$$\begin{aligned} f_1\left(\frac{a}{b}\right) &= f_1\left(\frac{a}{b}\right) - f_1(u_1) \\ &= \left(\frac{a}{b} - u_1\right) \left(\frac{a}{b} + u_1 - 4\right) \\ &= \left(\frac{a}{b} - u_1\right) \left(\frac{a}{b} - (2 + \sqrt{3})\right) \end{aligned} \quad (\text{A.4})$$

Hence, we have that

$$\begin{aligned} \frac{a}{b} - u_1 &= \frac{f_1\left(\frac{a}{b}\right)}{\frac{a}{b} - (2 + \sqrt{3})} \\ &= \frac{a^2 - 4ab + b^2}{b^2\left(\frac{a}{b} - (2 + \sqrt{3})\right)} \end{aligned}$$

which leads to

$$\begin{aligned} \left|\frac{a}{b} - u_1\right| &\geq \frac{1}{b^2\left|\frac{a}{b} - (2 + \sqrt{3})\right|} \\ &= \frac{1}{b^2\left(2 + \sqrt{3} - \frac{a}{b}\right)} \end{aligned} \tag{A.5}$$

since $|a^2 - 4ab + b^2| > 1$ for any nonzero integers a and b and $0 < \frac{a}{b} < 2 + \sqrt{3}$.

Now, combining Eq. (A.1) with Eq. (A.5) yields

$$\begin{aligned} |\Delta(a, b)| &\geq \left| \frac{2 + \sqrt{3} + \frac{a}{b}}{2 + \sqrt{3} - \frac{a}{b}} \right| \\ &= \frac{2 + \sqrt{3} + \frac{a}{b}}{2 + \sqrt{3} - \frac{a}{b}} \\ &> 1 \end{aligned}$$

Therefore, we can conclude in Case 1 that $|\Delta(a, b)| > 1$.

Case 2: $\frac{a}{b} < -\sqrt{3}$. In this case, similar to Case 1, let $\delta_2 = \frac{1}{8}$ and consider the following three situations:

1. $-2 - \sqrt{3} + \delta_2 < \frac{a}{b} < -\sqrt{3}$. In this situation, we have

$$\begin{aligned}
 |\Delta(a, b)| &= b^2 \left| \frac{a}{b} - (2 - \sqrt{3}) \right| \left| \frac{a}{b} + (2 + \sqrt{3}) \right| \\
 &> 4 \times \left| (2 - \sqrt{3}) + \sqrt{3} \right| \times \delta_2 \\
 &= 8\delta_2 = 1
 \end{aligned} \tag{A.6}$$

2. $\frac{a}{b} < -2 - \sqrt{3} - \delta_2$. Similar to Situation 1, we can obtain

$$\begin{aligned}
 |\Delta(a, b)| &= b^2 \left| \frac{a}{b} - (2 - \sqrt{3}) \right| \left| \frac{a}{b} + (2 + \sqrt{3}) \right| \\
 &> 4 \times \left| (-2 - \sqrt{3} - \delta_2) - (2 - \sqrt{3}) \right| \times \delta_2 \\
 &= 4\delta_2(4 + \delta_2) > 1
 \end{aligned} \tag{A.7}$$

3. $-2 - \sqrt{3} - \delta_2 < \frac{a}{b} < -2 - \sqrt{3} + \delta_2$. In this situation, for notational convenience, we let $u_2 = -2 - \sqrt{3}$ and $f_2(u) = u^2 + 4u + 1$. Then, $f_2(u_2) = 0$ and

$$\begin{aligned}
 f_2\left(\frac{a}{b}\right) &= f_2\left(\frac{a}{b}\right) - f_2(u_2) \\
 &= \left(\frac{a}{b} - u_2\right) \left(\frac{a}{b} + u_2 + 4\right) \\
 &= \left(\frac{a}{b} - u_2\right) \left(\frac{a}{b} + (2 - \sqrt{3})\right)
 \end{aligned} \tag{A.8}$$

Hence, we have that

$$\begin{aligned}
 \frac{a}{b} - u_2 &= \frac{f_2\left(\frac{a}{b}\right)}{\frac{a}{b} - (2 + \sqrt{3})} \\
 &= \frac{a^2 - 4ab + b^2}{b^2 \left(\frac{a}{b} + (2 - \sqrt{3})\right)}
 \end{aligned}$$

which leads to

$$\begin{aligned} \left| \frac{a}{b} - u_2 \right| &\geq \frac{1}{b^2 \left| \frac{a}{b} + (2 - \sqrt{3}) \right|} \\ &= \frac{1}{b^2 \left(-\frac{a}{b} - (2 - \sqrt{3}) \right)} \end{aligned} \quad (\text{A.9})$$

since $|a^2 - 4ab + b^2| > 1$ for any nonzero integers a and b and $\frac{a}{b} < -(2 - \sqrt{3}) < 0$.

Now, combining Eq. (A.1) with Eq. (A.9) yields

$$\begin{aligned} |\Delta(a, b)| &\geq \left| \frac{\frac{a}{b} - (2 - \sqrt{3})}{\frac{a}{b} + (2 - \sqrt{3})} \right| \\ &= \frac{-\frac{a}{b} + (2 - \sqrt{3})}{-\frac{a}{b} - (2 - \sqrt{3})} \\ &> 1 \end{aligned}$$

we can prove that $|\Delta(a, b)| > 1$ and thus, complete the proof of Lemma 2. \square

A.2 Proof of Lemma 3

Proof. The proof of Lemma 3 is similar to that of Lemma 2. First, we examine the case where $|b| = 1$. If $b = 1$, then, $\mathcal{E}(a, 1) = 2a + \sqrt{3}(a^2 - 1)$. The two roots of quadratic equation $\mathcal{E}(a, 1) = \sqrt{3}a^2 + 2a - \sqrt{3} = 0$ are $a_1 = -\sqrt{3}$ and $a_2 = \frac{\sqrt{3}}{3}$. There are only three integers belonging to the interval $[a_1, a_2]$, i.e., $-1, 0, 1$.

It is not difficult to check that $|\mathcal{E}(\pm 1, 1)| = 2 > 1$. In addition, we know that function $\mathcal{E}(a, 1)$ is monotonically decreasing and greater than 0 for $a < a_1$, and that $\mathcal{E}(a, 1)$ is monotonically increasing and greater than 0 for $a > a_2$. If we let a_R and a_L denote the two integers closest to a_1 and a_2 , respectively, then, $a_L = -2$ and $a_R = 2$.

Since $|\mathcal{E}(a_L, 1)| > 1$ and $|\mathcal{E}(a_R, 1)| > 1$, we obtain $|\mathcal{E}(a, 1)| > 1$ for either $a \leq a_L$ or $a \geq a_R$. Therefore, we always have $|\mathcal{E}(a, 1)| > 1$ for any nonzero integer a . Similarly, we can also prove that $|\mathcal{E}(a, -1)| > 1$ for any nonzero integer a .

Hence, in the following, we only need to examine the case where $|b| \geq 2$. Note that $\mathcal{E}(a, b)$ can be decomposed into a product of the following three factors:

$$\mathcal{E}(a, b) = \sqrt{3}b^2 \left(\frac{a}{b} - \frac{\sqrt{3}}{3} \right) \left(\frac{a}{b} + \sqrt{3} \right) \quad (\text{A.10})$$

We consider the following two cases:

Case 1: $\frac{a}{b} > -\frac{\sqrt{3}}{3}$. In this case, we let $\varepsilon_1 = \frac{1}{8}$ and discuss three possibilities:

1. $-\frac{\sqrt{3}}{3} < \frac{a}{b} < \frac{\sqrt{3}}{3} + \varepsilon_1$. In this situation, we have

$$\begin{aligned} |\mathcal{E}(a, b)| &= \sqrt{3}b^2 \left| \frac{a}{b} - \frac{\sqrt{3}}{3} \right| \left| \frac{a}{b} + \sqrt{3} \right| \\ &> 4\sqrt{3} \times \varepsilon_1 \times \left| \sqrt{3} - \frac{\sqrt{3}}{3} \right| \\ &= 8\varepsilon_1 = 1 \end{aligned} \quad (\text{A.11})$$

2. $\frac{a}{b} > \frac{\sqrt{3}}{3} + \varepsilon_1$. Similar to Situation 1, we can obtain

$$\begin{aligned} |\mathcal{E}(a, b)| &= \sqrt{3}b^2 \left| \frac{a}{b} - \frac{\sqrt{3}}{3} \right| \left| \frac{a}{b} + \sqrt{3} \right| \\ &> 4\sqrt{3} \times \delta_1 \times \left| \frac{\sqrt{3}}{3} + \varepsilon_1 + \sqrt{3} \right| \\ &= 4\varepsilon_1 \left(\frac{4\sqrt{3}}{3} + \varepsilon_1 \right) > 1 \end{aligned} \quad (\text{A.12})$$

3. $\frac{\sqrt{3}}{3} - \varepsilon_1 < \frac{a}{b} < \frac{\sqrt{3}}{3} + \varepsilon_1$. In this situation, for discussion convenience, we let

$v_1 = \frac{\sqrt{3}}{3}$ and $g_1(v) = 3v^2 - 1$. Then, $g_1(v_1) = 0$ and

$$\begin{aligned} g_1\left(\frac{a}{b}\right) &= g_1\left(\frac{a}{b}\right) - g_1(v_1) \\ &= 3\left(\frac{a}{b} - v_1\right)\left(\frac{a}{b} + v_1\right) \end{aligned}$$

Hence, we can obtain

$$\begin{aligned} \frac{a}{b} - v_1 &= \frac{g_1\left(\frac{a}{b}\right)}{3\left(\frac{a}{b} + v_1\right)} \\ &= \frac{3a^2 - b^2}{3b^2\left(\frac{a}{b} + v_1\right)} \end{aligned}$$

which leads to

$$\begin{aligned} \left|\frac{a}{b} - v_1\right| &\geq \frac{1}{3b^2\left|\frac{a}{b} + v_1\right|} \\ &= \frac{1}{3b^2\left(\frac{a}{b} + v_1\right)} \end{aligned} \tag{A.13}$$

since $|3a^2 - b^2| > 1$ for any nonzero integers a and b and $\frac{a}{b} > \frac{\sqrt{3}}{3} - \varepsilon_1 > 0$. Now, combining Eq.(A.10) with Eq.(A.13) yields

$$\begin{aligned} |\mathcal{E}(a, b)| &\geq \frac{\sqrt{3}}{3} \cdot \left| \frac{\frac{a}{b} + \sqrt{3}}{\frac{a}{b} + v_1} \right| \\ &= \frac{\sqrt{3}}{3} \cdot \frac{\frac{a}{b} + \sqrt{3}}{\frac{a}{b} + v_1} \\ &> \frac{\sqrt{3}}{3} \cdot \frac{1 + \sqrt{3}}{1 + v_1} \\ &= 1 \end{aligned}$$

since $\frac{a}{b} < \frac{\sqrt{3}}{3} - \varepsilon_1 < 1$ and function $\frac{a/b+\sqrt{3}}{a/b+v_1}$, with respect to variable $\frac{a}{b}$, is monotonically decreasing for $\frac{a}{b} > 0$. Therefore, we can conclude that $|\Delta(a, b)| > 1$ in this case.

Case 2: $\frac{a}{b} < -\frac{\sqrt{3}}{3}$. In this case, similar to Case 1, we let $\varepsilon_2 = \frac{1}{8}$ and consider the following three situations:

1. $-\sqrt{3} + \varepsilon_2 < \frac{a}{b} < -\frac{\sqrt{3}}{3}$. In this situation, we have

$$\begin{aligned}
 |\mathcal{E}(a, b)| &= \sqrt{3}b^2 \left| \frac{a}{b} - \frac{\sqrt{3}}{3} \right| \left| \frac{a}{b} + \sqrt{3} \right| \\
 &> 4\sqrt{3} \times \left| \frac{\sqrt{3}}{3} + \frac{\sqrt{3}}{3} \right| \times \varepsilon_2 \\
 &= 8\varepsilon_2 = 1
 \end{aligned} \tag{A.14}$$

2. $\frac{a}{b} < -\sqrt{3} - \varepsilon_2$. Similar to Situation 1, we can obtain

$$\begin{aligned}
 |\mathcal{E}(a, b)| &= \sqrt{3}b^2 \left| \frac{a}{b} - \frac{\sqrt{3}}{3} \right| \left| \frac{a}{b} + \sqrt{3} \right| \\
 &> 4\sqrt{3} \times \left| (-\sqrt{3} - \varepsilon_2) - \frac{\sqrt{3}}{3} \right| \times \varepsilon_2 \\
 &= 4\sqrt{3} \varepsilon_2 \left(\frac{4\sqrt{3}}{3} + \varepsilon_2 \right) > 1
 \end{aligned} \tag{A.15}$$

3. $-\sqrt{3} - \varepsilon_2 < \frac{a}{b} < -\sqrt{3} + \varepsilon_2$. In this situation, for notational convenience, we let $v_2 = -\sqrt{3}$ and $g_2(v) = v^2 - 3$. Then, $g_2(v_2) = 0$ and

$$\begin{aligned}
 g\left(\frac{a}{b}\right) &= g\left(\frac{a}{b}\right) - g_2(v_2) \\
 &= \left(\frac{a}{b} - v_2\right) \left(\frac{a}{b} + v_2\right) \\
 &= \left(\frac{a}{b} - v_2\right) \left(\frac{a}{b} + v_2\right)
 \end{aligned} \tag{A.16}$$

Hence, we have that

$$\begin{aligned} \frac{a}{b} - v_2 &= \frac{g_2\left(\frac{a}{b}\right)}{\frac{a}{b} + v_2} \\ &= \frac{a^2 - 3b^2}{b^2\left(\frac{a}{b} + v_2\right)} \end{aligned}$$

which leads to

$$\begin{aligned} \left| \frac{a}{b} - v_2 \right| &\geq \frac{1}{b^2 \left| \frac{a}{b} + v_2 \right|} \\ &= \frac{1}{b^2 \left(-\frac{a}{b} + \sqrt{3} \right)} \end{aligned} \tag{A.17}$$

since $|a^2 - 3b^2| > 1$ for any nonzero integers a and b and $\frac{a}{b} < -\sqrt{3} + \varepsilon_2 < 0$.

Now, combining Eq. (A.10) with (A.17) yields

$$\begin{aligned} |\mathcal{E}(a, b)| &\geq \sqrt{3} \left| \frac{\frac{a}{b} - \frac{\sqrt{3}}{3}}{\frac{a}{b} + v_2} \right| \\ &= \sqrt{3} \times \frac{-\frac{a}{b} + \frac{\sqrt{3}}{3}}{-\frac{a}{b} + \sqrt{3}} \\ &> \sqrt{3} \times \frac{1 + \frac{\sqrt{3}}{3}}{1 + \sqrt{3}} \\ &= 1 \end{aligned}$$

This completes the proof of Lemma 3. □

Appendix B

Proofs of Properties in Chapter 5

In this appendix we let $\bar{\rho} = \rho/8$ to simplify the calculations.

B.1 Proof of Property 3

Proof. Notice that $\mathbf{A} = \mathbf{R}^T \text{diag}(\lambda_1, \lambda_2) \mathbf{R}$. If we let $\bar{\mathbf{A}} = \mathbf{R}^T \text{diag}(\lambda_2, \lambda_1) \mathbf{R}$, then, we have

$$\begin{aligned} \mathbf{A} &= \begin{pmatrix} \cos \theta & -\sin \theta \\ \sin \theta & \cos \theta \end{pmatrix} \begin{pmatrix} 0 & -1 \\ 1 & 0 \end{pmatrix} \begin{pmatrix} \lambda_2 & 0 \\ 0 & \lambda_1 \end{pmatrix} \begin{pmatrix} 0 & 1 \\ -1 & 0 \end{pmatrix} \begin{pmatrix} \cos \theta & \sin \theta \\ -\sin \theta & \cos \theta \end{pmatrix} \\ &= \bar{\mathbf{R}}^T \begin{pmatrix} \lambda_2 & 0 \\ 0 & \lambda_1 \end{pmatrix} \bar{\mathbf{R}} \end{aligned} \tag{B.18}$$

On the other hand, we have

$$\begin{aligned}
\bar{\mathbf{R}} &= \begin{pmatrix} 0 & 1 \\ -1 & 0 \end{pmatrix} \begin{pmatrix} \cos \theta & \sin \theta \\ -\sin \theta & \cos \theta \end{pmatrix} \\
&= \begin{pmatrix} -\sin \theta & \cos \theta \\ -\cos \theta & -\sin \theta \end{pmatrix} \begin{pmatrix} 0 & -1 \\ 1 & 0 \end{pmatrix} \begin{pmatrix} 0 & 1 \\ -1 & 0 \end{pmatrix} \\
&= \begin{pmatrix} \cos \theta & \sin \theta \\ -\sin \theta & \cos \theta \end{pmatrix} \begin{pmatrix} 0 & 1 \\ -1 & 0 \end{pmatrix} = \mathbf{R} \begin{pmatrix} 0 & 1 \\ -1 & 0 \end{pmatrix} \tag{B.19}
\end{aligned}$$

Now, substituting Eq.(B.19) into Eq.(B.18) produces

$$\mathbf{A} = \begin{pmatrix} 0 & -1 \\ 1 & 0 \end{pmatrix} \bar{\mathbf{A}} \begin{pmatrix} 0 & 1 \\ -1 & 0 \end{pmatrix}$$

By combining this with $\Sigma_{\nu\nu} = \frac{1}{2\rho}\mathbf{A}$ and $\mathbf{z}_0 = -\mathbf{A}(1 \ 1)^T$, we can obtain

$$\begin{aligned}
\frac{1}{2}(\mathbf{z} - \mathbf{z}_0)^T \Sigma_{\nu\nu}^{-1} (\mathbf{z} - \mathbf{z}_0) &= \bar{\rho}(\mathbf{z} + \mathbf{A}(-1 \ -1)^T)^T \mathbf{A}^{-1} (\mathbf{z} + \mathbf{A}(-1 \ -1)^T) \\
&= \bar{\rho}(\bar{\mathbf{z}} + \bar{\mathbf{A}}(1 \ -1)^T)^T \bar{\mathbf{A}}^{-1} (\bar{\mathbf{z}} + \bar{\mathbf{A}}(1 \ -1)^T)
\end{aligned}$$

where $\bar{\mathbf{z}}$ is determined by

$$\bar{\mathbf{z}} = \begin{pmatrix} 0 & 1 \\ -1 & 0 \end{pmatrix} \mathbf{z} = \begin{pmatrix} 0 & 1 \\ -1 & 0 \end{pmatrix} \begin{pmatrix} z_1 \\ z_2 \end{pmatrix} = \begin{pmatrix} z_2 \\ -z_1 \end{pmatrix}$$

Therefore, we have

$$\begin{aligned}
p(\mathbf{z}|H_3, (\lambda_1 \ \lambda_2)^T, \theta) &= \frac{\bar{\rho}}{\pi \sqrt{\det(\bar{\mathbf{A}})}} \exp\left(-\frac{1}{2}(\mathbf{z} - \mathbf{z}_0)^T \Sigma_{\nu\nu}^{-1}(\mathbf{z} - \mathbf{z}_0)\right) \\
&= \frac{\bar{\rho}}{\pi \sqrt{\det(\bar{\mathbf{A}})}} \exp\left(-\bar{\rho}(\bar{\mathbf{z}} + \bar{\mathbf{A}}(1 \ -1)^T)^T \bar{\mathbf{A}}^{-1}(\bar{\mathbf{z}} + \bar{\mathbf{A}}(1 \ -1)^T)\right) \\
&= p(\bar{\mathbf{z}}|H_2, (\lambda_1 \ \lambda_2)^T, \theta)
\end{aligned}$$

This gives the proof of Eq.(5.7a) in Property 3. Similarly, we can obtain the proof of Eq.(5.7b) and thus, completes the proof of Property 3. \square

B.2 Proof of Property 4

Proof. We know from Eqs.(4.34) that for $a_{12} < 0$, the probability of the correct decision on $\tilde{\mathbf{s}} = \boldsymbol{\varsigma}_3 = (1 \ 1)^T$ is given by

$$P_c(\hat{\tilde{\mathbf{s}}}|H_3, \theta, \boldsymbol{\lambda}, \lambda_1 < \lambda_2) = \iint_{\mathcal{Z}_3|_{a_{12}<0}} p(\mathbf{z}|H_3, (\lambda_1 \ \lambda_2)^T, \theta) dz_2 dz_1$$

By Property 3, $P_c(\hat{\tilde{\mathbf{s}}}|H_3, \theta, \boldsymbol{\lambda}, \lambda_1 < \lambda_2)$ can be represented as

$$P_c(\hat{\tilde{\mathbf{s}}}|H_3, \theta, \boldsymbol{\lambda}, \lambda_1 < \lambda_2) = \iint_{\mathcal{Z}_3|_{a_{12}<0}} p(\bar{\mathbf{z}}|H_2, (\lambda_2 \ \lambda_1)^T, \theta) dz_2 dz_1 \quad (\text{B.20})$$

where $\bar{\mathbf{z}} = (z_2 \ -z_1)^T$. After transformation: $z_1 = -x_2$ and $z_2 = x_1$, the decision region, $\mathcal{Z}_3|_{a_{12}<0}$, changes to

$$\Gamma_3|_{a_{12}<0} = \{(x_1, x_2) : x_1 \leq -a_{12}, x_2 \geq -a_{12}\} \cup \{(x_1, x_2) : |x_2| \leq -a_{12}, x_1 \leq x_2\}$$

Correspondingly, Eq.(B.20) is transformed into

$$P_c(\hat{\mathbf{s}}|H_3, \theta, \boldsymbol{\lambda}, \lambda_1 < \lambda_2) = \iint_{\Gamma_3|_{a_{12}<0}} p(\mathbf{x}|H_2, (\lambda_2 \ \lambda_1)^T, \theta) dx_1 dx_2 \quad (\text{B.21})$$

Therefore, if we let $f(\lambda_1, \lambda_2) = \lambda_1 \lambda_2 e^{-(\lambda_1 + \lambda_2)}$, then, we have

$$\begin{aligned} P_c(\hat{\mathbf{s}}|H_3, \theta, \lambda_1 < \lambda_2) &= E_{\lambda_1 < \lambda_2} [P_c(\hat{\mathbf{s}}|H_3, \theta, \boldsymbol{\lambda}, \lambda_1 < \lambda_2)] \\ &= \iint_{\lambda_1 < \lambda_2} f(\lambda_1, \lambda_2) \iint_{\Gamma_3|_{a_{12}<0}} p(\mathbf{x}|H_2, (\lambda_2 \ \lambda_1)^T, \theta) dx_1 dx_2 d\lambda_1 d\lambda_2 \\ &= \iint_{\mu_2 < \mu_1} f(\mu_2, \mu_1) \iint_{Z_2|_{a_{12} \geq 0}} p(\mathbf{z}|H_2, (\mu_1 \ \mu_2)^T, \theta) dz_1 dz_2 d\mu_1 d\mu_2 \\ &= \iint_{\mu_1 \geq \mu_2} f(\mu_1, \mu_2) \iint_{Z_2|_{a_{12} \geq 0}} p(\mathbf{z}|H_2, (\mu_1 \ \mu_2)^T, \theta) dz_1 dz_2 d\mu_1 d\mu_2 \\ &= P_c(\hat{\mathbf{s}}|H_2, \theta, \lambda_1 \geq \lambda_2) \end{aligned} \quad (\text{B.22})$$

where we use the fact that $f(\mu_2, \mu_1) = f(\mu_1, \mu_2)$. This gives the proof of Eq.(5.8a).

Similarly, we can obtain the proof of Eq.(5.8b) and hence, this completes the proof of Property 4. \square

B.3 Proof of Property 5

Proof. For notational simplicity, let

$$\mathbf{B} = \begin{bmatrix} b_{11} & b_{12} \\ b_{12} & b_{22} \end{bmatrix} = \mathbf{A}^{-1} \quad (\text{B.23})$$

where \mathbf{A} is defined in Eq.(4.13). Then, we have $b_{11} \det(\mathbf{A}) = a_{22}$, $b_{22} \det(\mathbf{A}) = a_{11}$, $b_{12} \det(\mathbf{A}) = -a_{12}$, and thus,

$$\begin{aligned}
J_1(\boldsymbol{\lambda}, \theta) &= \int_{-\infty}^{\infty} \int_{a_{22}}^{\infty} p(\tilde{\mathbf{z}}|\boldsymbol{\lambda}, \theta) d\tilde{z}_2 d\tilde{z}_1 \\
&= \frac{1}{2\pi \sqrt{\det(\boldsymbol{\Sigma}_{\nu\nu})}} \int_{-\infty}^{\infty} \int_{a_{22}}^{\infty} \exp\left(-\frac{1}{2} \tilde{\mathbf{z}}^T \boldsymbol{\Sigma}_{\nu\nu}^{-1} \tilde{\mathbf{z}}\right) d\tilde{z}_2 d\tilde{z}_1 \\
&= \frac{\bar{\rho}}{\pi \sqrt{\det(\mathbf{A})}} \int_{-\infty}^{\infty} \int_{a_{22}}^{\infty} \exp\left(-\bar{\rho} (b_{11} \tilde{z}_1^2 + 2b_{12} \tilde{z}_1 \tilde{z}_2 + b_{22} \tilde{z}_2^2)\right) d\tilde{z}_2 d\tilde{z}_1 \\
&= \frac{\bar{\rho}}{\pi \sqrt{\det(\mathbf{A})}} \int_{-\infty}^{\infty} \int_{a_{22}}^{\infty} \exp\left(-\bar{\rho} \left(b_{11} \left(\tilde{z}_1 + \frac{b_{12}}{b_{11}} \tilde{z}_2\right)^2 + \left(\frac{b_{11} b_{22} - b_{12}^2}{b_{11}}\right) \tilde{z}_2^2\right)\right) d\tilde{z}_2 d\tilde{z}_1 \\
&= \frac{\bar{\rho}}{\pi \sqrt{\det(\mathbf{A})}} \int_{-\infty}^{\infty} \exp(-\bar{\rho} b_{11} \tilde{z}_1^2) d\tilde{z}_1 \int_{a_{22}}^{\infty} \exp\left(-\frac{\bar{\rho} \det(\mathbf{B}) \tilde{z}_2^2}{b_{11}}\right) d\tilde{z}_2 \\
&= \frac{1}{\sqrt{2\pi \det(\mathbf{A}) \det(\mathbf{B})}} \int_{a_{22} \sqrt{\frac{2\bar{\rho} \det(\mathbf{B})}{b_{11}}}}^{\infty} \exp\left(-\frac{\tilde{z}_2^2}{2}\right) d\tilde{z}_2 \\
&= \frac{1}{\sqrt{2\pi}} \int_{a_{22} \sqrt{\frac{2\bar{\rho}}{b_{11} \det(\mathbf{A})}}}^{\infty} \exp\left(-\frac{\tilde{z}_2^2}{2}\right) d\tilde{z}_2 = Q\left(\frac{a_{22} \sqrt{2\bar{\rho}}}{\sqrt{b_{11} \det(\mathbf{A})}}\right) \\
&= Q\left(\sqrt{2\bar{\rho} a_{22}}\right) = Q\left(\frac{\sqrt{\rho a_{22}}}{2}\right)
\end{aligned}$$

This completes the proof of Eq.(5.20a) in Property 5. Similarly, we can prove Eqs.(5.20b) and (5.20c). This completes the proof of Property 5. \square

B.4 Proof of Property 6

Proof. Using the first formula of Eq.(5.11) and the probability density function of λ_1 and λ_2 , $\lambda_1\lambda_2e^{-(\lambda_1+\lambda_2)}$, we can express $E_{\lambda_1 \geq \lambda_2} \left[Q \left(\sqrt{2\bar{\rho}\alpha(\lambda_1, \lambda_2)} \right) \right]$ as

$$\begin{aligned} E_{\lambda_1 \geq \lambda_2} \left[Q \left(\sqrt{2\bar{\rho}\alpha(\lambda_1, \lambda_2)} \right) \right] &= \frac{1}{\pi} \int_0^\infty \int_{\lambda_2}^\infty \lambda_1 \lambda_2 e^{-(\lambda_1+\lambda_2)} d\lambda_1 d\lambda_2 \\ &\quad \times \int_0^{\pi/2} \exp \left(-\frac{\bar{\rho}\alpha(\lambda_1, \lambda_2)}{\sin^2 \phi} \right) d\phi \end{aligned}$$

This, after linear transformation $\lambda_1 = u\lambda_2$ and then using the homogenous linear property $\alpha(u\lambda_2, \lambda_2) = \lambda_2\alpha(u, 1)$, can be changed into

$$\begin{aligned} E_{\lambda_1 \geq \lambda_2} \left[Q \left(\sqrt{2\bar{\rho}\alpha(\lambda_1, \lambda_2)} \right) \right] &= \frac{1}{\pi} \int_0^{\pi/2} \int_1^\infty u du d\phi \\ &\quad \times \int_0^\infty \lambda_2^3 \exp \left(-\left(1 + u + \frac{\bar{\rho}\alpha(u, 1)}{\sin^2 \phi} \right) \lambda_2 \right) d\lambda_2 \\ &= \frac{6}{\pi} \int_0^{\pi/2} \int_1^\infty \frac{u}{\left(1 + u + \frac{\bar{\rho}\alpha(u, 1)}{\sin^2 \phi} \right)^4} du d\phi \\ &= \frac{6}{\pi \bar{\rho}^4} \int_0^{\pi/2} \sin^8 \phi d\phi \int_1^\infty \frac{u}{\alpha^4(u, 1)} du + O(\bar{\rho}^{-5}) \\ &= \frac{105}{128 \bar{\rho}^4} \int_1^\infty \frac{u}{\alpha^4(u, 1)} du + O(\bar{\rho}^{-5}) \\ &= 3360 \bar{\rho}^{-4} \int_1^\infty \frac{u}{\alpha^4(u, 1)} du + O(\bar{\rho}^{-5}) \end{aligned} \tag{B.24}$$

This completes the proof of Property 6. \square

B.5 Proof of Property 7

Proof. First, we have

$$\begin{aligned}
E_{\lambda_1 \geq \lambda_2} [1] &= \iint_{\lambda_1 \geq \lambda_2} \lambda_1 \lambda_2 e^{-(\lambda_1 + \lambda_2)} d\lambda_1 d\lambda_2 \\
&= \int_0^\infty \lambda_2 e^{-\lambda_2} d\lambda_2 \int_{\lambda_2}^\infty \lambda_1 e^{-\lambda_1} d\lambda_1 \\
&= \int_0^\infty (\lambda_2^2 + \lambda_2) e^{-2\lambda_2} d\lambda_2 = \frac{1}{2} \int_0^\infty (2\lambda_2 + 1) e^{-2\lambda_2} d\lambda_2 \\
&= \frac{1}{4} [1 + 1] = \frac{1}{2}
\end{aligned} \tag{B.25}$$

This completes the proof of Eq.(5.22a) in Property 7. In addition, notice that a_{22} is the linearly homogenous function with respect to λ_1 and λ_2 . Hence, applying Property 6 to $J_1(\boldsymbol{\lambda}, \theta)$ yields

$$\begin{aligned}
E_{\lambda_1 \geq \lambda_2} [J_1(\boldsymbol{\lambda}, \theta)] &= \frac{105}{128\bar{\rho}^4} \int_1^\infty \frac{u}{a_{22}^4(u, 1)} du + O(\bar{\rho}^{-5}) \\
&= \frac{105}{8\bar{\rho}^4} \int_1^\infty \frac{u}{[(1 - \cos 2\theta)u + 1 + \cos 2\theta]^4} du + O(\bar{\rho}^{-5}) \\
&= \frac{105}{8\bar{\rho}^4(1 - \cos 2\theta)^2} \int_2^\infty \left(\frac{1}{u^3} - \frac{1 + \cos 2\theta}{u^4} \right) du + O(\bar{\rho}^{-5}) \\
&= \frac{105}{256\bar{\rho}^4 \sin^4 \theta} \left(1 - \frac{1 + \cos 2\theta}{3} \right) + O(\bar{\rho}^{-5}) \\
&= \frac{35(3 - 2 \cos^2 \theta)}{256\bar{\rho}^4 \sin^4 \theta} + O(\bar{\rho}^{-5}) \\
&= \frac{560(3 - 2 \cos^2 \theta)}{\rho^4 \sin^4 \theta} + O(\rho^{-5})
\end{aligned} \tag{B.26}$$

This completes the proof of Eq.(5.22b) in Property 7. Similarly, we can prove Eqs.(5.22c) and (5.22d). This completes the proof of Property 7. \square

B.6 Proof of Property 8

Proof. Applying Lemma 4 and taking expectation to J_4 yield

$$\begin{aligned}
\mathbb{E}_{\lambda_1 \geq \lambda_2} [J_4(\boldsymbol{\lambda}, \theta)] &= \mathbb{E}_{\lambda_1 \geq \lambda_2} \left[\frac{1}{2\pi \sqrt{\det(\boldsymbol{\Sigma}_{\nu\nu})}} \int_{-\tan^{-1} \frac{a_{22}}{a_{11}}}^{\tan^{-1} \frac{a_{22}}{a_{11}}} \frac{\exp\left(-\frac{a_{11}^2 \mathbf{z}^T(\phi) \boldsymbol{\Sigma}_{\nu\nu}^{-1} \mathbf{z}(\phi)}{2 \cos^2 \phi}\right)}{\mathbf{z}^T(\phi) \boldsymbol{\Sigma}_{\nu\nu}^{-1} \mathbf{z}(\phi)} d\phi \right. \\
&\quad \left. - \frac{1}{2\pi \sqrt{\det(\boldsymbol{\Sigma}_{\nu\nu})}} \int_{-\tan^{-1} \frac{a_{22}}{a_{11}}}^{\tan^{-1} \frac{a_{22}}{a_{11}}} \frac{\exp\left(-\frac{a_{22}^2 \mathbf{z}^T(\phi) \boldsymbol{\Sigma}_{\nu\nu}^{-1} \mathbf{z}(\phi)}{2 \sin^2 \phi}\right)}{\mathbf{z}^T(\phi) \boldsymbol{\Sigma}_{\nu\nu}^{-1} \mathbf{z}(\phi)} d\phi \right] \\
&= \mathbb{E}_{\lambda_1 \geq \lambda_2} [J_{4a}(\boldsymbol{\lambda}, \theta)] - \mathbb{E}_{\lambda_1 \geq \lambda_2} [J_{4b}(\boldsymbol{\lambda}, \theta)] \tag{B.27}
\end{aligned}$$

where $\mathbf{z}(\phi) = (\cos \phi \ \sin \phi)^T$ and J_{4a} and J_{4b} are defined as

$$J_{4a}(\boldsymbol{\lambda}, \theta) = \frac{1}{2\pi \sqrt{\det(\boldsymbol{\Sigma}_{\nu\nu})}} \int_{-\tan^{-1} \frac{a_{22}}{a_{11}}}^{\tan^{-1} \frac{a_{22}}{a_{11}}} \frac{\exp\left(-\frac{a_{11}^2 \mathbf{z}^T(\phi) \boldsymbol{\Sigma}_{\nu\nu}^{-1} \mathbf{z}(\phi)}{2 \cos^2 \phi}\right)}{\mathbf{z}^T(\phi) \boldsymbol{\Sigma}_{\nu\nu}^{-1} \mathbf{z}(\phi)} d\phi \tag{B.28a}$$

$$J_{4b}(\boldsymbol{\lambda}, \theta) = \frac{1}{2\pi \sqrt{\det(\boldsymbol{\Sigma}_{\nu\nu})}} \int_{-\tan^{-1} \frac{a_{22}}{a_{11}}}^{\tan^{-1} \frac{a_{22}}{a_{11}}} \frac{\exp\left(-\frac{a_{22}^2 \mathbf{z}^T(\phi) \boldsymbol{\Sigma}_{\nu\nu}^{-1} \mathbf{z}(\phi)}{2 \sin^2 \phi}\right)}{\mathbf{z}^T(\phi) \boldsymbol{\Sigma}_{\nu\nu}^{-1} \mathbf{z}(\phi)} d\phi \tag{B.28b}$$

Therefore, recalling $\boldsymbol{\Sigma}_{\nu\nu} = \frac{\mathbf{A}}{2\rho}$ and letting $\lambda_1 = u\lambda_2$, we have

$$\begin{aligned}
&\mathbb{E}_{\lambda_1 \geq \lambda_2} [J_{4a}(\boldsymbol{\lambda}, \theta)] \\
&= \frac{1}{2\pi} \int_1^\infty \sqrt{u} du \int_{-\tan^{-1} \frac{a_{22}(u,1)}{a_{11}(u,1)}}^{\tan^{-1} \frac{a_{22}(u,1)}{a_{11}(u,1)}} \int_0^\infty \lambda_2^3 e^{-(u+1)\lambda_2} \frac{\exp\left(-\frac{\bar{\rho}\lambda_2(a_{11}^2(u,1)\mathbf{z}^T(\phi)\mathbf{A}^{-1}(u,1)\mathbf{z}(\phi))}{\cos^2 \phi}\right)}{\mathbf{z}^T(\phi)\mathbf{A}^{-1}(u,1)\mathbf{z}} d\lambda_2 d\phi \\
&= \frac{1}{2\pi} \int_1^\infty \sqrt{u} du \int_{-\tan^{-1} \frac{a_{22}(u,1)}{a_{11}(u,1)}}^{\tan^{-1} \frac{a_{22}(u,1)}{a_{11}(u,1)}} \frac{d\phi}{\left(1 + u + \frac{\bar{\rho}a_{11}^2(u,1)\mathbf{z}^T(\phi)\mathbf{A}^{-1}(u,1)\mathbf{z}(\phi)}{\cos^2 \phi}\right)^4 \mathbf{z}^T(\phi)\mathbf{A}^{-1}(u,1)\mathbf{z}(\phi)} \tag{B.29}
\end{aligned}$$

If we let $\mathbf{A}^{-1}(u, 1) = \mathbf{B}(u, 1)$, then, $b_{11}(u, 1) = a_{22}(u, 1)/u$, $b_{22}(u, 1) = a_{11}(u, 1)/u$ and $b_{12}(u, 1) = -a_{12}(u, 1)/u$. Thus, we obtain

$$\begin{aligned}
\mathbf{z}^T(\phi)\mathbf{A}^{-1}(u, 1)\mathbf{z}(\phi) &= \mathbf{z}^T(\phi)\mathbf{B}(u, 1)\mathbf{z}(\phi) \\
&= b_{11}(u, 1)\cos^2\phi + 2b_{12}(u, 1)\cos\phi\sin\phi + b_{22}(u, 1)\sin^2\phi \\
&= \sin^2\phi(b_{11}(u, 1)\cot^2\phi + 2b_{12}(u, 1)\cot\phi + b_{22}(u, 1)) \\
&= \frac{\sin^2\phi}{u}(a_{22}(u, 1)\cot^2\phi - 2a_{12}(u, 1)\cot\phi + a_{11}(u, 1))
\end{aligned} \tag{B.30a}$$

$$\begin{aligned}
&= \frac{\cos^2\phi}{u}(a_{11}(u, 1)\tan^2\phi - 2a_{12}(u, 1)\tan\phi + a_{22}(u, 1))
\end{aligned} \tag{B.30b}$$

Substituting Eq.(B.30b) into Eq.(B.29) yields

$$\begin{aligned}
&E_{\lambda_1 \geq \lambda_2} [J_{4a}(\boldsymbol{\lambda}, \theta)] \\
&= \frac{1}{2\pi\bar{\rho}^4} \int_1^\infty \frac{u^{11/2}}{a_{11}^8(u, 1)} du \int_{-\tan^{-1}\frac{a_{22}(u, 1)}{a_{11}(u, 1)}}^{\tan^{-1}\frac{a_{22}(u, 1)}{a_{11}(u, 1)}} \frac{1 + \tan^2\phi}{(a_{11}(u, 1)\tan^2\phi - 2a_{12}(u, 1)\tan\phi + a_{22}(u, 1))^5} d\phi \\
&\quad + O(\bar{\rho}^{-5}) \\
&= \frac{1}{2\pi\bar{\rho}^4} \int_1^\infty \frac{u^{11/2}}{a_{11}^8(u, 1)} du \int_{-\frac{a_{22}(u, 1)}{a_{11}(u, 1)}}^{\frac{a_{22}(u, 1)}{a_{11}(u, 1)}} \frac{dt}{(a_{11}(u, 1)t^2 - 2a_{12}(u, 1)t + a_{22}(u, 1))^5} + O(\bar{\rho}^{-5}) \\
&= \frac{1}{2\pi\bar{\rho}^4} \int_1^\infty \frac{u^{11/2}}{a_{11}^8(u, 1)} du \int_{-\frac{a_{22}(u, 1)}{\delta(u, 1)}}^{\frac{a_{22}(u, 1)}{a_{11}(u, 1)}} \frac{dt}{\left(a_{11}(u, 1)\left(t - \frac{a_{12}(u, 1)}{a_{11}(u, 1)}\right)^2 + \frac{u}{a_{11}(u, 1)}\right)^5} + O(\bar{\rho}^{-5}) \\
&= \frac{1}{2\pi\bar{\rho}^4} \int_1^\infty \frac{u^{11/2}}{a_{11}^4(u, 1)} du \int_{-a_{22}(u, 1) - a_{12}(u, 1)}^{a_{22}(u, 1) - a_{12}(u, 1)} \frac{dt}{(t^2 + u)^5} + O(\bar{\rho}^{-5}) \\
&= \frac{1}{2\pi\bar{\rho}^4} \int_1^\infty \frac{u}{a_{11}^4(u, 1)} du \int_{-\frac{a_{22}(u, 1) - a_{12}(u, 1)}{\sqrt{u}}}^{\frac{a_{22}(u, 1) + a_{12}(u, 1)}{\sqrt{u}}} \frac{dt}{(t^2 + 1)^5} + O(\bar{\rho}^{-5})
\end{aligned} \tag{B.31}$$

Similarly, using Eq.(B.30a) we can obtain

$$\begin{aligned}
& E_{\lambda_1 \geq \lambda_2} [J_{4b}(\lambda, \theta)] \\
&= \frac{1}{2\pi\bar{\rho}^4} \int_1^\infty \frac{u^{11/2}}{a_{22}^8(u, 1)} du \int_{-\tan^{-1} \frac{a_{22}(u, 1)}{a_{11}(u, 1)}}^{\tan^{-1} \frac{a_{22}(u, 1)}{a_{11}(u, 1)}} \frac{1 + \cot^2 \phi}{(a_{22}(u, 1) \cot^2 \phi - 2a_{12}(u, 1) \cot \phi + a_{11}(u, 1))^5} d\phi \\
&\quad + O(\bar{\rho}^{-5}) \\
&= \frac{1}{2\pi\bar{\rho}^4} \int_1^\infty \frac{u^{11/2}}{a_{22}^8(u, 1)} du \int_0^{\tan^{-1} \frac{a_{22}(u, 1)}{a_{11}(u, 1)}} \frac{1 + \cot^2 \phi}{(a_{22}(u, 1) \cot^2 \phi - 2a_{12}(u, 1) \cot \phi + a_{11}(u, 1))^5} d\phi \\
&\quad + \frac{1}{2\pi\bar{\rho}^4} \int_1^\infty \frac{u^{11/2}}{a_{11}^8(u, 1)} du \int_{-\tan^{-1} \frac{a_{22}(u, 1)}{a_{11}(u, 1)}}^0 \frac{1 + \cot^2 \phi}{(a_{22}(u, 1) \cot^2 \phi - 2a_{12}(u, 1) \cot \phi + a_{11}(u, 1))^5} d\phi \\
&\quad + O(\bar{\rho}^{-5}) \\
&= \frac{1}{2\pi\bar{\rho}^4} \int_1^\infty \frac{u^{11/2}}{a_{22}^8(u, 1)} du \int_{\frac{a_{11}(u, 1)}{a_{22}(u, 1)}}^\infty \frac{dt}{(a_{22}(u, 1)t^2 - 2a_{12}(u, 1)t + a_{11}(u, 1))^5} \\
&\quad + \frac{1}{2\pi\bar{\rho}^4} \int_1^\infty \frac{u^{11/2}}{a_{22}^8(u, 1)} du \int_{\frac{a_{11}(u, 1)}{a_{22}(u, 1)}}^\infty \frac{dt}{(a_{22}(u, 1)t^2 + 2a_{12}(u, 1)t + a_{11}(u, 1))^5} + O(\bar{\rho}^{-5}) \\
&= \frac{1}{2\pi\bar{\rho}^4} \int_1^\infty \frac{u}{a_{22}^4(u, 1)} du \int_{\frac{a_{11}(u, 1) - a_{12}(u, 1)}{\sqrt{u}}}^\infty \frac{dt}{(t^2 + 1)^5} \\
&\quad + \frac{1}{2\pi\bar{\rho}^4} \int_1^\infty \frac{u}{a_{22}^4(u, 1)} du \int_{\frac{a_{11}(u, 1) + a_{12}(u, 1)}{\sqrt{u}}}^\infty \frac{dt}{(t^2 + 1)^5} + O(\bar{\rho}^{-5}) \tag{B.32}
\end{aligned}$$

Therefore, substituting Eqs.(B.31) and (B.32) into (B.27) leads to

$$\begin{aligned}
\mathbb{E}_{\lambda_1 \geq \lambda_2} [J_4(\boldsymbol{\lambda}, \theta)] &= \frac{1}{2\pi\bar{\rho}^4} \int_1^\infty \frac{u}{a_{11}^4(u, 1)} du \int_{-\frac{a_{22}(u,1)-a_{12}(u,1)}{\sqrt{u}}}{\frac{a_{22}(u,1)+a_{12}(u,1)}{\sqrt{u}}} \frac{dt}{(t^2+1)^5} \\
&\quad - \frac{1}{2\pi\bar{\rho}^4} \int_1^\infty \frac{u}{a_{22}^4(u, 1)} du \int_{\frac{a_{11}(u,1)-a_{12}(u,1)}{\sqrt{u}}}{\frac{a_{11}(u,1)+a_{12}(u,1)}{\sqrt{u}}} \frac{dt}{(t^2+1)^5} \\
&\quad - \frac{1}{2\pi\bar{\rho}^4} \int_1^\infty \frac{u}{a_{22}^4(u, 1)} du \int_{\frac{a_{11}(u,1)+a_{12}(u,1)}{\sqrt{u}}}{\frac{a_{22}(u,1)-a_{12}(u,1)}{\sqrt{u}}} \frac{dt}{(t^2+1)^5} + O(\bar{\rho}^{-5}) \\
&= \frac{2048}{\pi\rho^4} \int_1^\infty \frac{u}{a_{11}^4(u, 1)} du \int_{-\frac{a_{22}(u,1)-a_{12}(u,1)}{\sqrt{u}}}{\frac{a_{22}(u,1)+a_{12}(u,1)}{\sqrt{u}}} \frac{dt}{(t^2+1)^5} \\
&\quad - \frac{2048}{\pi\rho^4} \int_1^\infty \frac{u}{a_{22}^4(u, 1)} du \int_{\frac{a_{11}(u,1)-a_{12}(u,1)}{\sqrt{u}}}{\frac{a_{11}(u,1)+a_{12}(u,1)}{\sqrt{u}}} \frac{dt}{(t^2+1)^5} \\
&\quad - \frac{2048}{\pi\rho^4} \int_1^\infty \frac{u}{a_{22}^4(u, 1)} du \int_{\frac{a_{11}(u,1)+a_{12}(u,1)}{\sqrt{u}}}{\frac{a_{22}(u,1)-a_{12}(u,1)}{\sqrt{u}}} \frac{dt}{(t^2+1)^5} + O(\rho^{-5})
\end{aligned} \tag{B.33}$$

This completes the proof of Property 8. \square

B.7 Proof of Property 9

Proof. Applying Lemma 5 and taking expectation to $J_5(\boldsymbol{\lambda}, \theta)$ yield

$$\begin{aligned}
&\mathbb{E}_{\lambda_1 \geq \lambda_2} [J_5(\boldsymbol{\lambda}, \theta)] \\
&= \mathbb{E}_{\lambda_1 \geq \lambda_2} \left[\frac{1}{2\pi\sqrt{\det(\boldsymbol{\Sigma}_{\nu\nu})}} \int_{-\tan^{-1}\frac{a_{22}}{a_{11}}}^{\tan^{-1}\frac{2a_{12}-a_{22}}{a_{11}}} \frac{\exp\left(-\frac{c^2\mathbf{z}^T(\phi)\boldsymbol{\Sigma}_{\nu\nu}^{-1}\mathbf{z}(\phi)}{2(\cos\phi-\sin\phi)^2}\right) - \exp\left(-\frac{a_{11}^2\mathbf{z}^T(\phi)\boldsymbol{\Sigma}_{\nu\nu}^{-1}\mathbf{z}(\phi)}{2\cos^2\phi}\right)}{\mathbf{z}^T(\phi)\boldsymbol{\Sigma}_{\nu\nu}^{-1}\mathbf{z}(\phi)} d\phi \right. \\
&\quad \left. + \frac{1}{2\pi\sqrt{\det(\boldsymbol{\Sigma}_{\nu\nu})}} \int_{-\frac{\pi}{2}-\tan^{-1}\frac{2a_{12}-a_{11}}{a_{22}}}^{-\tan^{-1}\frac{a_{22}}{a_{11}}} \frac{\exp\left(-\frac{c^2\mathbf{z}^T(\phi)\boldsymbol{\Sigma}_{\nu\nu}^{-1}\mathbf{z}(\phi)}{2(\cos\phi-\sin\phi)^2}\right) - \exp\left(-\frac{a_{22}^2\mathbf{z}^T(\phi)\boldsymbol{\Sigma}_{\nu\nu}^{-1}\mathbf{z}(\phi)}{2\sin^2\phi}\right)}{\mathbf{z}^T(\phi)\boldsymbol{\Sigma}_{\nu\nu}^{-1}\mathbf{z}(\phi)} d\phi \right] \\
&= \mathbb{E}_{\lambda_1 \geq \lambda_2} [J_{5a}(\boldsymbol{\lambda}, \theta)] + \mathbb{E}_{\lambda_1 \geq \lambda_2} [J_{5b}(\boldsymbol{\lambda}, \theta)]
\end{aligned} \tag{B.34}$$

where $c = a_{11} + a_{22} - 2a_{12}$, $\mathbf{z}(\phi) = (\cos \phi \ \sin \phi)^T$ and $J_{5a}(\boldsymbol{\lambda}, \theta)$ and $J_{5b}(\boldsymbol{\lambda}, \theta)$ are defined as

$$\begin{aligned} & J_{5a}(\boldsymbol{\lambda}, \theta) \\ &= \frac{1}{2\pi \sqrt{\det(\boldsymbol{\Sigma}_{\nu\nu})}} \int_{-\tan^{-1} \frac{a_{22}}{a_{11}}}^{\tan^{-1} \frac{2a_{12}-a_{22}}{a_{11}}} \frac{\exp\left(-\frac{c^2 \mathbf{z}^T(\phi) \boldsymbol{\Sigma}_{\nu\nu}^{-1} \mathbf{z}(\phi)}{2(\cos \phi - \sin \phi)^2}\right) - \exp\left(-\frac{a_{11}^2 \mathbf{z}^T(\phi) \boldsymbol{\Sigma}_{\nu\nu}^{-1} \mathbf{z}(\phi)}{2 \cos^2 \phi}\right)}{\mathbf{z}^T(\phi) \boldsymbol{\Sigma}_{\nu\nu}^{-1} \mathbf{z}(\phi)} d\phi \end{aligned} \quad (\text{B.35a})$$

$$\begin{aligned} & J_{5b}(\boldsymbol{\lambda}, \theta) \\ &= \frac{1}{2\pi \sqrt{\det(\boldsymbol{\Sigma}_{\nu\nu})}} \int_{-\frac{\pi}{2} - \tan^{-1} \frac{2a_{12}-a_{11}}{a_{22}}}^{-\tan^{-1} \frac{a_{22}}{a_{11}}} \frac{\exp\left(-\frac{c^2 \mathbf{z}^T(\phi) \boldsymbol{\Sigma}_{\nu\nu}^{-1} \mathbf{z}(\phi)}{2(\cos \phi - \sin \phi)^2}\right) - \exp\left(-\frac{a_{22}^2 \mathbf{z}^T(\phi) \boldsymbol{\Sigma}_{\nu\nu}^{-1} \mathbf{z}(\phi)}{2 \sin^2 \phi}\right)}{\mathbf{z}^T(\phi) \boldsymbol{\Sigma}_{\nu\nu}^{-1} \mathbf{z}(\phi)} d\phi \end{aligned} \quad (\text{B.35b})$$

Following the way similar to the proof of Property 8, we can obtain

$$\begin{aligned} \mathbb{E}_{\lambda_1 \geq \lambda_2} [J_{5a}(\boldsymbol{\lambda}, \theta)] &= \frac{1}{2\pi \bar{\rho}^4} \int_1^\infty \frac{u^5 du}{a_{11}^4(u, 1) c^8(u, 1)} \int_{\frac{a_{22}(u, 1) - a_{12}(u, 1)}{\sqrt{u}}}^{\frac{a_{22}(u, 1) + a_{12}(u, 1)}{\sqrt{u}}} \frac{\left(t + \frac{a_{11}(u, 1) - a_{12}(u, 1)}{\sqrt{u}}\right)^8 dt}{(t^2 + 1)^5} \\ &\quad - \frac{1}{2\pi \bar{\rho}^4} \int_1^\infty \frac{u}{a_{11}^4(u, 1)} du \int_{\frac{a_{22}(u, 1) - a_{12}(u, 1)}{\sqrt{u}}}^{\frac{a_{22}(u, 1) + a_{12}(u, 1)}{\sqrt{u}}} \frac{dt}{(t^2 + 1)^5} + O(\bar{\rho}^{-5}) \end{aligned} \quad (\text{B.36})$$

In the same token, we can also obtain

$$\begin{aligned} \mathbb{E}_{\lambda_1 \geq \lambda_2} [J_{5b}(\boldsymbol{\lambda}, \theta)] &= \frac{1}{2\pi \bar{\rho}^4} \int_1^\infty \frac{u^5 du}{a_{22}^4(u, 1) c^8(u, 1)} \int_{\frac{a_{11}(u, 1) - a_{12}(u, 1)}{\sqrt{u}}}^{\frac{a_{11}(u, 1) + a_{12}(u, 1)}{\sqrt{u}}} \frac{\left(t + \frac{a_{22}(u, 1) - a_{12}(u, 1)}{\sqrt{u}}\right)^8 dt}{(t^2 + 1)^5} \\ &\quad - \frac{1}{2\pi \bar{\rho}^4} \int_1^\infty \frac{u}{a_{22}^4(u, 1)} du \int_{\frac{a_{11}(u, 1) - a_{12}(u, 1)}{\sqrt{u}}}^{\frac{a_{11}(u, 1) + a_{12}(u, 1)}{\sqrt{u}}} \frac{dt}{(t^2 + 1)^5} + O(\bar{\rho}^{-5}) \end{aligned} \quad (\text{B.37})$$

Substituting $\rho/8 = \bar{\rho}$ and substituting Eqs.(B.36) and (B.37) into Eq.(B.34), we can complete the proof of Property 9. \square

Appendix C

Proofs of Lemmas in Chapter 5

C.1 Proof of Lemma 4

Proof. Since $\mathcal{D} = \mathcal{D}_1 \cup \mathcal{D}_2$, where $\mathcal{D}_1 = \{(x_1, x_2) : x_1 \geq a, -b \leq x_2 \leq 0\}$ and $\mathcal{D}_2 = \{(x_1, x_2) : x_1 \geq a, 0 \leq x_2 \leq b\}$, we obtain

$$I_1 = \iint_{\mathcal{D}} f(\mathbf{x}) dx_2 dx_1 = \iint_{\mathcal{D}_1} f(\mathbf{x}) dx_2 dx_1 + \iint_{\mathcal{D}_2} f(\mathbf{x}) dx_2 dx_1 \quad (\text{C.38})$$

Using the polar system, $x_1 = r \cos \phi$, $x_2 = r \sin \phi$ and $f(\mathbf{x}(\phi)) = \exp(-r^2 \mathbf{x}(\phi)^T \mathbf{P} \mathbf{x}(\phi))$, where $\mathbf{x}(\phi) = (\cos \phi \quad \sin \phi)^T$. Hence,

$$\begin{aligned} \iint_{\mathcal{D}_1} f(\mathbf{x}) dx_2 dx_1 &= \int_{-\tan^{-1} b/a}^0 \int_{a/\cos \phi}^{b/\sin \phi} r f(r \cos \phi, r \sin \phi) dr d\phi \\ &= -\frac{1}{2} \int_{-\tan^{-1} b/a}^0 \int_{a/\cos \phi}^{b/\sin \phi} r \exp(-r^2 \mathbf{x}(\phi)^T \mathbf{P} \mathbf{x}(\phi)) d(-r^2 \mathbf{x}(\phi)^T \mathbf{P} \mathbf{x}(\phi)) d\phi \\ &= \int_{-\tan^{-1} b/a}^0 \frac{\exp\left(-\frac{a^2 \mathbf{x}^T(\phi) \mathbf{P} \mathbf{x}(\phi)}{\cos^2 \phi}\right) - \exp\left(-\frac{b^2 \mathbf{x}^T(\phi) \mathbf{P} \mathbf{x}(\phi)}{\sin^2 \phi}\right)}{2 \mathbf{x}^T(\phi) \mathbf{P} \mathbf{x}(\phi)} d\phi \end{aligned} \quad (\text{C.39})$$

Similarly, we can obtain

$$\iint_{D_2} f(\mathbf{x}) dx_2 dx_1 = \int_0^{\tan^{-1} b/a} \frac{\exp\left(-\frac{a^2 \mathbf{x}^T(\phi) \mathbf{P} \mathbf{x}(\phi)}{\cos^2 \phi}\right) - \exp\left(-\frac{b^2 \mathbf{x}^T(\phi) \mathbf{P} \mathbf{x}(\phi)}{\sin^2 \phi}\right)}{2 \mathbf{x}^T(\phi) \mathbf{P} \mathbf{x}(\phi)} d\phi. \quad (\text{C.40})$$

Therefore, combining Eqs.(C.39) and (C.40) yields

$$I_1 = \int_{-\tan^{-1} b/a}^{\tan^{-1} b/a} \frac{\exp\left(-\frac{a^2 \mathbf{x}^T(\phi) \mathbf{P} \mathbf{x}(\phi)}{\cos^2 \phi}\right) - \exp\left(-\frac{b^2 \mathbf{x}^T(\phi) \mathbf{P} \mathbf{x}(\phi)}{\sin^2 \phi}\right)}{2 \mathbf{x}^T(\phi) \mathbf{P} \mathbf{x}(\phi)} d\phi \quad (\text{C.41})$$

This completes the proof of Lemma 4. \square

C.2 Proof of Lemma 5

Proof. Since the intersection point between line $x_2 = -x_1 \tan \frac{b}{a}$ and line $x_2 = x_1 - c$ is $x_1 = \frac{c}{1 + \tan \frac{b}{a}}, x_2 = \frac{c \tan \frac{b}{a}}{1 + \tan \frac{b}{a}}$, the integral domain \mathcal{D} can be segmented into $\mathcal{D} = \mathcal{D}_1 \cup \mathcal{D}_2$, where $\mathcal{D}_1 = \{(x_1, x_2) : \frac{c}{1 + \tan \frac{b}{a}} \leq x_1 \leq a, -x_1 \tan \frac{b}{a} \leq x_2 \leq x_1 - c\}$ and $\mathcal{D}_2 = \{(x_1, x_2) : c - b \leq x_1 \leq \frac{c}{1 + \tan \frac{b}{a}}, -b \leq x_2 \leq x_1 - c\}$ or $\frac{c}{1 + \tan \frac{b}{a}} \leq x_1 \leq a, -x_1 \tan \frac{b}{a} \leq x_2 \leq x_1 - c\}$. Hence, we have

$$I_2 = \iint_{\mathcal{D}} f(\mathbf{x}) dx_2 dx_1 = \iint_{\mathcal{D}_1} f(\mathbf{x}) dx_2 dx_1 + \iint_{\mathcal{D}_2} f(\mathbf{x}) dx_2 dx_1 \quad (\text{C.42})$$

We consider the following two cases.

1. $c \leq b$. In this case, using the polar transformation; $x_1 = r \cos \phi$ and $x_2 = r \sin \phi$, we have $f(\mathbf{x}(\phi)) = \exp(-r^2 \mathbf{x}(\phi)^T \mathbf{P} \mathbf{x}(\phi))$, where $\mathbf{x}(\phi) = (\cos \phi \ \sin \phi)^T$. Therefore,

we obtain

$$\begin{aligned}
\iint_{\mathcal{D}_1} f(\mathbf{x}) dx_2 dx_1 &= \int_{-\tan^{-1} \frac{b}{a}}^{-\tan^{-1} \frac{a-c}{a}} \int_{\frac{c}{\cos \phi - \sin \phi}}^{\frac{a}{\cos \phi}} r f(r \cos \phi, r \sin \phi) dr d\phi \\
&= -\frac{1}{2} \int_{-\tan^{-1} \frac{b}{a}}^{-\tan^{-1} \frac{a-c}{a}} \int_{\frac{c}{\cos \phi - \sin \phi}}^{\frac{b}{\sin \phi}} \exp(-r^2 \mathbf{x}(\phi)^T \mathbf{P} \mathbf{x}(\phi)) d(-r^2 \mathbf{x}(\theta)^T \mathbf{P} \mathbf{x}(\theta)) d\theta \\
&= \int_{-\tan^{-1} \frac{b}{a}}^{-\tan^{-1} \frac{a-c}{a}} \frac{\exp\left(-\frac{c^2 \mathbf{x}^T(\phi) \mathbf{P} \mathbf{x}(\phi)}{(\cos \phi - \sin \phi)^2}\right) - \exp\left(-\frac{a^2 \mathbf{x}^T(\theta) \mathbf{P} \mathbf{x}(\theta)}{\cos^2 \phi}\right)}{2 \mathbf{x}^T(\phi) \mathbf{P} \mathbf{x}(\phi)} d\phi \tag{C.43}
\end{aligned}$$

Similarly, we can obtain

$$\begin{aligned}
\iint_{\mathcal{D}_2} f(\mathbf{x}) dx_2 dx_1 &= \int_{-\frac{\pi}{2} - \tan^{-1} \frac{b-c}{b}}^{-\tan^{-1} \frac{b}{a}} \int_{\frac{c}{\cos \phi - \sin \phi}}^{\frac{b}{\sin \phi}} r f(r \cos \phi, r \sin \phi) dr d\phi \\
&= \int_{-\frac{\pi}{2} - \tan^{-1} \frac{b-c}{b}}^{-\tan^{-1} \frac{b}{a}} \frac{\exp\left(-\frac{c^2 \mathbf{x}^T(\phi) \mathbf{P} \mathbf{x}(\phi)}{(\cos \phi - \sin \phi)^2}\right) - \exp\left(-\frac{b^2 \mathbf{x}^T(\theta) \mathbf{P} \mathbf{x}(\theta)}{\cos^2 \phi}\right)}{2 \mathbf{x}^T(\phi) \mathbf{P} \mathbf{x}(\phi)} d\phi \tag{C.44}
\end{aligned}$$

Now, substituting Eqs.(C.43) and (C.44) into Eq.(C.42) yields

$$\begin{aligned}
I_2 &= \int_{-\tan^{-1} \frac{b}{a}}^{\tan^{-1} \frac{a-c}{a}} \frac{\exp\left(-\frac{c^2 \mathbf{x}^T(\theta) \mathbf{P} \mathbf{x}(\theta)}{(\cos \theta - \sin \theta)^2}\right) - \exp\left(-\frac{a^2 \mathbf{x}^T(\theta) \mathbf{P} \mathbf{x}(\theta)}{\cos^2 \theta}\right)}{2 \mathbf{x}^T(\theta) \mathbf{P} \mathbf{x}(\theta)} d\theta \\
&\quad + \int_{-\frac{\pi}{2} - \tan^{-1} \frac{b-c}{b}}^{-\tan^{-1} \frac{b}{a}} \frac{\exp\left(-\frac{c^2 \mathbf{x}^T(\theta) \mathbf{P} \mathbf{x}(\theta)}{(\cos \theta - \sin \theta)^2}\right) - \exp\left(-\frac{b^2 \mathbf{x}^T(\theta) \mathbf{P} \mathbf{x}(\theta)}{\sin^2 \theta}\right)}{2 \mathbf{x}^T(\theta) \mathbf{P} \mathbf{x}(\theta)} d\theta \tag{C.45}
\end{aligned}$$

Therefore, Lemma 5 is true for $c \leq b$.

2. $c > b$. In this case, the integral over the domain \mathcal{D}_1 does not change, but the

integral over the domain \mathcal{D}_2 becomes

$$\begin{aligned} \iint_{\mathcal{D}_2} f(\mathbf{x}) dx_2 dx_1 &= \int_{-\tan^{-1} \frac{b}{c-b}}^{-\tan^{-1} \frac{b}{a}} \int_{\frac{c}{\cos \phi - \sin \phi}}^{\frac{b}{\sin \phi}} r f(r \cos \phi, r \sin \phi) dr d\phi \\ &= \int_{-\tan^{-1} \frac{b}{c-b}}^{-\tan^{-1} \frac{b}{a}} \frac{\exp\left(-\frac{c^2 \mathbf{x}^T(\phi) \mathbf{P} \mathbf{x}(\phi)}{(\cos \phi - \sin \phi)^2}\right) - \exp\left(-\frac{b^2 \mathbf{x}^T(\theta) \mathbf{P} \mathbf{x}(\phi)}{\sin^2 \phi}\right)}{2 \mathbf{x}^T(\phi) \mathbf{P} \mathbf{x}(\phi)} d\phi \end{aligned}$$

Hence, in this case, proving the lemma is equivalent to proving

$$\begin{aligned} &\int_{-\tan^{-1} \frac{b}{c-b}}^{-\tan^{-1} \frac{b}{a}} \frac{\exp\left(-\frac{c^2 \mathbf{x}^T(\phi) \mathbf{P} \mathbf{x}(\phi)}{(\cos \phi - \sin \phi)^2}\right) - \exp\left(-\frac{b^2 \mathbf{x}^T(\theta) \mathbf{P} \mathbf{x}(\phi)}{\sin^2 \phi}\right)}{2 \mathbf{x}^T(\phi) \mathbf{P} \mathbf{x}(\phi)} d\phi \\ &= \int_{-\frac{\pi}{2} - \tan^{-1} \frac{b-c}{b}}^{-\tan^{-1} \frac{b}{a}} \frac{\exp\left(-\frac{c^2 \mathbf{x}^T(\phi) \mathbf{P} \mathbf{x}(\phi)}{(\cos \phi - \sin \phi)^2}\right) - \exp\left(-\frac{b^2 \mathbf{x}^T(\theta) \mathbf{P} \mathbf{x}(\phi)}{\cos^2 \phi}\right)}{2 \mathbf{x}^T(\phi) \mathbf{P} \mathbf{x}(\phi)} d\phi \quad (\text{C.46}) \end{aligned}$$

To do that, we let

$$F(\phi) = \frac{\exp\left(-\frac{c^2 \mathbf{x}^T(\phi) \mathbf{P} \mathbf{x}(\phi)}{(\cos \phi - \sin \phi)^2}\right) - \exp\left(-\frac{b^2 \mathbf{x}^T(\theta) \mathbf{P} \mathbf{x}(\phi)}{\cos^2 \phi}\right)}{2 \mathbf{x}^T(\phi) \mathbf{P} \mathbf{x}(\phi)} \quad (\text{C.47})$$

Then, on one hand, we obtain

$$\begin{aligned} \int_{-\tan^{-1} \frac{b}{c-b}}^{-\tan^{-1} \frac{b}{a}} F(\phi) d\phi &= - \int_{\tan^{-1} \frac{b}{c-b}}^{\tan^{-1} \frac{b}{a}} F(-\varphi) d\varphi \\ &= \int_{\frac{c-b}{b}}^{\frac{a}{b}} \frac{F(-\cot^{-1} t)}{1+t^2} dt \quad (\text{C.48}) \end{aligned}$$

On the other hand, we obtain

$$\begin{aligned}
 \int_{-\frac{\pi}{2}-\tan^{-1}\frac{b-c}{b}}^{-\tan^{-1}\frac{b}{a}} F(\phi)d\phi &= -\int_{\frac{\pi}{2}+\tan^{-1}\frac{b-c}{b}}^{\tan^{-1}\frac{b}{a}} F(-\varphi)d\varphi \\
 &= \int_{\frac{c-b}{b}}^{\frac{a}{b}} \frac{F(-\cot^{-1}t)}{1+t^2} dt
 \end{aligned} \tag{C.49}$$

Comparing Eq.(C.47) with Eq.(C.49) produces the proof of Eq.(C.46).

This completes the proof of Lemma 5. □

Bibliography

- [1] W. Su and X.-G. Xia, "Signal constellations for quasi-orthogonal space-time block codes with full diversity," *IEEE Trans. Inform. Theory*, vol. 50, pp. 2331–2347, Oct. 2004.
- [2] M. K. Simon and M. S. Alouini, *Digital Communication over Fading Channels: A Unified Approach to Performance Analysis*. New York: Wiley, 2000.
- [3] L. Zheng and D. N. C. Tse, "Diversity and multiplexing: A fundamental tradeoff in multiple-antennas channels," *IEEE Trans. Inform. Theory*, vol. 49, pp. 1073–1096, May 2004.
- [4] A. Goldsmith, *Wireless Communications*. Cambridge: Cambridge University Press, 2005.
- [5] V. Tarokh, N. Seshadri, and A. R. Calderbank, "Space-time codes for high data rate wireless communication: Performance criterion and code construction," *IEEE Trans. Inform. Theory*, vol. 44, pp. 744–765, Mar. 1998.
- [6] G. J. Foschini and M. J. Gans, "On limits of wireless communications in a fading environment when using multiple antennas," *Wireless Personal Communications*, vol. 6, pp. 311–335, January 1998.

- [7] E. Telatar, "Capacity of multi-antenna gaussian channels," *European Transactions on Telecommunications*, vol. 10, pp. 585–595, November 1999.
- [8] B. Hassibi and B. M. Hochwald, "High-rate codes that are linear in space and time," *IEEE Trans. Inform. Theory*, vol. 50, pp. 1804–1824, Jul. 2002.
- [9] H. E. Gamal and M. O. Damen, "Universal space-time coding," *IEEE Trans. Inform. Theory*, vol. 49, pp. 1097–1119, May. 2003.
- [10] X. Ma and G. B. Giannakis, "Full-diversity full rate complex-field space-time coding," *IEEE Trans. Signal Processing*, vol. 51, pp. 2917–2930, Nov. 2003.
- [11] B. A. Sethuraman, B. S. Rajan, and V. Shashidhar, "Full-diversity, high rate space-time block codes from division algebras," *IEEE Trans. Inform. Theory*, vol. 49, pp. 2596–2616, Oct. 2003.
- [12] T. Kiran and B. S. Rajan, "STBC-schemes with nonvanishing determinant for certain number of transmitters," *IEEE Trans. Inform. Theory*, vol. 51, pp. 2984–2992, Aug. 2005.
- [13] F. Oggier, G. Rekaya, J.-C. Belfiore, and E. Viterbo, "Perfect space-time block codes," *IEEE Trans. Inform. Theory*, vol. 52, pp. 3885–3902, Sep. 2006.
- [14] P. Elia, K. R. Kumar, S. A. Pawar, P. V. Kumar, and H.-F. Lu, "Explicit space-time codes achieving the diversity-multiplexing gain tradeoff," *IEEE Trans. Inform. Theory*, vol. 52, pp. 3869–3884, Sep. 2006.
- [15] S. M. Alamouti, "A simple transmitter diversity scheme for wireless communications," *IEEE J. Select. Areas Commun.*, vol. 16, pp. 1451–1458, Oct. 1998.

- [16] V. Tarokh, H. Jafarkhani, and A. R. Calderbank, "Space-time block codes from orthogonal designs," *IEEE Trans. Inform. Theory*, vol. 45, pp. 1456–1467, July. 1999.
- [17] O. Tirkkonen and A. Hottinen, "Square-matrix embeddable space-time codes for complex signal constellations," *IEEE Trans. Inform. Theory*, vol. 48, pp. 1122–1126, Feb. 2002.
- [18] X.-B. Liang, "Orthogonal designs with maximal rates," *IEEE Trans. Inform. Theory*, vol. 49, pp. 2468–2503, Oct. 2003.
- [19] S. Sandhu and A. J. Paulraj, "Space-time block coding: A capacity perspective," *IEEE Commun. Letters*, vol. 4, pp. 384–386, Dec. 2000.
- [20] H. Jafarkhani, "A quasi-orthogonal space-time block code," *IEEE Trans. Commun.*, vol. 49, pp. 1–4, Jan. 2001.
- [21] O. Tirkkonen, A. Boariu, and A. Hottinen, "Minimal nonorthogonality rate 1 space-time block code for 3+ tx antennas," in *Proc. IEEE 6th Int. Symp. Spread-Spectrum Techniques and Applications*, pp. 429–432, Sept. 2000.
- [22] C. B. Papadias and G. J. Foschini, "Capacity-approaching space-time codes for systems employing four transmitter antennas," *IEEE Trans. Inform. Theory*, vol. 49, pp. 726–732, Mar. 2003.
- [23] L.-K. Hua, *Introduction to Number Theory*. Berlin ; New York: Springer-Verlag, 1982.

- [24] C. Yuen, Y. L. Guan, and T. T. Tjhung, "Quasi-orthogonal STBC with minimum decoding complexity," *IEEE Trans. Wireless Commun.*, vol. 4, pp. 2089–2094, Sept. 2005.
- [25] S. Karmakar and B. S. Rajan, "Multi-group quasi-orthogonal STBCs from clifford algebras," in *IEEE Inform. Theory Workshop*, (Chengdu, China), pp. 448–452, Oct. 2006.
- [26] D. N. Dao, C. Yuen, C. Tellambura, Y. L. Guan, and T. T. Tjhung, "Four-group decodable space-time block codes," *IEEE Trans. Signal Processing*, vol. 56, pp. 424–430, Jan. 2008.
- [27] S. Sezginer and H. Sari, "A full-rate full-diversity 2×2 space-time code for mobil WiMAX systems," in *Proc. IEEE 6th Int. Conf. Signal Processing and Communications*, (Dubai), November 2007.
- [28] J. Paredes, A. B. Gershman, and M. G. Alkhansari, "A new full-rate full-diversity space-time block code with non-vanishing determinants and simplified maximum likelihood decoding," *IEEE Trans. Signal Processing*, vol. 56, pp. 2461–2469, June 2008.
- [29] E. Biglieri, Y. Yong, and E. Viterbo, "On fact-decodable space-time block codes," *IEEE Trans. Inform. Theory*, vol. 55, pp. 524–530, Feb. 2009.
- [30] A. V. Geramita and J. Seberry, "Orthogonal design, quadratic forms and hadamard matrices," in *Lecture Notes in Pure and Applied Mathematics*, (New York: Marcel Dekker INC), 1979.

- [31] M. K. Simon and M.-S. Alouini, "A unified approach to the performance analysis of digital communication over generalized fading channels," *Proc. of the IEEE*, vol. 86, pp. 1860–1877, Sept. 1998.
- [32] R. A. Horn and C. R. Johnson, *Topics in matrix analysis*. The Pitt Building, Trumping Street, Cambridge CB2 IRP England: Cambridge University Press, 1991.
- [33] J. Liu, J.-K. Zhang, and K. M. Wong, "Full diversity codes for MISO systems equipped with linear or ML detectors," *IEEE Trans. Inform. Theory*, vol. 54, pp. 4511–4527, Oct. 2008.
- [34] G. D. Forney and G. U. Ungerboeck, "Modulation and coding for linear Gaussian channel," *IEEE Trans. Inform. Theory*, vol. 44, pp. 2384–2415, May 1998.
- [35] Y. Xin, Z. Wang, and G. Giannakis, "Space-time diversity systems based on linear constellation precoding," *IEEE Trans. Wireless Communications*, vol. 2, pp. 294–309, March 2003.
- [36] C. Yuen, Y. L. Guan, and T. T. Tjhung, "A class of four-group quasi-orthogonal space-time block code achieving full rate and full diversity for any number of antennas," in *Proc. IEEE Personal, Indoor and Mobile Radio Communications Symp. (PIMRC)*, (Berlin, Germany), pp. 92–96, Sep. 2005.
- [37] J. W. Craig, "A new, simple, and exact result for calculating the probability of error for two-dimensional signal constellations," in *Proc. IEEE Milit. Commun. Conf.*, (McLean, VA), pp. 571–575, Oct. 1991.